JUMONJI 30 and JUMONJI 32 regulate abscisic acid-dependent growth arrest

（JMJ30 と JMJ32 は、ABA 依存の成長抑制を制御する）

Jinfeng Wu

Nara Institute of Science and Technology of Biological Sciences,

Laboratory of Plant Stem Cell Regulation and Floral Patterning

(Professor Toshiro Ito)

Submitted on August 20, 2019

Contents

List of Abbreviations

ABA	Abscisic Acid
ABFs	ABA-responsive Element Binding Factors
ABI1	ABSCISIC ACID INSENSITIVE 1
ABI3	ABA INSENSITIVE3
ABI5	ABSCISIC ACID INSENSITIVE5
ABRE	ABA-Responsive Elements
ARR9	AUTHENTIC RESPONSE REGULATOR9
CCA1	CIRCADIAN CLOCK ASSOCIATED 1
ChIP	Chromatin Immunoprecipitation
DEGs	Different Expression Genes
ELF6	EARLY FLOWERING 6
FC	Fold Change
FDR	False Discovery Rate
FLC	FLOWERING LOCUS C
FUS3	FUSCA3
GO	Gene Ontology
GUS	β-glucuronidase
H3K27me3	H3 Lysine 27 Trimethylation

HAB1	HYPERSENSITIVE TO ABA1
HAT	Histone Acetyltransferase
HDAC	Histone de-acetylase
HDM	Histone de-methylase
HMT	Histone Methyltransferase
JMJ30/32	JUMONJI-C DOMAIN-CONTAINING PROTEIN30/32
LEC1/2	LEAFY COTYLEDON1/2
LHY	LATE ELONGATED HYPOCOTYL
MAP18	MICROTUBULE-ASSOCIATED PROTEIN18
PcG	Polycomb Group
PP2Cs	Type 2C Protein Phosphatases
PRC1	POLYCOMB REPRESSIVE COMPLEX 1
PRC2	POLYCOMB REPRESSIVE COMPLEX 2
REF6	RELATIVE OF EARLY FLOWERING 6
REVIGO	REduced VIsualize Gene Ontology
RNA-seq	RNA Sequencing
RT-qPCR	Quantitive Reverse Transcription Polymerase Chain Reaction
SnRK2.8	SNF1-RELATED PROTEIN KINASE 2.8
SnRK2s	SNF1-RELATED PROTEIN KINASE 2s

TEM	Transmission Electron Micrography
ZRF	ZUOTIN-RELATED FACTOR1

Part I Abscisic acid-dependent histone demethylation during post-germination growth arrest in *Arabidopsis*

Abstract

After germination, seedlings undergo growth arrest in response to unfavorable conditions, a critical adaptation enabling plants to survive harsh environments. The plant hormone abscisic acid (ABA) plays a key role in this arrest. To arrest growth, ABA-dependent transcription factors change gene expression patterns in a flexible and reversible manner. Although the control of gene expression has important roles in growth arrest, the epigenetic mechanisms in the response to ABA are not fully understood. Here, I show that the histone demethylases JUMONJI-C DOMAIN-CONTAINING PROTEIN30 (JMJ30) and JMJ32 control ABA-mediated growth arrest in *Arabidopsis thaliana*.

The early seedling development phase was divided into seed germination and seedling establishment stage. I conducted RT-qPCR to test whether *JMJ30/JMJ32* is induced by ABA during these two stages. The results indicated that *JMJ30* is specifically induced by ABA only during the seedling establishment stage but it is not induced by ABA during seed germination stage. However, *JMJ32* is not induced by ABA in both two stages. These data promoted me to do further studies on the seedling establishment stage. I found that during this stage, the ABA-dependent transcription factor ABA INSENSITIVE3 (ABI3) activates the expression of *JMJ30*

in response to ABA, showing that ABI3 as an upstream regulator for ABA-dependent *JMJ30* induction. Furthermore, I made mutation on the RY motif (ATGCAT) of the *JMJ30* promoter then compared the JMJ30-GUS levels between native RY motif and mutated RY motif lines. The results suggested that ABA-dependent *JMJ30* expression is controlled by ABI3 through the conserved RY motif.

Next, I performed phenotypical analyses. Under mock treatment, there was no significate differences among WT, *jmj30*, *jmj32* and *jmj30 jmj32* on seed germination ratio, seedling establishment ratio and fresh weight. Under ABA treatment, no significant differences were detected among WT and *jmj* single mutants, but *jmj30 jmj32* double mutants were less sensitive to ABA as compared to WT and *jmj* single mutants. To understand the mechanism of JMJ-mediated ABA responses, I performed RNA-seq analyses to find the downstream targets of JMJ30 and JMJ32. The results showed that 60 genes were differentially expressed only in ABA-treated *jmj30 jmj32* plants; 31 genes and 29 genes were downregulated and upregulated in the double mutant, respectively. Pervious study demonstrated that JMJ30/JMJ32 are the histone demethylases for H3 lysine 27 trimethylation (H3K27me3) and then activate gene expression. Therefore, the 31 downregulated genes were used for further analyses as putative targets of JMJ30/JMJ32. After GO analysis and filtering based on the annotation from TAIR database, *SNF1-RELATED PROTEIN KINASE 2.8 (SnRK2.8)*, *AT1G62660* and *AT4G23670* were previously shown to be responsive to ABA. Further studies supported that JMJ30 removes

a repressive histone mark, H3 lysine 27 trimethylation (H3K27me3), from the promoter of *SnRK2.8*, and hence activates *SnRK2.8* expression. The overexpression of *SnRK2.8* can rescue the ABA less sensitivity of *jmj30 jmj32* double mutant. SnRK2.8 encodes a kinase that activates ABI3 and is responsible for JMJ30- and JMJ32-mediated growth arrest.

In summary, I uncovered a feedback activation loop which involve in ABI3 transcription factor, JMJ histone demethylases, and the SnRK2.8 kinase during post-germination phase. My findings highlight the importance of the histone demethylases in mediating adaptation of plants to the environment.

1. Introduction

1.1 Seed germination and subsequent seedling establishment

Seed dormancy and post-germination growth arrest are critical adaptations that allow plants to survive unfavorable conditions (Bewley 1997; Lopez-Molina et al. 2001; Bentsink and Koornneef 2008; Li et al. 2018). Before germination, seeds contain carbohydrates, proteins, lipids, and phosphates as energy sources and remain in a metabolically quiescent, desiccation-tolerant state (Bentsink and Koornneef 2008). Once the seed senses environmental signals favorable for the release of dormancy, such as water imbibition or stratification, the radicle emerges through the seed coat in the process known as germination (Penfield 2017). During a post-germination phase lasting 2–3 days, activation of metabolism results in the gradual hydrolysis and release of storage materials. During the process of seedling establishment, if the seedlings encounter stress conditions such as water deficit, they can arrest their growth until more favorable conditions return (Lopez-Molina et al., 2001).

Dormancy is always terminated by environmental stimuli and endogenous cues. Cold stratification (4°C) is the process which can break seed dormancy. When stratified seeds encounter stimuli such as light, water or suitable temperature condition, they will start elongating radicle which is embryonic root of the plant. The process of radicle emerges through the seed is known as germination (Penfield 2017). Subsequent post-germination growth leads to seedling establishment. After protrusion of radicle, cotyledons turn into green and root hairs

are formed before the cotyledons fully open (2-3 day after stratification) (Fig. 1).

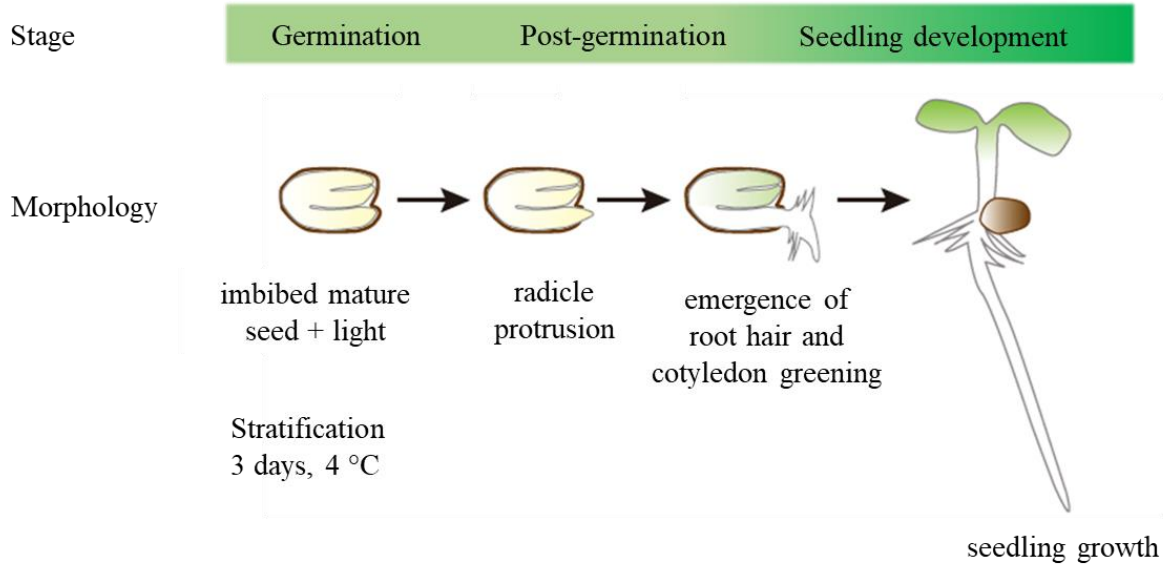

Figure 1 Morphological changes during early plant growth and development.

1.2 Environmental changes affect seed germination and seedling establishment

To overcome the environmental changes during early plant growth and development, plants have evolved adaptive mechanisms to sense and respond to environmental signals. The seed dormancy and subsequent growth arrest are critical adaptive strategies allowing plants to cope with unfavorable conditions for better survival. Seed germination stage is a critical phase in the life cycle in plants. Before germination, seeds which contain carbohydrates, proteins, lipids, and phosphate as energy sources remain in a metabolically quiescent state and confer tolerance to desiccation (Bentsink and Koornneef 2008). Once the seed senses environmental signals favorable for the release of dormancy such as water imbibition or stratification, the seed

will complete germination stage (Penfield 2017). During a post-germination phase which lasts for two to three days, activation of metabolism results in a gradual hydrolysis and release of stored materials. If seedlings encounter stress conditions such as water deficit during the process of establishment, the plants can execute growth arrest until more favorable growth conditions return (Lopez-Molina et al. 2001). Flexible and reversible control of gene expression is thought to have an important role in triggering growth arrest.

1.3 Hormonal control of gene expression in response to environment

To cope with the environmental stimuli and endogenous cues, plants have developed multiple and efficient protective mechanisms to minimize damage effects from stresses on their growth stages. Plant hormones which include abscisic acid (ABA), auxin, brassinosteroids (BRs), cytokinin, gibberlins (GA) and ethylene play central roles during many stress-related biological processes (Zhang et al. 2009; Asami and Nakagawa 2018). After sensing hormonal cues, plants start to activate stress response genes for better adaptation.

1.4 The role of ABA signaling pathway on gene expression in response to environment

ABA is a crucial signaling molecule for plant growth and development in response to stresses (Mustilli et al. 2002; Finkelstein 2013). When plants sense the stress signals, the level of endogenous ABA will be elevated. Recent researches revealed that ABA inhibits seed

germination and seedling establishment (Weitbrecht et al. 2011; Nee et al. 2017; Ryu et al. 2014). When plants produce and sense ABA, the receptors such as PYRABACTIN RESISTANCE1 (PYR1)/PYR1-LIKE (PYL)/REGULATORY COMPONENTS OF ABA RECEPTOR (RCAR) proteins undergo conformational changing to allow ABA binding to occur easier (Park et al. 2009; Cutler et al. 2010). The RCAR family of proteins contains 14 sub-members (Cutler et al. 2010). All of these proteins bind to ABA and interact with type 2C protein phosphatases（PP2Cs). The ABA receptor complexes then inhibit the PP2Cs, such as ABSCISIC ACID INSENSITIVE 1 (ABI1), ABI2 and HYPERSENSITIVE TO ABA1 (HAB1). Among the PP2Cs identified in *Arabidopsis*, six out of nine clade A PP2Cs act as negative regulators of ABA signaling (Merlot et al. 2001; Rodrigues et al. 2013). The PP2Cs bind to SNF1-RELATED PROTEIN KINASE 2s (SnRK2s) protein and inhibit phosphorylation in the absence of ABA (Mustilli et al. 2002; Umezawa et al. 2004; Nakashima et al. 2009; Umezawa et al. 2009; Lee et al. 2015). There are 10 members of the SnRK2a and SnRK2b groups in Arabidopsis. The members from SnRK2a subfamily such as SRK2D/SnRK2.2, SRK2E/SnRK2.6, SRK2I/SnRK2.3, SRK2F/SnRK2.7 and SRK2C/SnRK2.8 were reported as the ABA-activated protein kinases. These SnRK2s regulate many biological processes through the control of seed dormancy, bud dormancy and root development under harsh environmental conditions, as well as stress response. One of these protein kinases, SnRK2.8 was reported as a drought and systemic immune response regulator (Lee et al. 2015).

In the presence of ABA, the self-phosphorylated SnRK2s subsequently phosphorylate key transcription factors that mediate ABA response. The activated SnRK2s are able to phosphorylate and activate downstream transcription factors such as bZIP-type transcription factor ABSCISIC ACID INSENSITIVE5 (ABI5), AP2-type protein ABI4, the B3-type protein ABI3 and ABA-responsive element Binding Factors (ABFs) through the binding onto ABA-Responsive Elements (ABRE) (Lopez-Molina et al. 2002; Narusaka et al. 2003; Perruc et al. 2007; Lim et al. 2013). Among them, the B3 domain transcription factor ABSCISIC ACID INSENSITIVE3 (ABI3) and the basic domain/leucine zipper (bZIP) transcription factor ABI5 have important roles in seed dormancy and subsequent growth arrest (Finkelstein and Lynch 2000; Lopez-Molina et al. 2001; Lopez-Molina et al. 2002; Lim et al. 2013). Endogenous *ABI3* expression is transcriptionally induced during seed maturation stage and attenuated after germination (Delmas et al. 2013). ABA treatment leads to growth arrest through persistent high expression of *ABI3* (Teaster et al. 2007; Piskurewicz et al. 2009; Liu et al. 2013). ABI3 recognizes the conserved RY sequence motif which consists of alternating purine and pyrimidine nucleotides in its target genes (Suzuki et al. 1997; Sakata et al. 2010). On the other hands, *ABI5* acts as a downstream target of ABI3 in ABA-dependent growth arrest (Lopez-Molina et al. 2002).

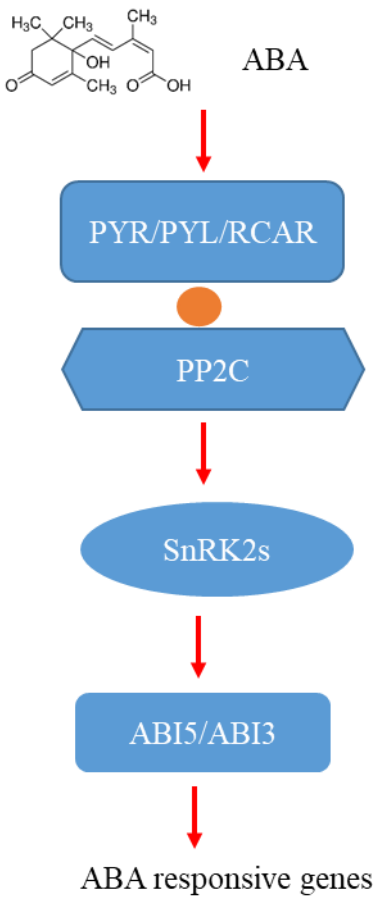

Figure 2 The ABA signaling pathway. ABA-bound PYR/PYL/RCAR receptors bind PPC2s to form a complex, thereby activates the protein kinases SnRK2s. Activated SnRK2 kinases phosphorylate transcription factors ABI5 and ABI3, then regulate ABA responsive genes to control stress responses.

1.5 Epigenetic control of gene expression by histone modification

The eukaryotic chromatin consists of histone protein and DNA (Chatterjee and Muir 2010). The histones can be divided into four different types of core histones that are H2A, H2B, H3 and H4 as well as linker histone H1 (Harshman et al. 2013; Vogler et al. 2010). There are two copies for each core histones. They form an eight-subunit complex, which is surrounded

by a 146 bp of DNA to form the basic unit of chromatin, nucleosome. Each core histone has a hydrophobic C-terminal which occupies the internal region. On the other hand, the hydrophilic N-terminal tail extends outward (Cutter and Hayes 2015; Marino-Ramirez et al. 2005). Histone tails play an important role in gene expression. Histone tails are the most common sites of post-translational modifications, such as methylation and demethylation, acetylation and deacetylation, phosphorylation and dephosphorylation, ubiquitination and deubiquitination (Hong and Shao 2011; Gan et al. 2015; Liu et al. 2016; Rossetto et al. 2012). Histone modifying enzymes specifically add or remove those epigenetic modifications. Histone methyltransferase (HMT), histone de-methylase (HDM), histone acetyltransferase (HAT), and histone de-acetylase (HDAC) are well-characterized not only in plants, but also in animals (Mathiyalagan et al. 2014; Javaid and Choi 2017).

Histone methylation has important roles in transcriptional regulation. Among histone methylation marks, trimethylation of lysine 27 on histone H3 (H3K27me3) is a well-characterized repressive chromatin mark of genes. H3K27me3 targets on many genes and represses their expression (Lafos et al. 2011). In *Arabidopsis*, more than 15 % of total expressed genes are marked by H3K27me3 (Lafos et al. 2011).

1.6 Polycomb Group proteins deposite H3K27me3 marks

Polycomb Group (PcG) protein complexes play as the writers and readers of H3K27me3 (Wang et al. 2015; Ficz et al. 2005). There are two classes of PcGs, namely polycomb repressive complex 1 (PRC1) and PRC2 (Wu et al. 2013; Kahn et al. 2016). These two complexes has the fundamental roles in repression of gene expression (Grossniklaus and Paro 2014). PRC2 has histone methyltransferase activity and primarily mediates H3K27me3. On the other hand, PRC1 interacts with H3K27me3 and maintains the PRC2-mediated gene repression (Boros et al. 2014). PRC1 also prevents the activated form of RNA polymerase II preinitiation complex to deposit H3K27me marks (Lehmann et al. 2012). Moreover, PRC1 binds to nucleosome which in turn decreases the accessibility of transcription factors to chromatin (Li and Reinberg 2011).

1.7 JMJ proteins remove H3K27me3 marks

The function of JUMONJI C DOMAIN-CONTAINING (JMJ) proteins is to demethylate histone marks (Takeuchi et al. 2006). In *Arabidopsis*, there are 21 JmjC proteins in total. JMJ family proteins are categorized into five different groups; KDM4/JHDM3/JMJD2, KDM5/JARID1, JMJD6, KDM3/JHDM2 and JmjC-domain-only groups (Lu et al. 2008). Among them, four JMJ proteins have been shown to act as demethylases of H3K27me3: EARLY FLOWERING 6 (ELF6)/AtPKD9A, RELATIVE OF EARLY FLOWERING 6

(REF6)/AtPKD9B (also known as JMJ11 and JMJ12, respectively), JMJ30 and JMJ32 (Cui et al. 2016; Lu et al. 2011; Crevillen et al. 2014; Gan et al. 2014).

The JMJ30 protein is necessary to maintain circadian oscillation, possibly by regulating diurnal histone modifications at promoters of core clock genes, including *CIRCADIAN CLOCK ASSOCIATED 1* (*CCA1*) and *LATE ELONGATED HYPOCOTYL* (*LHY*) (Jones et al. 2010). In addition, the JMJ30 and JMJ32 proteins mediate temperature-dependent flowering responses (Gan et al. 2014). JMJ30 and JMJ32 remove the H3K27me3 marks at the *FLOWERING LOCUS C* (*FLC*) promoter and prevents precocious flowering at high ambient temperatures (Fig. 3). Previous study revealed that *JMJ30* shows high induction after ABA treatment during vegetative stage (Qian et al. 2015). Despite its critical importance in H3K27me3 removal, the role of JMJ30 in the regulation of growth during seed germination and seedling establishment stages was unexplored.

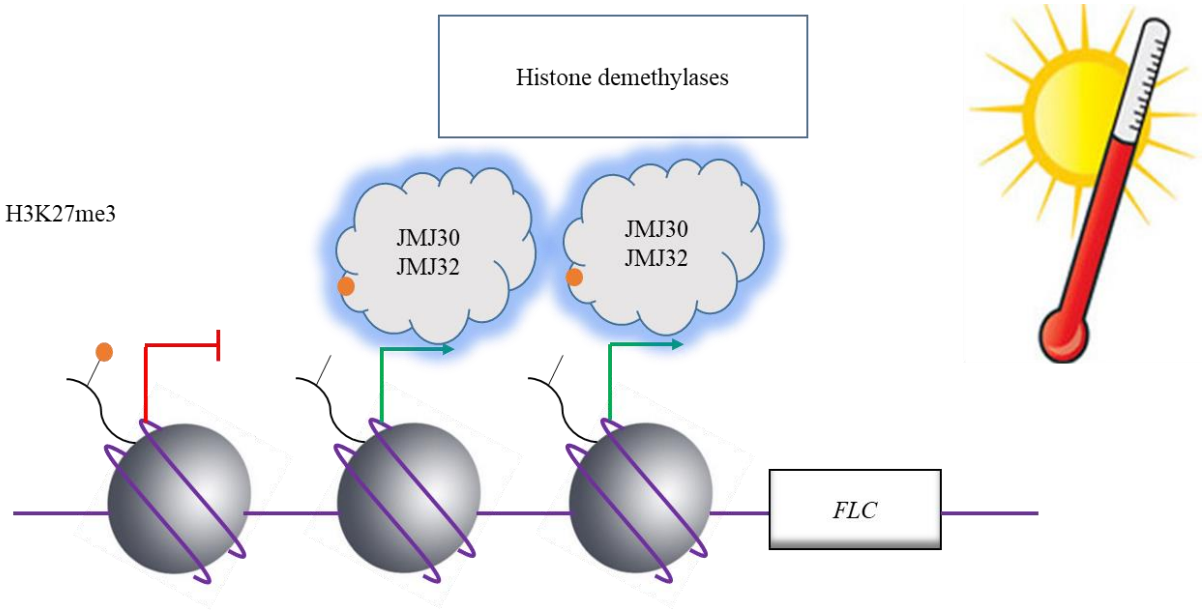

Figure 3 The molecular and biochemical functions of JMJ30 and JMJ32. Under high temperature condition, JMJ30 and JMJ32 directly bind to *FLC* loci and demethylate the repressive histone marks H3K27me3 then allow activation of *FLC*. This mechanism highlights the importance of JMJ30/JMJ32-mediated histone demethylation in preventing early flowering at warm temperatures.

2. Objectives of this study

1. To validate the JMJ induction by ABA during seed germination and seedling establishment

2. To identify the transcription factors mediating JMJ induction in response to ABA

3. To investigate the ABA sensitivity between wild type and *jmj* mutant during seed germination and seedling establishment

4. To identify direct targets of JMJ30 in response to ABA

3. Materials and Methods

3.1 Plant Materials and Growth Conditions

All of the *Arabidopsis thaliana* lines in this study were in the Columbia (Col-0) background. The *jmj30-2, jmj32-1, jmj30-2 jmj32-1*, *pJMJ30::JMJ30-GUS*, *pJMJ30::JMJ30-HA* and *JMJ30 ox* plants (Gan et al. 2014), the *abi3-8* mutants (Nambara et al. 2002) and the *abi5-7* mutants were described previously (Yamagishi et al. 2009), as was the genotyping method for *abi5-7* (Dekkers et al. 2016). Genotyping primers are described in Table 1. All of the plants used in experiments were grown at 22°C under 24-hour light conditions after stratification at 4°C for 3 days.

Table 1 Genotyping primers were used in this study.

Genotyping primers	Sequence
jmj30-2-FW	5'-CAAACTCTGCTGCAATCGATTTC-3'
jmj30-2-RV	5'-GAAAATGTCACAAGCTCTTGCTTC-3'
jmj32-1-FW	5'-GACTGAGAAAACCTGAACTCAGC-3'
jmj32-1-RV	5'-GTCGTGTAAAGGACTGAAGGTTG-3'
abi3-8-FW	5'-GAAGCGATGAAGCAGCTTTT-3'
abi3-8-RV	5'-AGGAACCCATGTTGAAGGTG-3'
abi5-7-FW	5'-CGTCAGAGCGAGAAGTAGAG-3'
abi5-7-RV	5'GCGGGGCGGGGGCACGGGGGGGATTGTTATTATTCTCCTCTGCGAT-3'

3.2 Plasmid Construction and Plant Transformation

To mutagenize the RY-like motif in the *JMJ30* promoter, pCR8-*pJMJ30::JMJ30-GUS* was used for site-directed mutagenesis with the PrimeSTAR Mutagenesis Basal Kit (Takara) (Gan et al. 2014). PCR was conducted using two primers, pJMJ30RYm::JMJ30-FW and pJMJ30RYm::JMJ30-RV. Replacement of the RY-like motif (ATGCAT) with RYm (ATGGTA) in the *JMJ30* promoter was confirmed by sequencing. The resulting pCR8-*pJMJ30RYm::JMJ30-GUS* construct was recombined into the pBGW vector using LR Clonase II (Invitrogen).

To generate an over-expression construct of *SnRK2.8*, the full-length coding sequence was amplified using Arabidopsis vegetative cDNA as template and cloned into the pENTR/D-TOPO vector (Invitrogen) using *SnRK2.8*–cds_FW and *SnRK2.8*–cds_RV. Then, the clone was

recombined into pB2GW7.0 vector using LR Clonase II for plant transformation (Invitrogen). All primer sequences are listed in Table 2. Transgenic lines were generated by floral dipping with *Agrobacterium tumefaciens* (GV3101) (Clough and Bent 1998). At least 30 transgenic plants were identified for each line and a representative line was used for further characterization.

Table 2 Gene cloning primers were used in this study.

Gene cloning primers	Sequence
gJMJ30-GUS-P1	5'-TAATCATCACTATTTACGACTTAAACC-3'
gJMJ30-GUS-P2	5'-AATCTACATATAAATTTTTGCAGCCA-3'
gJMJ30-GUS-P3	5'-TGAGATTTCATTTGTTAATTGAGCAT-3'
gJMJ30-GUS-P4	5'-ACCACAACAACCTCCGTCTC-3'
gJMJ30-GUS-P5	5'-TGTTGAAACTTGCAGGTCCTT-3'
gJMJ30-GUS-P6	5'-GTTTAAAATGCTATTCAGGTGGG-3'
gJMJ30-GUS-P7	5'-CAAAGAAATCGTTTGGCCTG-3'
gJMJ30-GUS-P8	5'-GAATTGATCAGCGTTGGTGG-3'
gJMJ30-GUS-P9	5'-GGGACTTTGCAAGTGGTGAA-3'
gJMJ30-GUS-P10	5'-AAGCAACGCGTAAACTCGAC-3'
gJMJ30-GUS-P11	5'-TCAGGTTCTAAGTTCACGTTGTG-3'
gJMJ30-GUS-P12	5'-CTCTACTAGCATTAAACTTTGGACA-3'
gJMJ30-GUS-P13	5'-CGTAAGTATGATCTATCCTTTCATCC-3'
pJMJ30RYm::JMJ30-FW	5'-TATTCATAAATTATAATATGTAGTGATGGTAATGGTAAACAAATAAACAAAAAGTA-3'
pJMJ30RYm::JMJ30-RV	5'-TACTTTTTGTTTATTTGTTTACCATTACCATCACTACATATTATAATTTATGAATA-3'
35S::SnRK2.8-FW	5'-CACCATGGAGAGGTACGAAATAGT-3'
35S:: SnRK2.8-RV	5'-TCACAAAGGGGAAAGGAGAT-3'

3.3 Phenotypic and Statistical Analyses

To make Murashige-Skoog (MS) plates, half-strength MS salt solution with minimal organics adjusted to pH 5.6 by KOH was mixed with 0.8% agar and autoclaved. Either 0.25 μM, 0.5 μM (final concentration) of ABA (Sigma-Aldrich) was added to the medium just before the medium was poured into plastic petri plates. For seed surface sterilization, mature seeds were sterilized with bleach (6% sodium hypochlorite) for 1 minute and then washed three times with sterilized water. For the seedling establishment assay, the sterilized wild-type, *jmj30-2, jmj32-1* and *jmj30-2 jmj32-1* seeds were placed on the ABA-containing plates, stratified at 4°C for 3 days and then placed in a growth chamber at 22°C under continuous light. The ratios of seedlings with green cotyledons over germinated seeds—defined morphologically as all those showing visible radicles—were determined at 5.5 days after incubation (Boyes et al. 2001; Weitbrecht et al. 2011; Silva et al. 2016). Statistical significance was computed using the Student's *t*-test and Chi-Squared test for seed germination and seedling establishment rate, respectively. To measure fresh weight, 81 wild-type, *jmj30-2*, *jmj32-1*, and *jmj30-2 jmj32-1* seeds were sown on plates and stratified at 4°C for 3 days. Three plates were prepared for each genotype. The resulting plants were grown for 5.5 days at 22°C under continuous light. All 81 seedlings were harvested and then measured with an analytical balance (Mettler Toledo XS104). Statistical significance was calculated using a Student's *t*-test for fresh weight.

3.4 GUS Staining

GUS staining was performed as previously described with modification (Sun et al. 2014). Tissues were fixed in 90% ice-cold acetone for 15 minutes and then rinsed with sterilized water and GUS staining solution without X-gluc (50 mM $NaPO_4$, 0.5 mM $K_3Fe(CN)_6$, 0.5 mM $K_4Fe(CN)_6$, pH 7.2). *JMJ30-GUS* and *JMJ32-GUS* lines were stained with a solution containing 1 mM X-gluc containing solution for 2 hours and a solution containing 2 mM X-gluc solution overnight, respectively. The resulting stained tissues were placed in 70% ethanol for a week or more to remove chlorophyll. An Axio Scope A1 microscope (ZEISS) was used to observe the tissues. GUS signal was categorized into two different groups and statistical significance was determined using a Chi-Squared test.

3.5 Transmission Electron Micrography (TEM)

For TEM, tissues grown on plates were harvested when approximately half of wild-type plants were at a stage just after germination but before greening for each treatment. Tissues were fixed in 2% paraformaldehyde and 1.25% glutaraldehyde in 0.05 M PB buffer for five hours at 4°C, washed five times with 0.05 M PB buffer for 10 minutes at 4°C, and fixed with OsO_4 buffer at 4°C overnight. The resulting tissues were washed with 8% sucrose in water for 2 hours at 4°C, dehydrated with an ethanol series, and infiltrated with Eponate 812 resin by incubating the samples at room temperature for several hours to overnight in increasing

concentrations of resin. Then, the resin was polymerized in an oven at 60°C for 48 hours. Resin-embedded samples were sectioned to 70 nm widths with a diamond knife on an ultramicrotome. Sections were collected on a 0.5% formvar-coated slot grid. Grids were post-stained for 5 min with 2% aqueous uranyl acetate and for 10 min with Reynolds lead citrate (Yamaguchi et al. 2018). Cortex cell images were taken using a H-7100 TEM (Hitachi).

3.6 RT-qPCR and RNA-seq

Total RNA was extracted using an RNeasy plant mini kit (Qiagen) for both RT-qPCR and RNA-seq. DNA was digested in column using an RNase-free DNase set (Qiagen) prior to cDNA synthesis. For RT-qPCR, cDNA was synthesized from 2.5 μg RNA in a 50 μL reaction volume using PrimeScript RT Master Mix (Takara). RT-qPCR with gene-specific primers was performed using a Light Cycler 480 (Roche) using FastStart DNA Essential DNA Green Master mix (Roche). *EIF4A1* (*AT3G13920*) was used as an internal control. Three independent biological replicates were performed for RT-qPCR analyses and four technical replicates were conducted for each experiment. RT-qPCR primers are described in Table 3. For RNA-seq, ABA-treated wild-type and *jmj30-2 jmj32-1* seedlings were harvested. RNA-seq was performed as previously described (Uemura et al. 2018). For ABA treatment, 1.5-day-old wild-type seedlings on 1/2 MS plates were sprayed with 100 μM ABA to produce rapid changes of gene expression. Seedlings were harvested 5 hours after treatment. Libraries for RNA-seq were

prepared by the Breath Adapter Directional sequencing method. The libraries were sequenced by Next-Seq 500 (Illumina). Mapping to the Arabidopsis reference (TAIR10) was conducted using Bowtie with the following options "--all --best --strata --trim5 8". The number of reads mapped to each reference was counted. After normalization, FDR and FC were calculated using the edgeR package for R. Differentially expressed genes were identified ($p < 0.05$). Among 85 differentially expressed genes, *JMJ30* was manually removed. Thus, the total number of differentially expressed genes was 84. The data were deposited into the DNA Data Bank of Japan (DRA007070).

Table 3 RT-qPCR primers were used in this study.

RT-PCR primers	Sequence
EIF4A1-FW	5'-TCTTGGTGAAGCGTGATGAG-3'
EIF4A1-RV	5'-AATCAACCTTACGCCTGGTG-3'
JMJ30-FW	5'-GAATCACTTGGACTACCTCAATGC-3'
JMJ30-RV	5'-CATTGGAGACGATTTATTGGTCC-3'
JMJ32-FW	5'-GTTTCATTGTACTGTCAAGGCTGG-3'
JMJ32-RV	5'-CATACTTGATGTCAAACTGCATGTC-3'
ABI5-FW	5'-ACCTAATCCAAACCCGAACC-3'
ABI5-RV	5'-TACCCTCCTCCTCCTGTCCT-3'
AT1G62660-FW	5'-TGGACACAAGGACGCATAAA-3'
AT1G62660-RV	5'-GTCTAGCTGAGTGGCGGAAC-3'
SnRK2.8-FW	5'-GTTGCCAACCCTGAAAAGAG-3'
SnRK2.8-RV	5'-CCGAGCTTCTTCAATGATCC-3'
AT2G43530-FW	5'-GACAGAGAAGATGGGCATGG-3'
AT2G43530-RV	5'-GCTTAAAGGCGCATCAATGT-3'
ARR9-FW	5'-GCATCAAATCCCGGAGATAG-3'
ARR9-RV	5'-GCCATACCCATTGCAGAAAC-3'
AT4G23670-FW	5'-CCAAAATGTCGTTGTTCACG-3'
AT4G23670-RV	5'-CATCACGTGACCATCCAGTC-3'
ARI1-FW	5'-CACCGGAATATCCCTCCTTT-3'
ARI1-RV	5'-TCTTCCTCCGCGCTAAAATA-3'
RAD4-FW	5'-AGGTGGTTCTTCTTGCATGG-3'
RAD4-RV	5'-CTGTTCCAGGTGGGAGACAT-3'
AHG1-FW	5'-ATTGTGCAGCACGACTATGC-3'
AHG1-RV	5'-GTTGCCATCTCATCCATCCT-3'

3.7 Chromatin Immunoprecipitation (ChIP)

ChIP was performed as previously described with minor modifications (Yamaguchi et al. 2014). Briefly, 1 g of tissue from 1.5-day-old whole seedlings that had received the ABA spray treatment was used for chromatin-protein extraction. The extracted chromatin was immunoprecipitated using 5 μL/sample of the anti-H3K27me3 antibody ab6002 (Abcam) or 10 μL/sample of the anti-HA antibody 12CA5 (Roche). After reverse crosslinking and DNA purification using a QIAquick PCR Purification Kit (Qiagen), the amount of DNA was quantified with a Light Cycler 480 (Roche) using FastStart DNA Essential DNA Green Master mix (Roche). *ACT7* (*AT5G09810*) was used as an internal control. For the H3K27me3 ChIP, the relative enrichment was calculated after normalization of the input DNA. Similarly, the HA binding ChIP, the genetic control ChIP without transgenes was set to 1.0 and the relative enrichment was calculated. Three independent experiments were conducted for the ChIP assay. ChIP primers are described in Table 4.

Table 4 ChIP primers were used in this study.

ChIP primers	Sequence
ACT7-FW	5’-CGAGAGCAGTGTTCCCAAGT-3’
ACT7-RV	5’-TGGACTGAGCTTCATCACCA-3’
SnRK2.8-P1-FW	5’-GGAGACAGCTCAGAGGGACA-3’
SnRK2.8-P1-RV	5’-CCGTTTGAGCAATCACAAAA-3’
SnRK2.8-P2-FW	5’-CGACAGTCGACGACAAATAAG-3’
SnRK2.8-P2-RV	5’-CTTCCGTCTCGATGTGATCT-3’
SnRK2.8-P3-FW	5’-GCAGCGATAGCTCCTCTCAC-3’
SnRK2.8-P3-RV	5’-AAGGTGGATCGCACATTTTC-3’
SnRK2.8-P4-FW	5’-CATGAACCATAGGTCGCTGA-3’
SnRK2.8-P4-RV	5’-GGCGGCGTATTCCATTACTA-3’
SnRK2.8-P5-FW	5’-TGGTCCATCGACTCAGACAG-3’
SnRK2.8-P5-RV	5’-CACCATTACTGCTTCCACCA-3’
SnRK2.8-P6-FW	5’-TGCTCAACTTGTTCCCATGA-3’
SnRK2.8-P6-RV	5’-TGTGATTGTTGGTTTCAGGTG-3’
AT1G62660-P1-FW	5’-TGTCGTCTGCAAACGTGATT-3’
AT1G62660-P1-RV	5’-TTGGGTTGGCAAATTAGAGC-3’
AT1G62660-P2-FW	5’-ACGGAGTCACGTCCTCGTAT-3’
AT1G62660-P2-RV	5’-CTCAGGCTGGAAATGAAACG-3’
AT1G62660-P3-FW	5’-ACGTGAGTCATGTGCATATTGT-3’
AT1G62660-P3-RV	5’-GTCAAATGGGGACTGTCCAA-3’
AT1G62660-P4-FW	5’-ACCATCGGTTCCAAAATCAA-3’
AT1G62660-P4-RV	5’-CGGGTAAAAATCAACGCACT-3’
AT1G62660-P5-FW	5’-TTCGAGATCAAGACCGATGA-3’
AT1G62660-P5-RV	5’-GTCAGCGAGAACCGAGAATC-3’
AT1G62660-P6-FW	5’-ATTGCGTGATGCATGATGTT-3’
AT1G62660-P6-RV	5’-ACGGCTTTGTGTACGAAGGT-3’
AT4G23670-P1-FW	5’-GGGCCCATACAATTGGTCTT-3’
AT4G23670-P1-RV	5’-GGGTTTGTTTATCTGCTTCCA-3’
AT4G23670-P2-FW	5’-ACGCACATAGGCCGTAAAAG-3’
AT4G23670-P2-RV	5’-ACGAAGGCGAACATGACTCT-3’
AT4G23670-P3-FW	5’-GCTAGTGGGATGTTGGAAATTG-3’
AT4G23670-P3-RV	5’-CATCACGTGACCATCCAGTC-3’
AT4G23670-P4-FW	5’-AACTCCACAAGACCCCCTTT-3’
AT4G23670-P4-RV	5’-TCGTCAAGCAAATGGTTGTT-3’
AT4G23670-P5-FW	5’-TGTGCATATGGAGTCAGTTGC-3’
AT4G23670-P5-RV	5’-CCATCACAACGATCGAAATC-3’

4. Results

4.1 *JMJ30* expression is induced by ABA during post-germination

Abscisic acid (ABA) promotes seed dormancy and prevents germination (Bentsink and Koornneef 2008; Bewley 1997). In my growth conditions, almost 100% of seeds germinated 24 hours after the end of stratification (4°C, 3 days). To confirm the ABA-induced response of *JMJ30* and one of its close homologs, *JMJ32*, during germination, I first conducted reverse transcription quantitative PCR (RT-qPCR) to compare gene expression in seeds sprayed with ABA to that in mock-treated controls. I sprayed the seeds with ABA at 24 hours after the end of stratification. At 0, 3, and 5 hours after treatment, induction of *JMJ30* or *JMJ32* expression was not observed when I used samples at the germination stage ($p > 0.05$ by two-tailed Student's *t*-test) (Fig. 4).

During the post-germination stage (2–3 days after germination), ABA triggers growth arrest in germinated embryos that encounter water stress. I sprayed ABA onto 1.5-day-old plants (36-hours-old) after stratification. Within 3 hours after treatment, I detected a statistically significant increase in *JMJ30* mRNA accumulation in ABA-treated wild-type (WT) plants compared to the mock-treated sample during the post-germination stage ($p < 0.05$ two-tailed Student's *t*-test) (Fig. 5A). The *JMJ30* expression levels remained high for 5 hours after ABA treatment (5 hr: $p < 0.05$ by two-tailed Student's *t*-test). On the other hand, *JMJ32* expression was not affected by ABA (3 hr: $p > 0.05$, 5 hr: $p > 0.05$ two-tailed Student's *t*-test) (Fig. 5B).

The *ABI5* was used as a positive control ($p < 0.05$ by two-tailed Student's *t*-test) (Fig. 5C). These results suggest that *JMJ30* is specifically induced by ABA during the post-germination stage but not the germination stage.

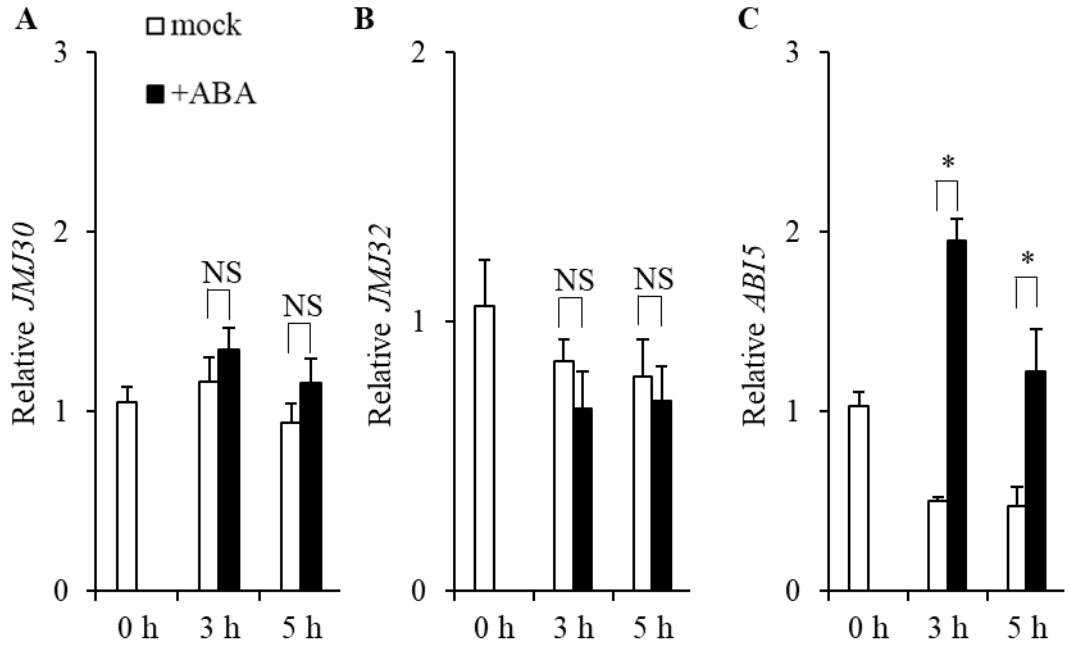

Figure 4. *JMJ30* and *JMJ32* expression after ABA treatment during germination.

Expression of *JMJ30* (A), *JMJ32* (B), and *ABI5* (C) in wild-type seedlings in response to ABA during germination. The WT with 0 hour mock treatment was set to 1.0 and the relative expression was calculated. Results are from three independent experiments. Values represent mean ± SEM. Asterisks indicate significant differences between mock- and ABA-treated plants based on two-tailed Student's *t*-test, $p < 0.05$.

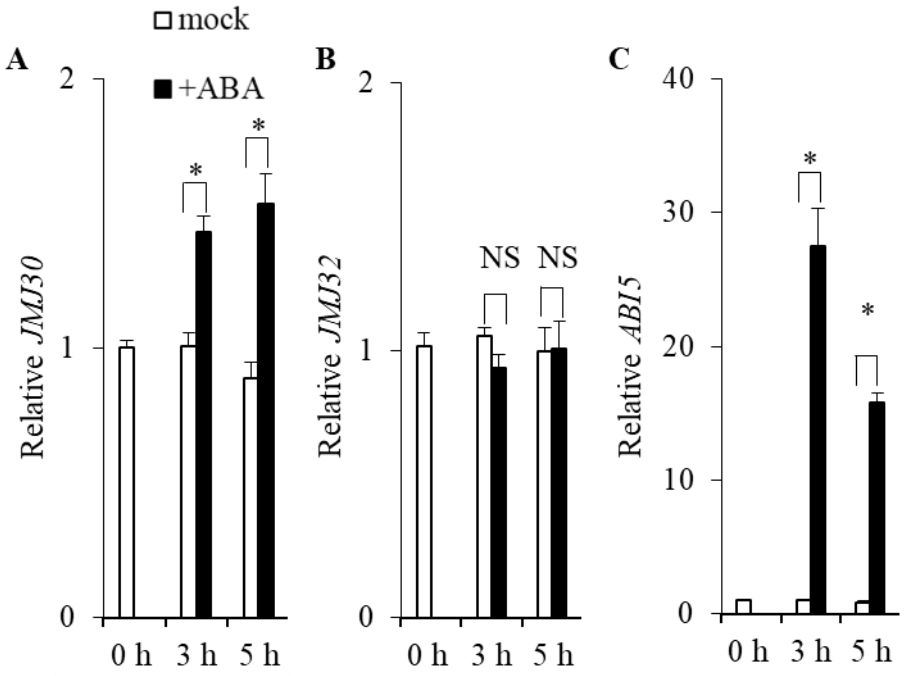

Figure 5. *JMJ30* and *JMJ32* expression after ABA treatment during post-germination.

Expression of *JMJ30* (A), *JMJ32* (B), and *ABI5* (C) in wild-type seedlings in response to ABA during post-germination.The WT with 0 hour mock treatment was set to 1.0 and the relative expression was calculated. Results are from three independent experiments. Values represent mean ± SEM. Asterisks indicate significant differences between mock- and ABA-treated plants based on two-tailed Student's *t*-test, $p < 0.05$.

To investigate the spatial distribution of JMJ30 in seedlings with and without ABA treatment during post-germination, I next examined *pJMJ30::JMJ30-GUS* accumulation. In the absence of ABA, JMJ30-GUS was expressed in the root meristem and root differentiation area (Fig. 6A). Upon ABA treatment, JMJ30-GUS levels became higher than in the mock-treated control, but its pattern of expression was largely unchanged (Fig. 6). As a control, I also made a reporter line for JMJ32, a protein with high sequence similarity to JMJ30. In good agreement with the RT-qPCR result, JMJ32-GUS accumulation in root meristem was not altered by ABA treatment (Fig. 5, Fig. 7). Taken together, my results suggest that ABA induces *JMJ30* expression during post-germination.

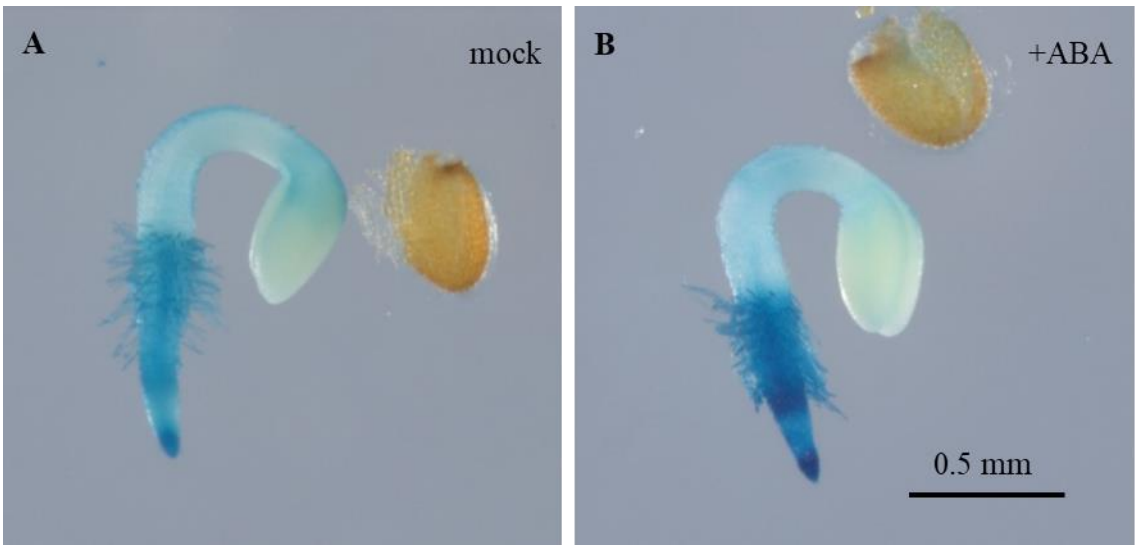

Figure 6. *pJMJ30::JMJ30-GUS* expression in response to ABA.

pJMJ30::JMJ30-GUS expression in wild-type background 5 hours after mock (A) or ABA (B) treatment. Scale bar = 0.5 mm.

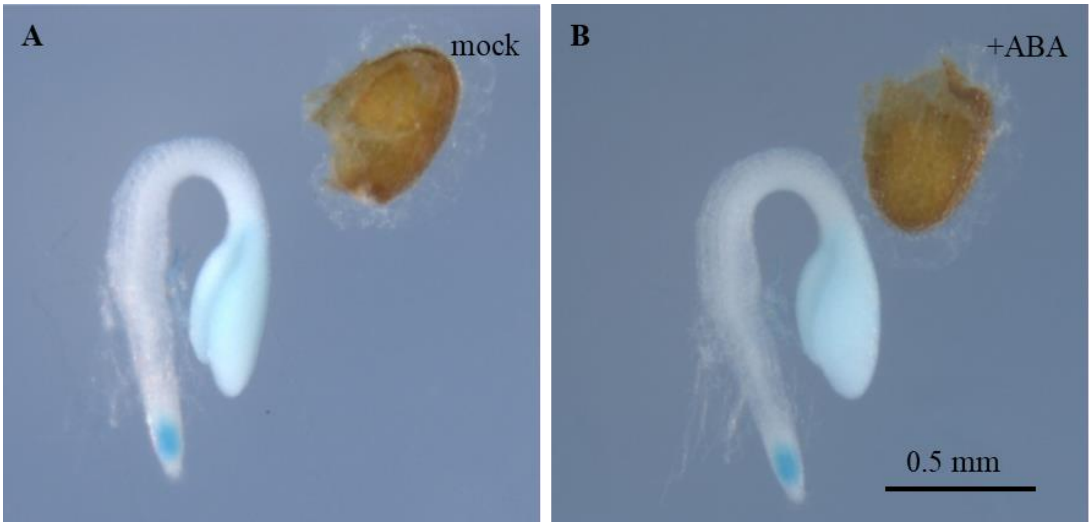

Figure 7. *pJMJ32::JMJ32-GUS* expression in response to ABA.

pJMJ32::JMJ32-GUS expression 5 hours after mock (A) or ABA (B) treatment. Scale bar = 0.5 mm.

4.2 ABI3 activates JMJ30 expression in response to ABA during post-germination

I next investigated whether *JMJ30* upregulation in response to ABA is mediated by ABIs. Transcription factors belonging to two different classes, the B3 domain transcription factor ABI3 and the bZIP transcription factor ABI5, play key roles during post-germination (Finkelstein et al. 2002; Arroyo et al. 2003). Therefore, I tested the effects of mutations causing loss of function of those two proteins on *JMJ30* expression. In the *abi3-8* background, I did not observe *JMJ30* upregulation in response to ABA in RT-qPCR experiments at two different time points (mock 3 h vs. ABA 3 h in WT: $p = 5.3 \times 10^{-5}$; mock 5 h vs. ABA 5 h in WT: $p = 1.0 \times 10^{-5}$) (mock 3 h vs. ABA 3 h in *abi3-8* and mock 5 h vs. ABA 5 h in *abi3-8*: $p > 0.05$) (Fig. 8). In the *abi5-7* background, however, *JMJ30* was induced in response to ABA, as it was in the wild type (Fig. 9). To confirm that *JMJ30* upregulation in response to ABA is dependent on ABI3, I probed the expression of *pJMJ30::JMJ30-GUS* in the *abi3-8* mutant (Fig. 10). In the wild type, JMJ30-GUS accumulation was enhanced by ABA treatment (mock vs. ABA in WT: $p = 1.4 \times 10^{-5}$) (Fig. 10A-B). But the increase in JMJ30-GUS accumulation in response to ABA was alleviated in the *abi3-8* mutant, as expected (mock vs. ABA in *abi3-8*: $p > 0.05$) (Fig. 10C-D).

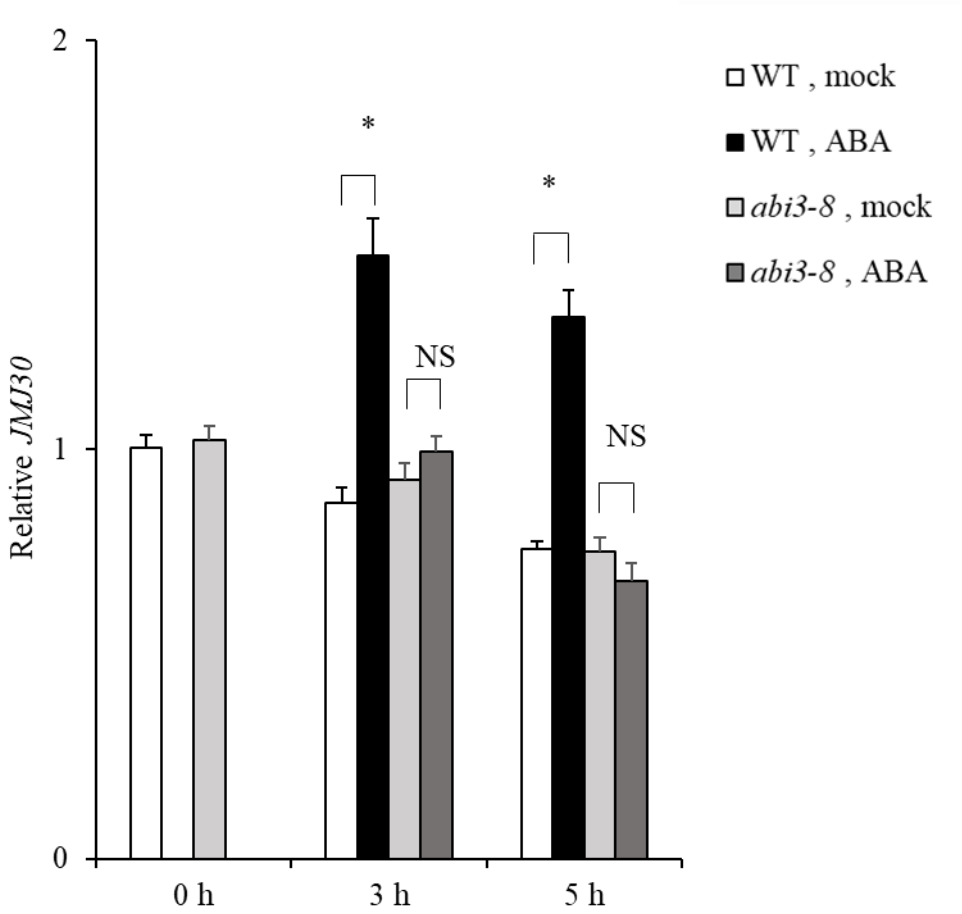

Figure 8. *JMJ30* expression in *abi3* with and without ABA treatment.

Expression of *JMJ30* in wild type and *abi3-8* in response to ABA. The WT with 0 hour mock treatment was set to 1.0 and the relative expressions were calculated. Results are from three independent experiments. Values represent mean ± SEM. Asterisks indicate significant differences between mock- and ABA-treated plants based on two-tailed Student's *t*-test.

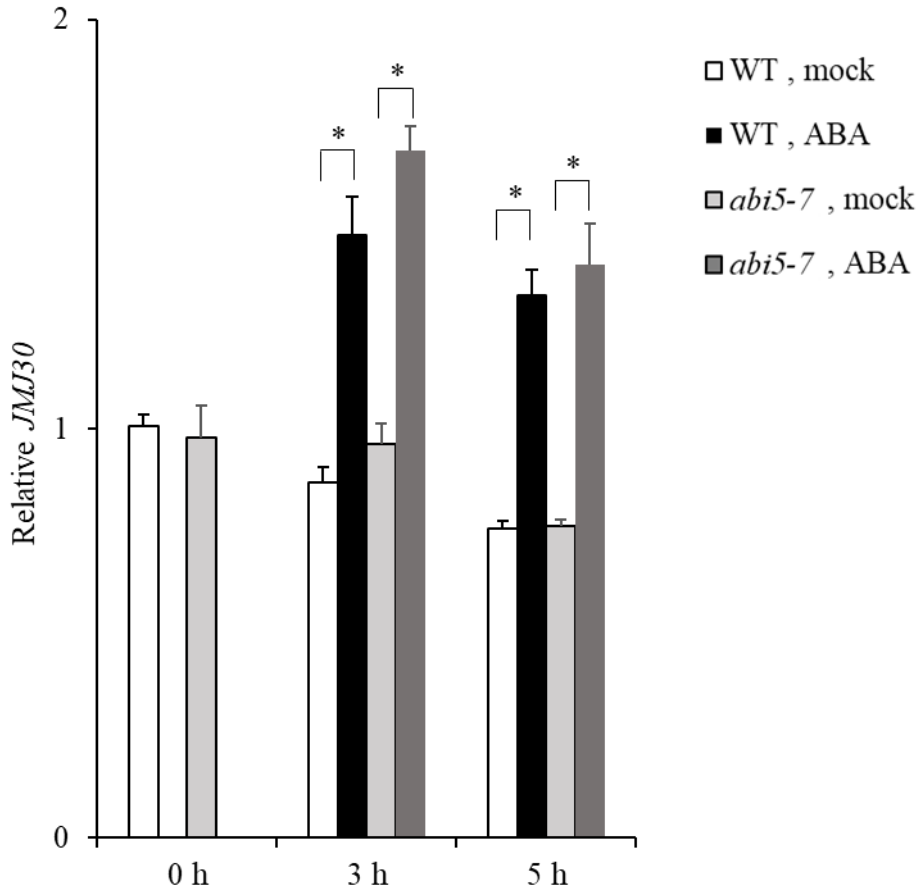

Figure 9. *JMJ30* expression in *abi5* with and without ABA treatment.

Expression of *JMJ30* in *abi5-7* in response to ABA. The WT with 0 hour mock treatment was set to 1.0 and the relative expressions were calculated. Results are from three independent experiments. For wild-type data, the same bars are shown in Figure 8. Values represent mean ± SEM. Asterisks indicate significant differences based on two-tailed Student's *t*-test.

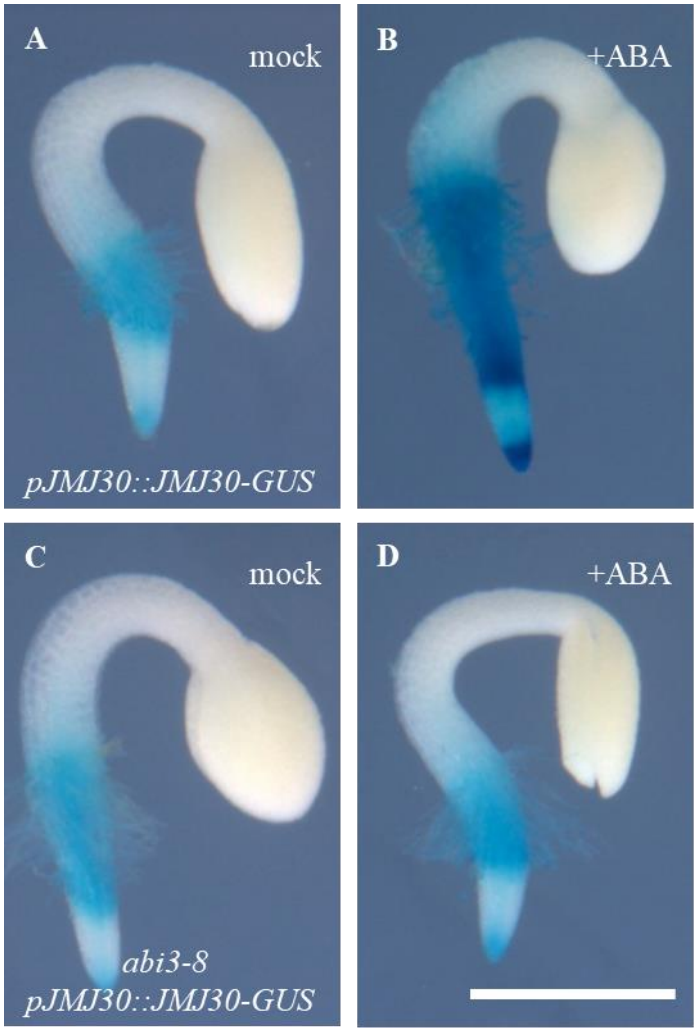

Figure 10. *pJMJ30::JMJ30-GUS* expression in *abi3* in response to ABA.

Expression of *JMJ30* in wild type and *abi3-8* in response to ABA. Results are from three independent experiments. Values represent mean ± SEM. Asterisks indicate significant differences between mock- and ABA-treated plants based on two-tailed Student's *t*-test. (B-F) *pJMJ30::JMJ30-GUS* expression 5 hours after mock (B, D) or ABA (C, E) treatment in wild-type (B, C) and *abi3-8* (D, E) seedlings. Scale bar = 0.5 mm.

To further examine the role of *ABI3* in *JMJ30* upregulation in response to ABA, I compared *JMJ30* promoter sequences between 9 *Brassica* species (Waese et al. 2016). Consistent with the earlier finding that ABI3 recognizes the conserved RY motif (Suzuki et al. 1997; Sakata et al. 2010), I found a potential RY motif at the distal region of the *JMJ30* promoter. The motif and short flanking sequences are highly conserved between species (Fig. 11). To confirm the biological function of this conserved RY motif, I examined JMJ30-GUS reporter expression under the control of the endogenous *JMJ30* gene with a mutated promoter (Fig. 11). When I replaced the sequence CAT in the RY motif (ATGCAT) of the *JMJ30* promoter with GTA, ABA-induced *JMJ30* expression was compromised (mock vs. ABA in the *pJMJ30m* promoter lines: $p > 0.05$) (Fig. 12-13). These results suggest that ABA-dependent *JMJ30* expression is controlled by ABI3 through the conserved RY motif.

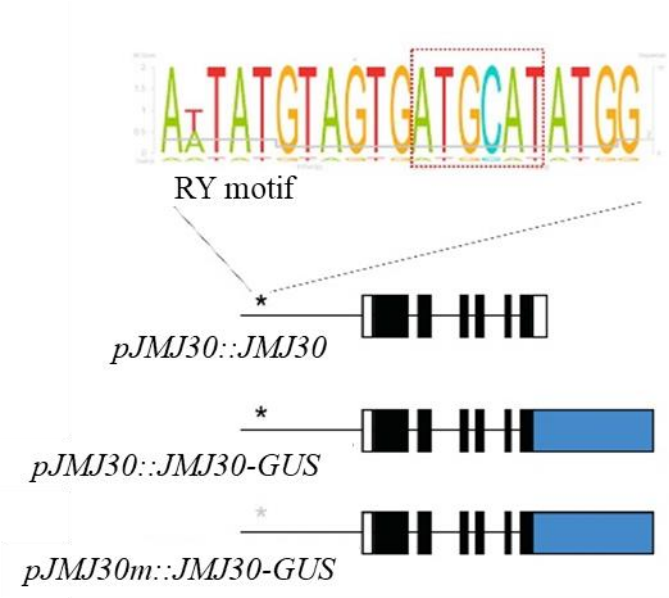

Figure 11. Schematic structure of the *pJMJ30::JMJ30-GUS* and *pJMJ30m::JMJ30-GUS*.

Above, schematic structure of the *JMJ30* gene structure and RY-like motif. Below, RY-like motif evolutionarily conserved between nine *Brassica* species identified by the Gene Slider.

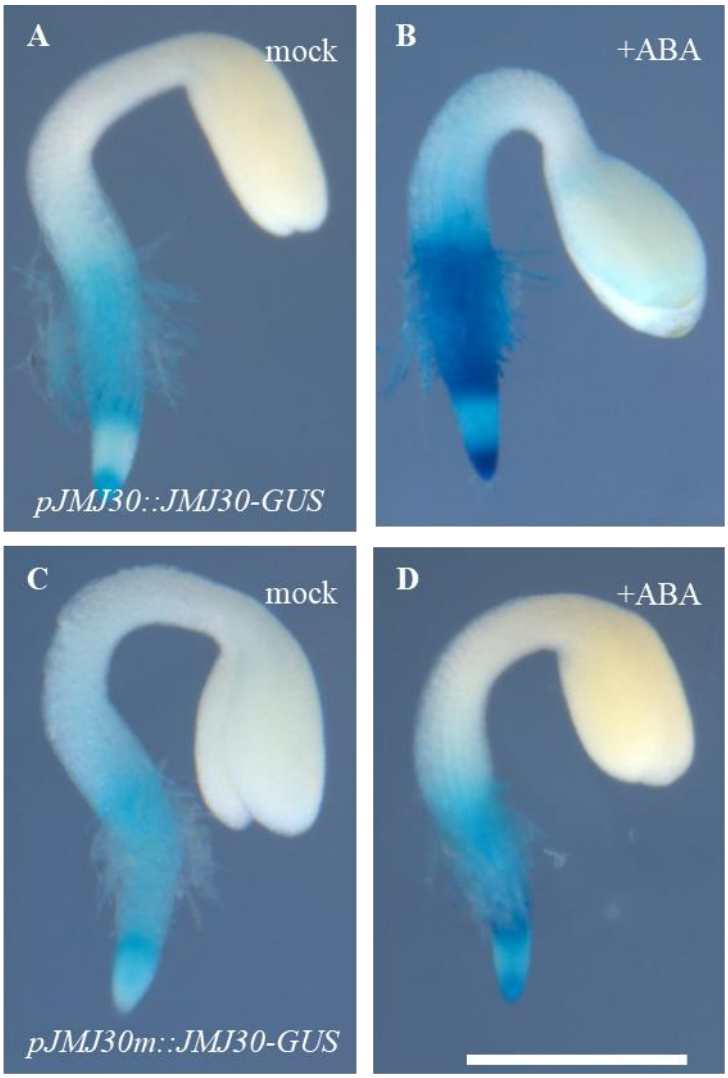

Figure 12. *pJMJ30::JMJ30-GUS* and *pJMJ30m::JMJ30-GUS* expression in response to ABA.

JMJ30-GUS expression 5 hours after mock (A, C) or ABA (B, D) treatment under the control of the *JMJ30* promoter (A, B) and a mutated version of the *JMJ30* promoter (C, D). Scale bar = 0.5 mm.

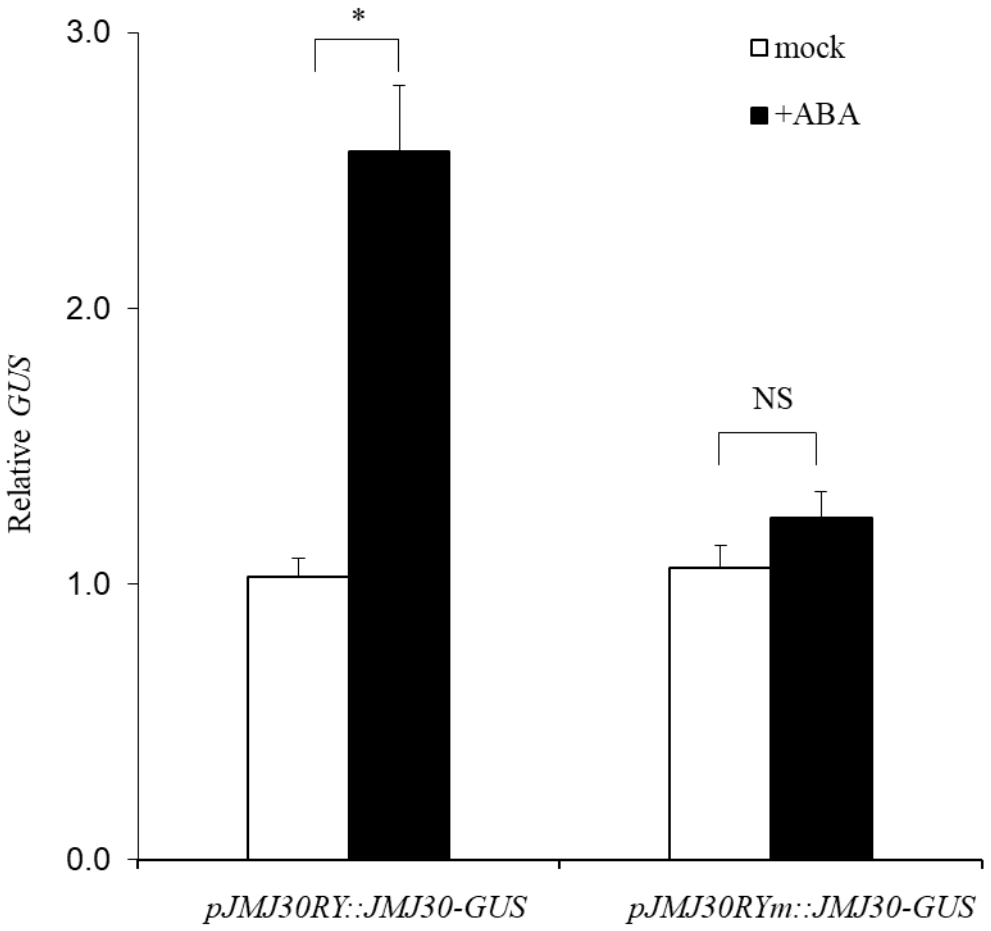

Figure 13. GUS expression after ABA treatment during post-germination.

Expression of *GUS* in *pJMJ30::JMJ30-GUS* and *pJMJ30m::JMJ30-GUS* seedlings in response to ABA during post-germination.The *pJMJ30::JMJ30-GUS* with 0 hour mock treatment was set to 1.0 and the relative expressions were calculated. Results are from three independent experiments. Values represent mean ± SEM. Asterisks indicate significant differences between mock- and ABA-treated plants based on two-tailed Student's *t*-test, $p < 0.05$.

4.3 JMJ30 and JMJ32 are redundantly required for ABA-dependent growth arrest during post-germination

In order to understand the role of JMJ30 in ABA responses during post-germination, I performed phenotypic analysis using mutants of *JMJ30* and *JMJ32* (Fig. 14-20). I used the previously published knockout alleles *jmj30-1*, *jmj30-2*, and *jmj32-1* (Gan et al. 2014) (Fig. 17). In the absence of ABA, almost all seedlings developed normally to form green cotyledons, a pair of true leaves, and copious root hairs not only in the wild type, but also in the *jmj30-1*, *jmj30-2*, and *jmj32-1* single mutants and *jmj30-2 jmj32-1* double mutants (mock: $p > 0.05$ by one-way ANOVA test) (Fig. 14A-D, Fig. 15-16, Fig. 18-20). In the presence of 0.25 μM ABA, approximately 60% of germinated wild-type plants failed to develop green cotyledons and the first pair of true leaves and were arrested just after germination (Fig. 14E-H, Fig. 15-16). Both single mutants showed similar responses, with no significant differences from the wild type. However, the percentage of arrested plants was significantly lower in *jmj30-2 jmj32-1* double mutants (seedling establishment at 0.25 μM ABA: $p < 0.05$ by one-way ANOVA test; fresh weight at 0.25 μM ABA: $p < 0.05$ by one-way ANOVA test) (seedling establishment in *jmj30 jmj32* + 0.25 μM ABA vs. the other samples: $p < 0.05$; fresh weight in *jmj30 jmj32* + 0.25 μM ABA vs. the other samples: $p < 0.05$ by post-hoc Tukey's HSD) (Fig. 14E-H, Fig. 15-16). The 0.5 μM ABA treatment also led to a reduced number of arrested plants in the *jmj30-2 jmj32-1* double mutant compared to the wild-type or parental single-mutant lines (Fig. 14I-L, Fig. 15-

16) (seedling establishment at 0.5 μM ABA: $p < 0.05$ by one-way ANOVA test) (seedling establishment in *jmj30 jmj32* + 0.5 μM ABA vs. the other samples: $p < 0.05$ by post-hoc Tukey's HSD). Correlating well with the rate of seedling establishment, the fresh weight in bulk after ABA treatment was greater in the *jmj30-2 jmj32-1* mutant than in wild-type seedlings (fresh weight at 0.5 μM ABA: $p < 0.05$ by one-way ANOVA test) (fresh weight in *jmj30 jmj32* + 0.5 μM ABA vs. the other samples: $p < 0.05$ by post-hoc Tukey's HSD).

Furthermore, overexpression of *JMJ30* led to an increased number of arrested plants in response to ABA (Fig. 18-20). The lack of a growth-arrest phenotype in the single mutants could be due to functional redundancy resulting from the fact that the highly similar *JMJ32* was expressed at a basal level in the *jmj30* mutants regardless of ABA treatment ($p > 0.05$ by one-way ANOVA test) (Fig. 21B). On the other hand, *JMJ30* was induced by ABA in the *jmj32* mutant background, just as in the wild type ($p < 0.05$ by one-way ANOVA test) (Fig. 21A). These data imply that both JMJ30 and JMJ32 contribute to ABA-dependent growth arrest during the post-germination stage.

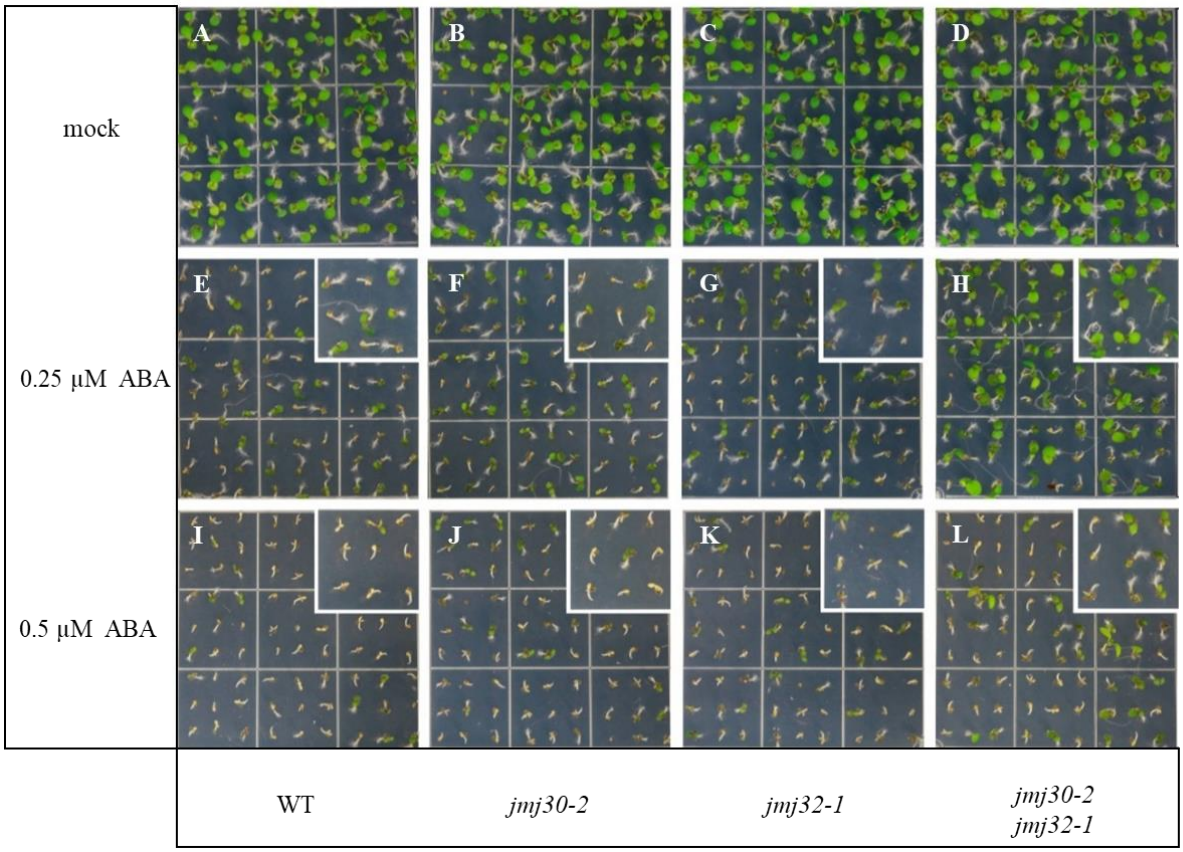

Figure 14. *jmj30 jmj32* mutants are less sensitive to ABA during post-germination.

(A-L) Representative images of wild type (A, E, I), *jmj30-2* (B, F, J) and *jmj32-1* (C, G, K) mutants, and *jmj30-2 jmj32-1* double mutants (D, H, L) grown for 5.5 days on 1/2 MS medium containing 0 µM (A-D), 0.25 µM (E-H), and 0.5 µM ABA (I-L). Insets in E-L show close-ups of representative seedlings.

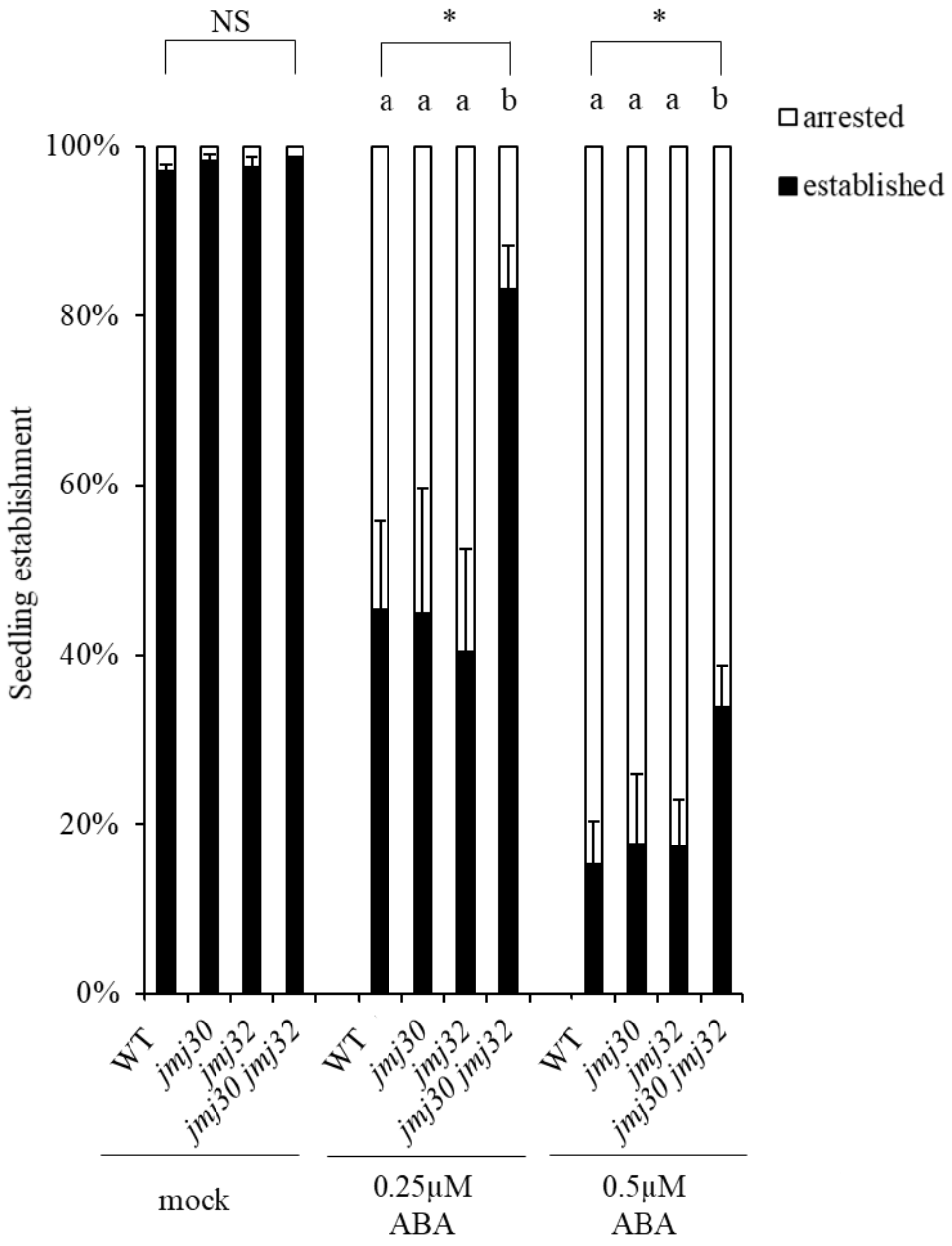

Figure 15. *jmj30 jmj32* mutants are less sensitive to ABA during post-germination.

Percentages of established and arrested seedlings in wild type, *jmj30-2*, *jmj32-1*, and *jmj30-2 jmj32-1* in the absence and presence of ABA. *p*-values were determined by Chi-Squared test.

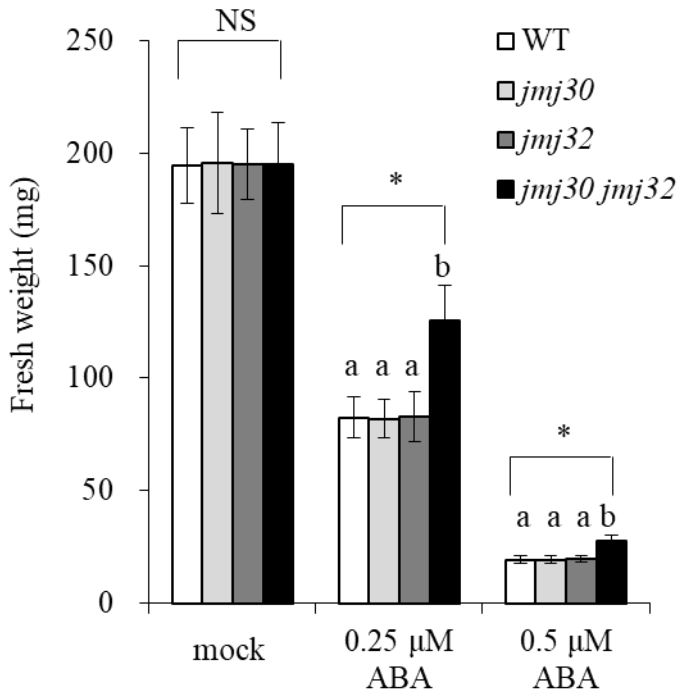

Figure 16. *jmj30 jmj32* mutants are less sensitive to ABA during post-germination.

Measurement of fresh weight in wild type, *jmj30-2*, *jmj32-1*, and *jmj30-2 jmj32-1* in the absence and presence of ABA. A two-tailed Student's *t*-test was performed to obtain *p*-values.

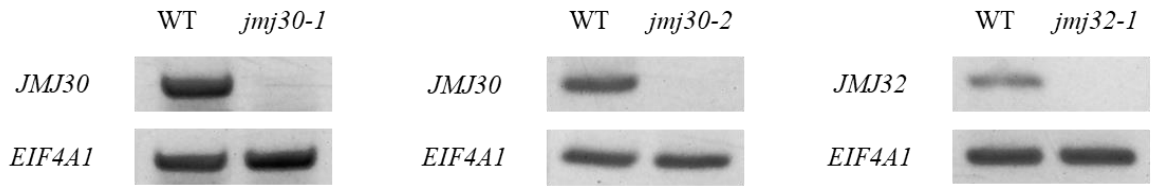

Figure 17. Confirmation of *JMJ30* and *JMJ32* expression in each mutant based on RT-PCR.

(a-c) Expression of *JMJ30* (above) and *EIF4A1* (below) in wild-type and *jmj30-1* (a), wild-type and *jmj30-2* (b), and wild-type and *jmj32-1* (c) seedlings. *EIF4A1* was used for a loading control.

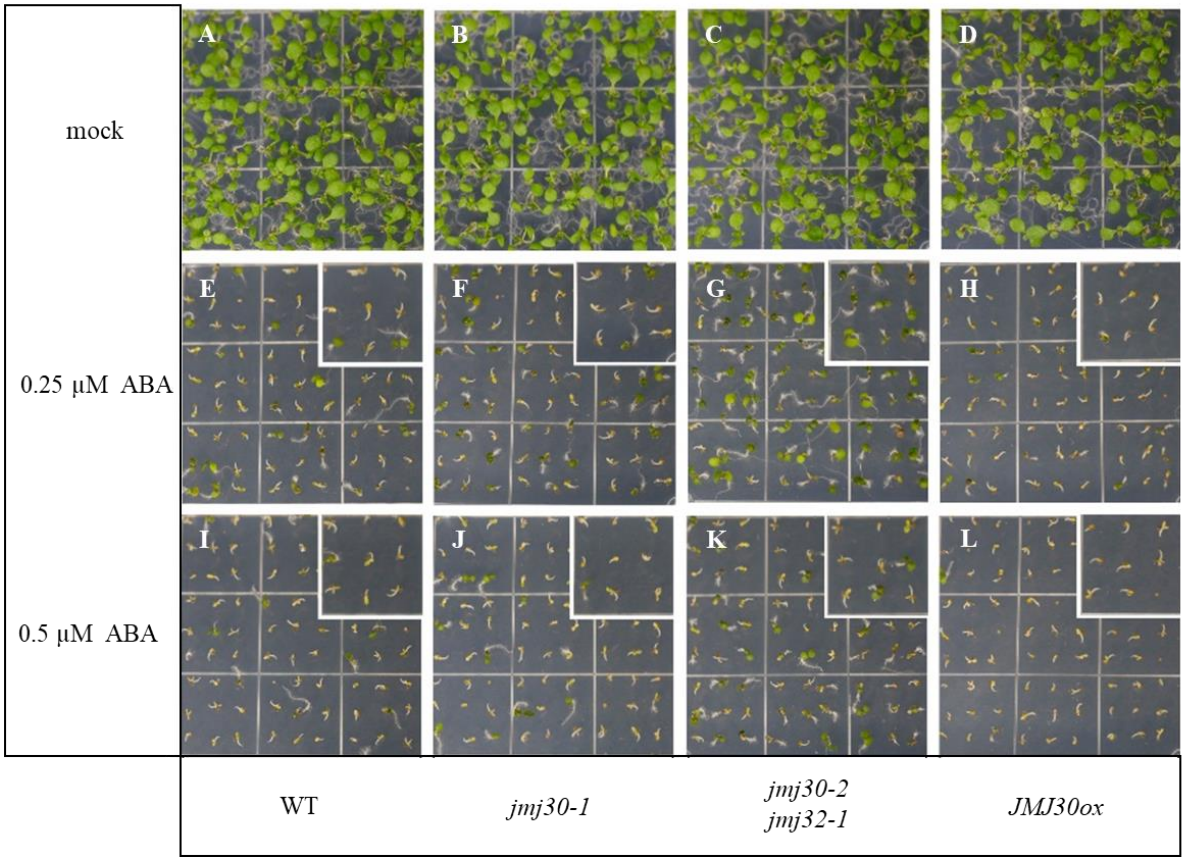

Figure 18. Phenotypes of the *jmj30-1* single mutant and a *JMJ30* overexpression line in response to ABA during post-germination.

(A-L) Representative images of the wild type (A, E, I), the *jmj30-1* mutant (B, F, J), the *jmj30-2 jmj32-1* double mutant (C, G, K), and the *JMJ30 ox* line (D, H, L) grown for 5.5 days on 1/2 MS medium with 1% sucrose containing 0 μM (A-D), 0.25 μM (E-H), and 0.5 μM ABA (I-L). Wild type and the *jmj30-2 jmj32-1* double mutant were included as controls. Insets in e-l show close-ups of representative seedlings.

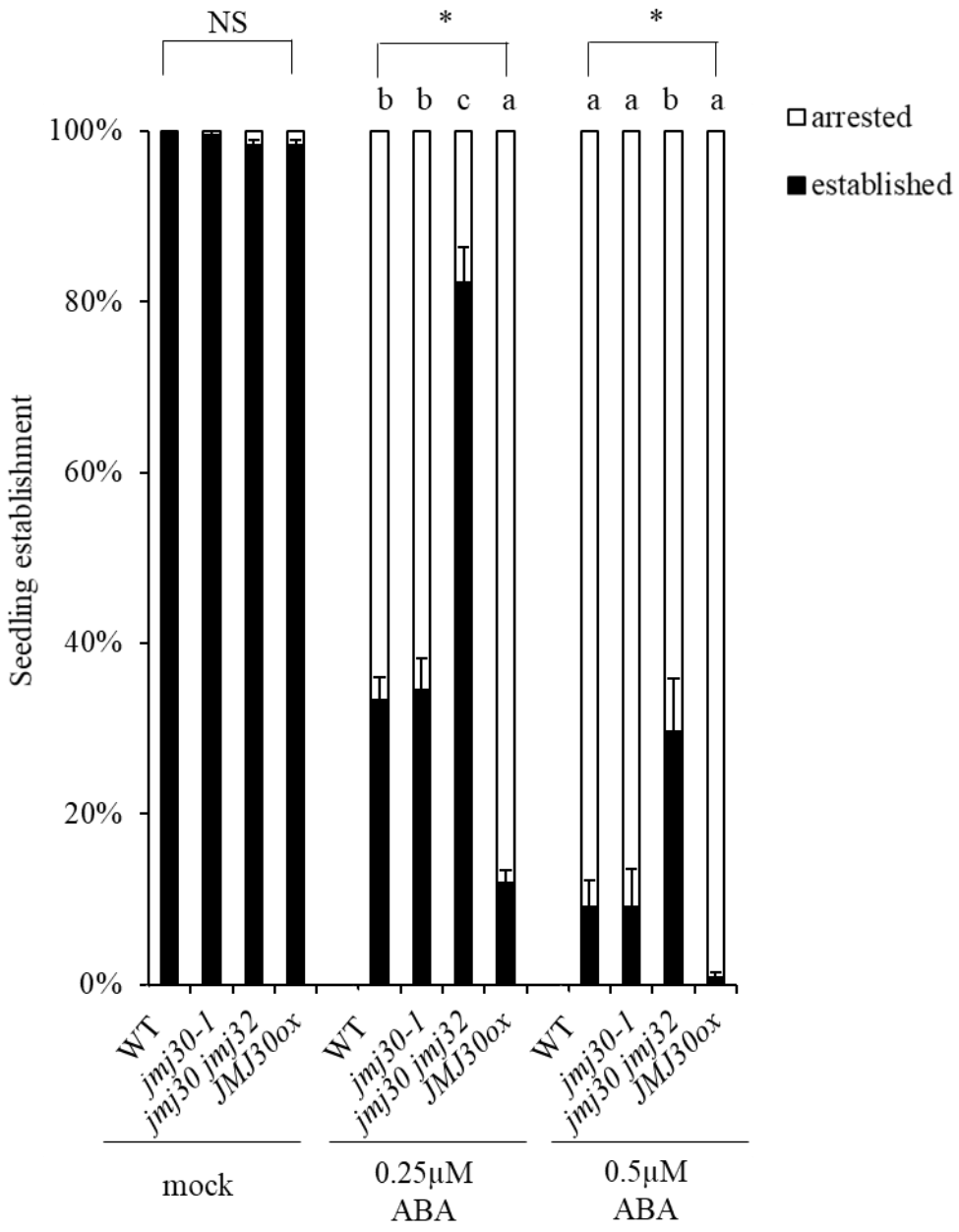

Figure 19. Seedling establishment of the *jmj30-1* single mutant and a *JMJ30* overexpression line in response to ABA during post-germination.

Percentages of established and arrested seedlings in wild-type, *jmj30-1*, *jmj30-2 jmj32-1* double mutant, and *JMJ30 ox* plants in the absence and presence of ABA. Asterisks indicate significant differences based on one-way ANOVA test. $p < 0.05$. Different letters indicate significant

differences based on post-hoc Tukey's HSD test. n = 243. NS, non significant. Values represents mean ± SD of 243 and 81 plants, respectively.

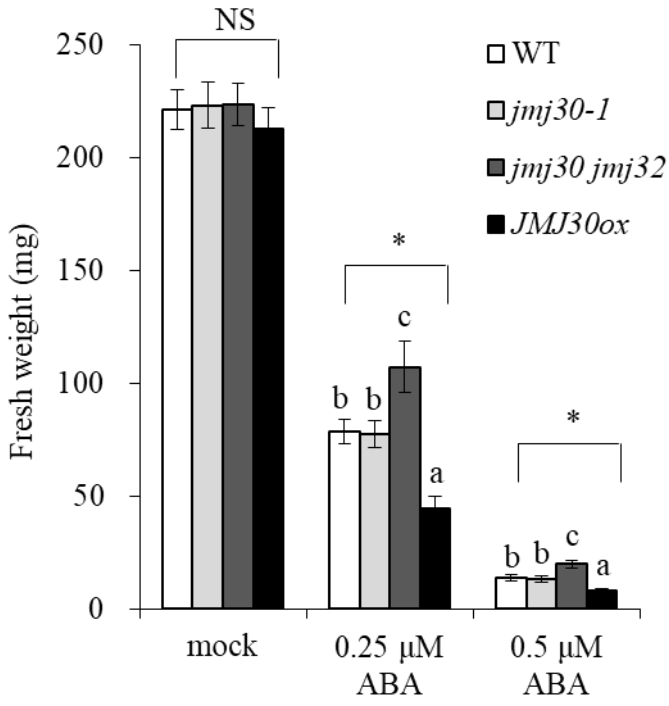

Figure 20. Fresh weight of the *jmj30-1* single mutant and a *JMJ30* overexpression line in response to ABA during post-germination.

Measurement of the fresh weight of wild type, *jmj30-1*, *jmj30-2 jmj32-1* double mutant, and *JMJ30 ox* seedlings in the absence and presence of ABA. Asterisks indicate significant differences based on one-way ANOVA test. $p < 0.05$. Different letters indicate significant differences based on post-hoc Tukey's HSD test. NS, non significant. Values represents mean ± SD of 243 and 81 plants, respectively.

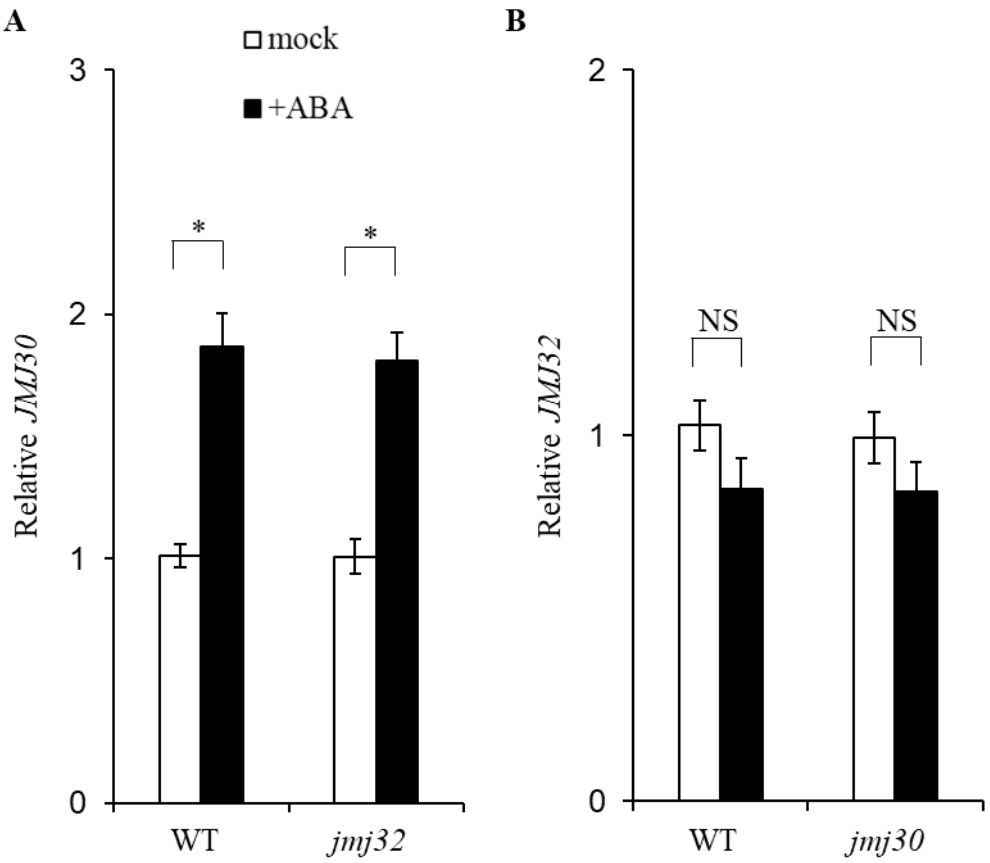

Figure 21. *JMJ30* and *JMJ32* expression in single mutants after ABA treatment during post-germination.

(A, B) Expression of *JMJ30* in wild type and *jmj32-1* mutant (A), and *JMJ32* in wild type and *jmj30-2* mutant (B), in response to ABA during post-germination. The WT with 0 hour mock treatment was set to 1.0 and the relative expressions were calculated. Results are from three independent experiments. Values represent mean ± SEM. Asterisks indicate significant differences between mock- and ABA-treated plants based on two-tailed Student's *t*-test.

I also examined the effects of JMJ30 and JMJ32 on ABA responses during germination. Consistent with the expression analysis during germination in response to ABA, no phenotypic difference in germination timing was observed between wild-type, *jmj* single mutants, the *jmj30-2 jmj32-1* double mutant, and *JMJ30 ox* seedlings in either the absence or the presence of ABA (Fig. 22). Thus, I concluded that the role of JMJ30 and JMJ32 in the ABA response is specifically important for ABA-dependent growth arrest after germination.

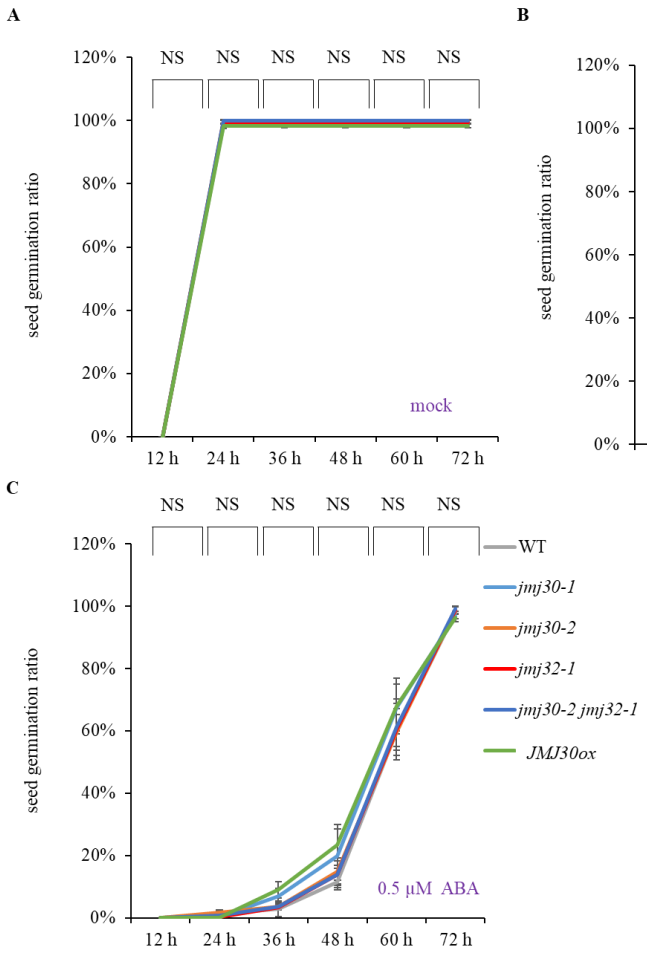

Figure 22. Germination rates of wild type and *jmj30 jmj32* double mutants with and without ABA. (A-C) Rates of seed germination on 1/2 MS agar plates in the absence of ABA (A) and in the presence of 0.25 μM (B) and 0.5 μM (C) ABA. Values represent mean ±SD.

4.4 JMJ30 and JMJ32 affect genes involved in stimulus and signaling pathways in response to ABA during post-germination

To identify genes and pathways regulated by JMJ30 and JMJ32 in response to ABA during post-germination, I performed RNA-seq analysis using mock- and ABA-treated wild-type and *jmj30-2 jmj32-1* double mutant plants. The sequencing depth for five technical replicates from two different genetic backgrounds was at least 10 M reads. The resulting sequences were mapped based on TAIR10 and total numbers of reads were obtained by converting counts to reads per million mapped reads. I found that 106 and 84 genes were differentially expressed between mock-treated wild-type and *jmj30-2 jmj32-1* plants and ABA-treated wild-type and *jmj30-2 jmj32-1* plants, respectively (FDR < 0.05) (Fig. 23, Table 5-6). Among those genes, 60 genes were differentially expressed only in ABA-treated *jmj30-2 jmj32-1* plants; 31 genes and 29 genes were downregulated and upregulated in the double mutant, respectively (Fig. 23).

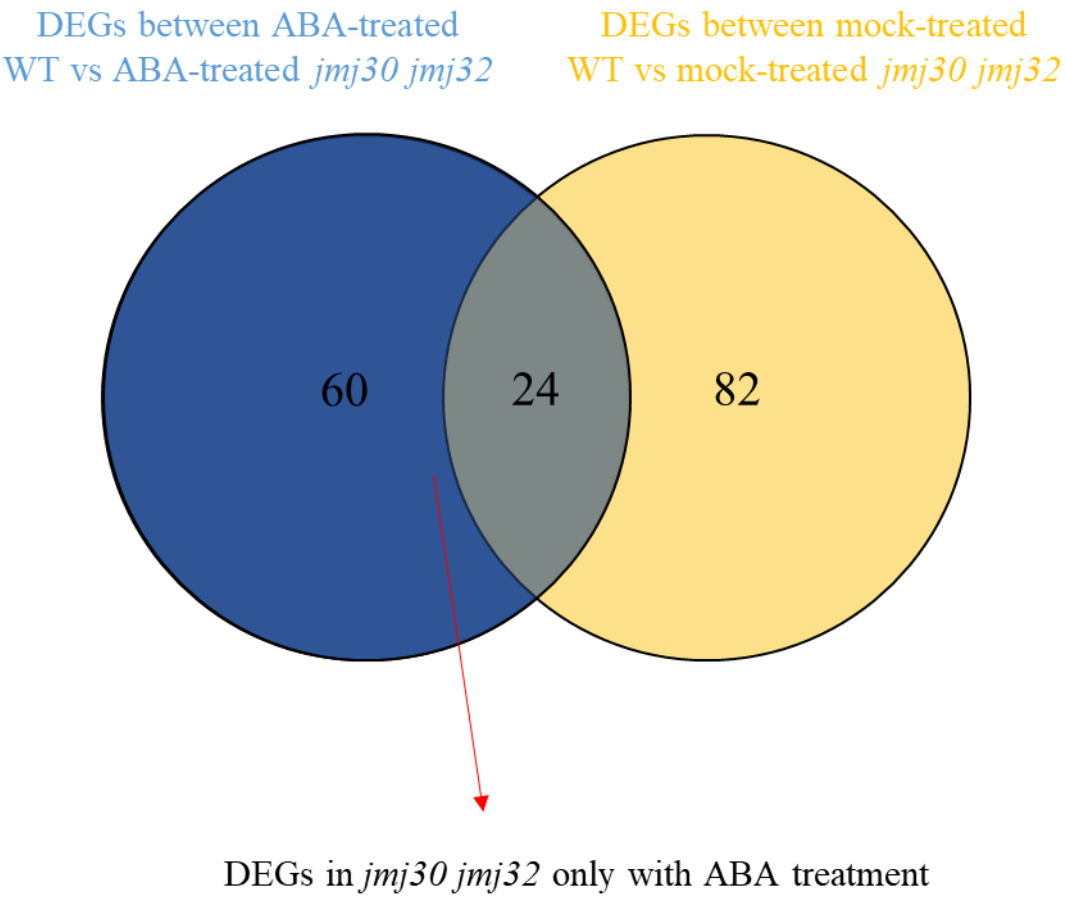

Figure 23. Identification of ABA-dependent JMJ downstream genes by RNA-seq.

Venn diagram showing the number of genes differentially expressed in ABA-treated wild-type (WT) and *jmj30-2 jmj32-1* seedlings and mock-treated WT and *jmj30-2 jmj32-1* seedlings. 60 genes differentially expressed in *jmj30-2 jmj32-1* only with ABA treatment were used for further study.

Table 5 High confident upregulated and downregulated genes (106 genes) in *jmj30 jmj32* under mock condition. The columns of expression level represents up-regulation (+) or down-regulation (-) in *jmj30 jmj32* mutant as compared to WT. The different expression genes with $p < 0.05$ were selected for further studies.

GO biological process	AGI ID	Description	Expression level
Response to ABA	AT2G18050	histone H1-3	+
	AT2G21490	dehydrin LEA	+
	AT2G40170	Stress induced protein	+
	AT3G51810	Stress induced protein	+
	AT3G50980	dehydrin xero 1	+
	AT5G66400	Dehydrin family protein	+
	AT5G52300	CAP160 protein	+
	AT3G02480	Late embryogenesis abundant protein (LEA) family protein	+
	AT4G25580	CAP160 protein	+
	AT2G47770	TSPO(outer membrane tryptophan-rich sensory protein)-related	+
Response to freezing	AT1G52690	Late embryogenesis abundant protein (LEA) family protein	+
Response to gibberellin	AT1G67100	LOB domain-containing protein 40	+
Response to osmotic stress	AT2G35300	Late embryogenesis abundant protein, group 1 protein	+
	AT5G62490	HVA22 homologue B	+
Lipid metabolism	AT3G27660	oleosin 4	+
	AT5G46890	Bifunctional inhibitor/lipid-transfer protein/seed storage 2S albumin superfamily protein	-
	AT5G46900	Bifunctional inhibitor/lipid-transfer protein/seed storage 2S albumin superfamily protein	-
	AT2G25890	Oleosin family protein	+
	AT5G40420	oleosin 2	+
	AT5G56100	glycine-rich protein / oleosin	+
	AT5G55410	Bifunctional inhibitor/lipid-transfer protein/seed storage 2S albumin superfamily protein	+
	AT4G12520	Bifunctional inhibitor/lipid-transfer protein/seed storage 2S albumin superfamily protein	-
	AT5G54740	seed storage albumin 5	+
Seed dormancy	AT1G72100	late embryogenesis abundant domain-containing protein / LEA domain-containing protein	+
	AT3G15670	Late embryogenesis abundant protein (LEA) family protein	+
	AT4G28520	cruciferin 3	+
	AT5G44310	Late embryogenesis abundant protein (LEA) family protein	+
	AT4G21020	Late embryogenesis abundant protein (LEA) family protein	+
	AT3G53040	late embryogenesis abundant protein, putative / LEA protein, putative	+
	AT5G06760	Late Embryogenesis Abundant 4-5	+
	AT2G36640	embryonic cell protein 63	+
	AT2G42560	late embryogenesis abundant domain-containing protein / LEA domain-containing protein	+
Atg8 ligase activity	AT5G61500	autophagy 3 (APG3)	+

(Continued)

GO biological process	AGI ID	Description	Expression level
Autophagy	AT1G73190	Aquaporin-like superfamily protein	+
Defense response	AT1G58848	Disease resistance protein (CC-NBS-LRR class) family	-
	AT1G59218	Disease resistance protein (CC-NBS-LRR class) family	-
	AT1G75830	low-molecular-weight cysteine-rich 67	+
Integral component of membrane	AT3G03341	cold-regulated protein	+
	AT3G47990	SUGAR-INSENSITIVE 3	+
	AT5G08500	Transmembrane CLPTM1 family protein	+
Carbohydrate binding	AT5G49850	Mannose-binding lectin superfamily protein	-
Carbohydrate metabolic process	AT2G28420	Lactoylglutathione lyase / glyoxalase I family protein	+
Chloroplast	AT3G27340	unknown protein	-
Chloroplast biogenesis	AT4G01800	Albino or Glassy Yellow 1	-
Cysteine-type endopeptidase inhibitor activity	AT2G31980	PHYTOCYSTATIN 2	+
DNA binding	AT5G57150	basic helix-loop-helix (bHLH) DNA-binding superfamily protein	+
DNA replication origin binding	AT2G37560	origin recognition complex second largest subunit 2	+
Endoplasmic reticulum	AT3G17520	Late embryogenesis abundant protein (LEA) family protein	+
	AT4G36600	Late embryogenesis abundant (LEA) protein	+
Endoplasmic reticulum tubular network organization	AT2G23640	Reticulan like protein B13	+
Endoribonuclease activity	AT1G68290	endonuclease 2	-
Glucosinolate catabolic process	AT2G33070	nitrile specifier protein 2	+
Glycolate oxidase activity	AT5G06580	FAD-linked oxidases family protein	+
Glycoside hydrolase	AT2G06845	Beta-galactosidase related protein	-
Histone demethylase	AT3G20810	2-oxoglutarate (2OG) and Fe(II)-dependent oxygenase superfamily protein	-
Meiotic cell cycle	AT1G53490	RING/U-box superfamily protein	-
Negative regulation of translation	AT3G20800	Cell differentiation, Rcd1-like protein	+
Oxidation-reduction process	AT5G50700	HSD1	+
Peroxidase activity	AT1G48130	1-cysteine peroxiredoxin 1	+
Phosphatidylinositol dephosphorylation	AT1G65580	Endonuclease/exonuclease/phosphatase family protein	+
Protein ADP-ribosylase activity	AT5G22470	NAD+ ADP-ribosyltransferases;NAD+ ADP-ribosyltransferases	+
Protein binding	AT5G05410	DRE-binding protein 2A	+
Protein histidine kinase binding	AT4G27160	seed storage albumin 3	+
Proteolysis	AT5G38510	Rhomboid-related intramembrane serine protease family protein	+
	AT3G54940	Papain family cysteine protease	+
Receptor serine/threonine kinase binding	AT1G34210	somatic embryogenesis receptor-like kinase 2	-
Regulation of gene expression	AT4G20480	Putative endonuclease or glycosyl hydrolase	+
RNA polymerase II complex binding	AT5G10060	ENTH/VHS family protein	+
Serine-type carboxypeptidase activity	AT2G22970	serine carboxypeptidase-like 11	-
Sulfate transmembrane transporter activity	AT3G12520	sulfate transporter 4;2	+
Thylakoid lumen	AT1G77090	Mog1/PsbP/DUF1795-like photosystem II reaction center PsbP family protein	+
TIM23 mitochondrial import inner membrane Translocase complex	AT4G16160	ATOEP16-2	+

(Continued)

GO biological process	AGI ID	Description	Expression level
Unknown	AT1G59865	transmembrane protein	+
	AT1G65090	nucleolin	+
	AT1G68250	hypothetical protein	+
	AT2G18540	RmlC-like cupins superfamily protein	+
	AT3G56210	ARM repeat superfamily protein	+
	AT4G36700	RmlC-like cupins superfamily protein	+
	AT5G24130	polypyrimidine tract-binding-like protein	+
	AT5G60590	DHBP synthase RibB-like alpha/beta domain-containing protein	-
	AT1G01770	unknown protein	+
	AT1G04560	AWPM-19-like family protein	+
	AT1G04660	glycine-rich protein	+
	AT1G27990	unknown protein	+
	AT1G32560	Late embryogenesis abundant protein, group 1 protein	+
	AT2G05915	unknown protein	-
	AT2G21820	unknown protein	+
	AT3G01570	Oleosin family protein	+
	AT4G08093	pseudogene	-
	AT4G15030	unknown protein	+
	AT4G25140	oleosin 1	+
	AT5G07330	unknown protein	+
	AT5G15360	unknown protein	-
	AT5G23830	MD-2-related lipid recognition domain-containing protein	-
	AT5G35660	Glycine-rich protein family	+
	AT5G01300	PEBP (phosphatidylethanolamine-binding protein) family protein	+
	AT1G22140	unknown protein	+
	AT3G31161	pseudogene	-
	AT1G53480	mto 1 responding down 1	-
	AT3G01345	Expressed protein	-
	AT5G06180	Protein of unknown function (DUF1022)	+
	AT2G44970	alpha/beta-Hydrolases superfamily protein	-
	AT1G52050	Mannose-binding lectin superfamily protein	-
	AT2G28490	AT2G28490	+
	AT5G44120	AT5G44120	+
	AT5G50600	hydroxysteroid dehydrogenase 1	+

Table 6 High confident upregulated and downregulated genes (84 genes) in *jmj30 jmj32* after ABA treatment. The columns of expression level represents up-regulation (+) or down-regulation (-) in *jmj30 jmj32* mutant as compared to WT. The different expression genes with $p < 0.05$ were selected for further studies.

GO biological process	AGI ID	Description	Expression level
Response to ABA	AT1G78290	Protein kinase superfamily protein	-
	AT1G62660	Glycosyl hydrolases family 32 protein	-
	AT4G23670	Polyketide cyclase/dehydrase and lipid transport superfamily protein	-
Response to BRs	AT1G75080	Brassinosteroid signalling positive regulator (BZR1) family protein	-
Response to cytokinin	AT1G13420	sulfotransferase 4B	-
	AT1G13430	sulfotransferase 4C	-
	AT3G57040	response regulator 9	-
Response to stress	AT2G38750	annexin 4	-
Defence response	AT2G43530	Scorpion toxin-like knottin superfamily protein	+
	AT3G03300	dicer-like 2	-
	AT4G11190	Disease resistance-responsive (dirigent-like protein) family protein	+
	AT1G14940	Polyketide cyclase/dehydrase and lipid transport superfamily protein	+
Lipid metabolism	AT1G06250	alpha/beta-Hydrolases superfamily protein	-
	AT2G04570	GDSL-like Lipase/Acylhydrolase superfamily protein	-
	AT4G12510	Bifunctional inhibitor/lipid-transfer protein/seed storage 2S albumin superfamily protein	-
	AT4G12520	Bifunctional inhibitor/lipid-transfer protein/seed storage 2S albumin superfamily protein	-
	AT5G46900	Bifunctional inhibitor/lipid-transfer protein/seed storage 2S albumin superfamily protein	+
Seed dormancy	AT1G48130	1-cysteine peroxiredoxin 1	+
Seed growth	AT1G17145	RING/U-box superfamily protein	
Cell-cell signaling	AT1G72970	Glucose-methanol-choline (GMC) oxidoreductase family protein	-
GTP biosynthetic process	AT1G17410	Nucleoside diphosphate kinase family protein	+
Autophagy	AT3G60640	Ubiquitin-like superfamily protein	+
Auxin-activated signaling pathway	AT3G11220	Paxneb protein-related	+
Carbohydrate metabolic process	AT3G06770	Pectin lyase-like superfamily protein	-
	AT1G55740	seed imbibition 1	+
Cell morphogenesis	AT5G44610	microtubule-associated protein 18	-
Flower development	AT5G10140	K-box region and MADS-box transcription factor family protein	-
Golgi to vacuole transport	AT3G55480	protein affected trafficking 2	+
Histone demethylase	AT3G20810	2-oxoglutarate (2OG) and Fe(II)-dependent oxygenase superfamily protein	-
Histone modification	AT1G06645	2-oxoglutarate (2OG) and Fe(II)-dependent oxygenase superfamily protein	+
Hydrolase activity	AT2G06845	Beta-galactosidase related protein	-
Lactate catabolic process	AT5G06580	FAD-linked oxidases family protein	+
Lateral root formation	AT5G49660	Leucine-rich repeat transmembrane protein kinase family protein	-
Meiotic cell cycle	AT1G53490	RING/U-box superfamily protein	-
Microtubule-based movement	AT1G73860	P-loop containing nucleoside triphosphate hydrolases superfamily protein	-
Mismatch repair	AT5G16630	DNA repair protein Rad4 family	+
Mitochondrial mRNA 5'-end Processing	AT2G28050	Pentatricopeptide repeat (PPR) superfamily protein	-
Mitochondrion	AT4G21490	NAD(P)H dehydrogenase B3	+
Negative regulation of translation	AT3G20800	Cell differentiation, Rcd1-like protein	+
N-terminal peptidyl-glycine N-myristoylation	AT4G20260	plasma-membrane associated cation-binding protein 1	-
Nutrient reservoir activity	AT4G27140	seed storage albumin 1	+
	AT4G27160	seed storage albumin 3	+

(Continued)

GO biological process	AGI ID	Description	Expression level
Oxidation-reduction process	AT3G56840	FAD-dependent oxidoreductase family protein	+
Protein dephosphorylation	AT5G51760	Protein phosphatase 2C family protein	+
Protein polyubiquitination	AT4G34370	RING/U-box superfamily protein	+
Protein ubiquitination	AT3G47990	SUGAR-INSENSITIVE 3	+
	AT5G62800	Protein with RING/U-box and TRAF-like domains	+
Proteolysis	AT5G38510	Rhomboid-related intramembrane serine protease family protein	+
	AT5G48430	Eukaryotic aspartyl protease family protein	+
Regulation of gene expression	AT4G20480	Putative endonuclease or glycosyl hydrolase	+
Regulation of transcription	AT5G57150	basic helix-loop-helix (bHLH) DNA-binding superfamily protein	+
RNA polyadenylation	AT4G32850	nuclear poly(a) polymerase	-
Seed maturation	AT4G28520	cruciferin 3	+
Transferase activity	AT5G01250	alpha 1,4-glycosyltransferase family protein	-
Translational initiation	AT1G73180	Eukaryotic translation initiation factor eIF2A family protein	+
Ubiquitin binding	AT1G64470	Ubiquitin-like superfamily protein	-
vernalization response	AT5G57380	Fibronectin type III domain-containing protein	+
Unknown	AT1G27460	no pollen germination related 1	+
	AT1G27565	unknown protein	+
	AT1G29418	unknown protein	+
	AT1G52905	unknown protein	+
	AT1G53480	mto 1 responding down 1	-
	AT2G32560	F-box family protein	-
	AT2G44970	alpha/beta-Hydrolases superfamily protein	-
	AT3G01345	Expressed protein	-
	AT3G27420	unknown protein	+
	AT3G55646	unknown protein	-
	AT3G56210	ARM repeat superfamily protein	+
	AT4G02810	Protein of unknown function (DUF3049)	-
	AT4G08093	pseudogene	-
	AT4G15030	unknown protein	+
	AT4G30630	unknown protein	+
	AT4G31830	unknown protein	+
	AT4G37420	Domain of unknown function (DUF23)	+
	AT5G01300	PEBP (phosphatidylethanolamine-binding protein) family protein	+
	AT5G06180	Protein of unknown function (DUF1022)	+
	AT5G08500	Transmembrane CLPTM1 family protein	+
	AT5G10210	unknown protein	-
	AT5G15360	unknown protein	-
	AT5G24750	UDP-Glycosyltransferase superfamily protein	+
	AT5G26610	D111/G-patch domain-containing protein	-
	AT5G40450	unknown protein	-
	AT5G41810	unknown protein	-
	AT5G56370	F-box/RNI-like/FBD-like domains-containing protein	-

Table 7 GO term analysis using differentially genes in *jmj30 jmj32* only when treated with ABA.

dowregulated in *jmj*						
GO term	Ontology	Description	Number in input list	Number in BG/Ref	p-value	FDR
GO:0010033	P	response to organic substance	12	2754	1.70E-05	0.0039
GO:0009725	P	response to hormone stimulus	8	1375	8.90E-05	0.01
GO:0009719	P	response to endogenous stimulus	8	1615	0.00027	0.015
GO:0006970	P	response to osmotic stress	6	842	0.00027	0.015
GO:0050896	P	response to stimulus	16	6292	0.00032	0.015
GO:0023052	P	signaling	9	2376	0.00074	0.019
GO:0051716	P	cellular response to stimulus	9	2355	0.0007	0.019
GO:0042221	P	response to chemical stimulus	12	3978	0.0006	0.019
GO:0032870	P	cellular response to hormone stimulus	5	641	0.00062	0.019
GO:0009651	P	response to salt stress	5	788	0.0016	0.036
GO:0071310	P	cellular response to organic substance	6	1234	0.002	0.038
GO:0071495	P	cellular response to endogenous stimulus	5	815	0.0018	0.038
GO:0023060	P	signal transmission	7	1767	0.0025	0.042
GO:0023046	P	signaling process	7	1768	0.0025	0.042
GO:0006950	P	response to stress	11	4089	0.0029	0.044
GO:0070887	P	cellular response to chemical stimulus	6	1417	0.0039	0.056
GO:0006952	P	defense response	6	1653	0.0082	0.11
GO:0007165	P	signal transduction	6	1670	0.0086	0.11
GO:0006519	P	cellular amino acid and derivative metabolic process	5	1324	0.014	0.17
GO:0009628	P	response to abiotic stimulus	7	2635	0.021	0.23
GO:0033554	P	cellular response to stress	5	1473	0.021	0.23
GO:0006810	P	transport	8	3577	0.035	0.36
GO:0051234	P	establishment of localization	8	3652	0.039	0.39
upregulated in *jmj*						
GO:0051716	P	cellular response to stimulus	6	2355	0.029	1
GO:0006629	P	lipid metabolic process	5	1772	0.032	1

Since JMJ30 and JMJ32 have been shown to act as demethylases of H3K27me3 and induce gene expression, I first carried out Gene Ontology (GO) term enrichment analysis based on the agriGO website using downregulated genes in the ABA-treated double mutant (Tian et al. 2017). I identified 23 significantly enriched GO terms by theses analysis ($p < 0.05$) (Table 7). To minimize duplication of GO terms, I used REduced VIsualize Gene Ontology (REVIGO) (Supek et al. 2011). I identified six categories containing multiple GO terms: "response to organic substance", "response to stimulus", "signal transmission", "signaling", "cellular amino acid metabolism", and "transport" (Fig. 24-25). Among these, "response to organic substance" was the largest group, containing 11 GO terms including "response to stress" and "response to abiotic stress" (Fig. 24, Table 7). Stimulus and signaling have been implicated in proper seedling establishment (Bewley 1997) (Fig. 24). Next, I identified "lipid metabolism" and "response to stimulus" based on the GO term analysis using upregulated genes. Those two biological processes have been implicated in proper seedling establishment (Fig. 26-27). Indeed, I found that lipid accumulation was lower in ABA-treated *jmj30-2 jmj32-1* double mutants than in mock-treated wild-type or *jmj30-2 jmj32-1* plants or in ABA-treated wild-type plants (Fig. 28).

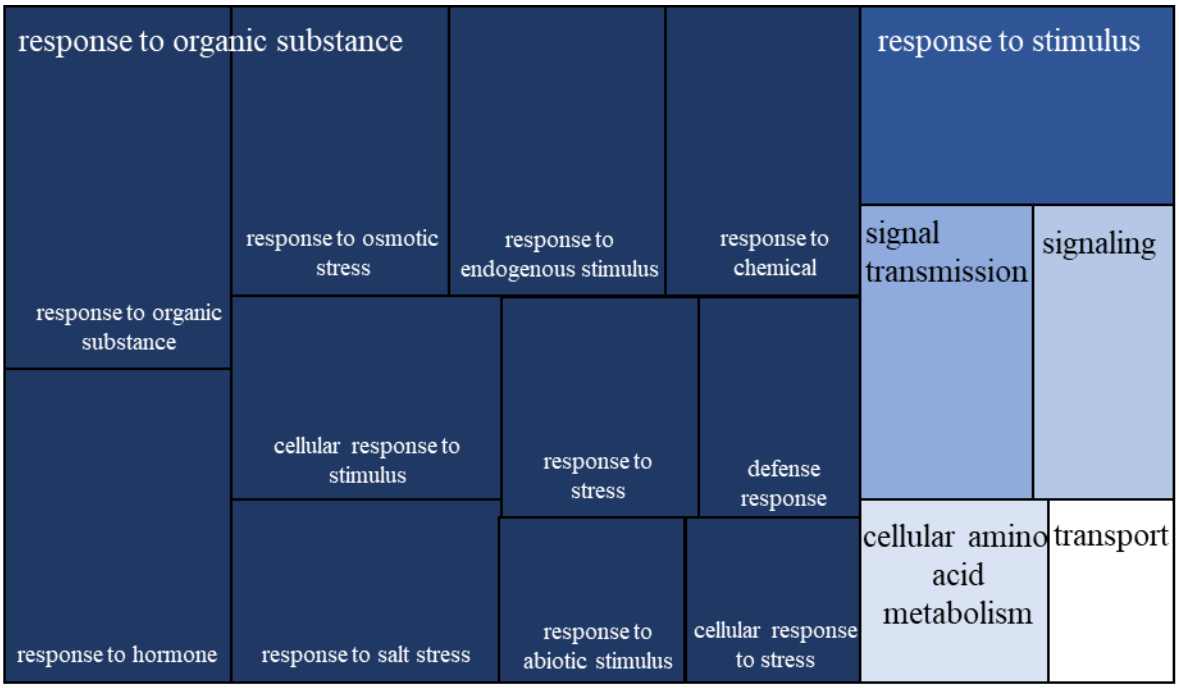

Figure 24. TreeMap view of GO terms generated by REVIGO (31 genes).

Dark and pale colors indicate lower and higher *p*-values, respectively. The sizes of boxes indicate the frequency of the GO terms in the underlying GOA database.

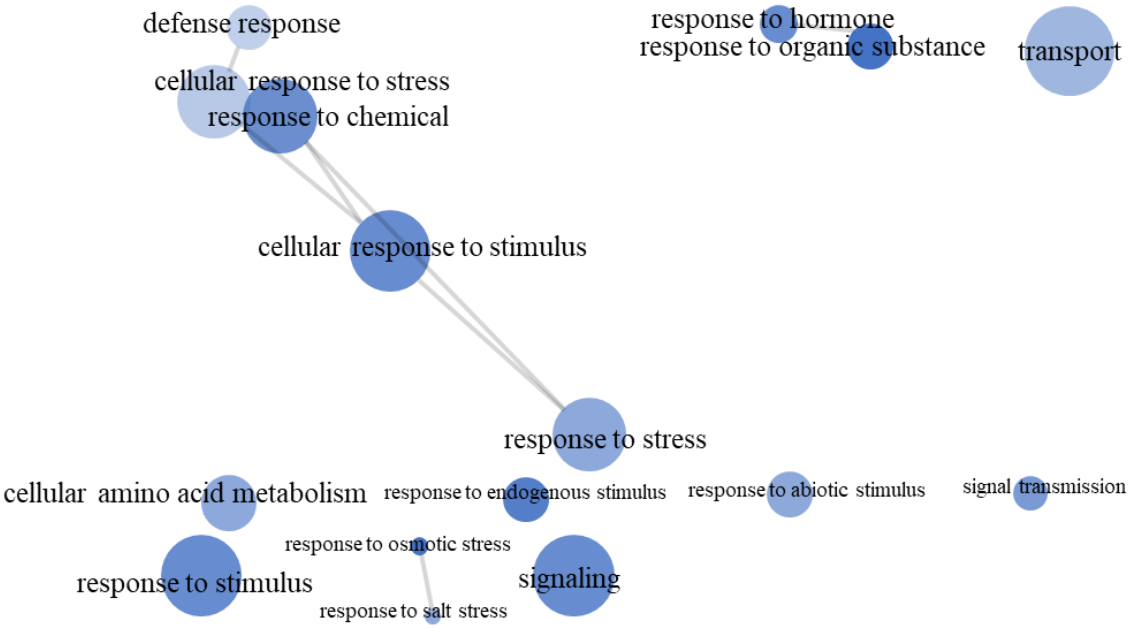

Figure 25. Interactive graph view generated with REVIGO (31 genes).

Dark and pale colors indicate lower and higher *p*-values, respectively. The sizes of circles indicate the frequency of the GO terms in the underlying GOA database.

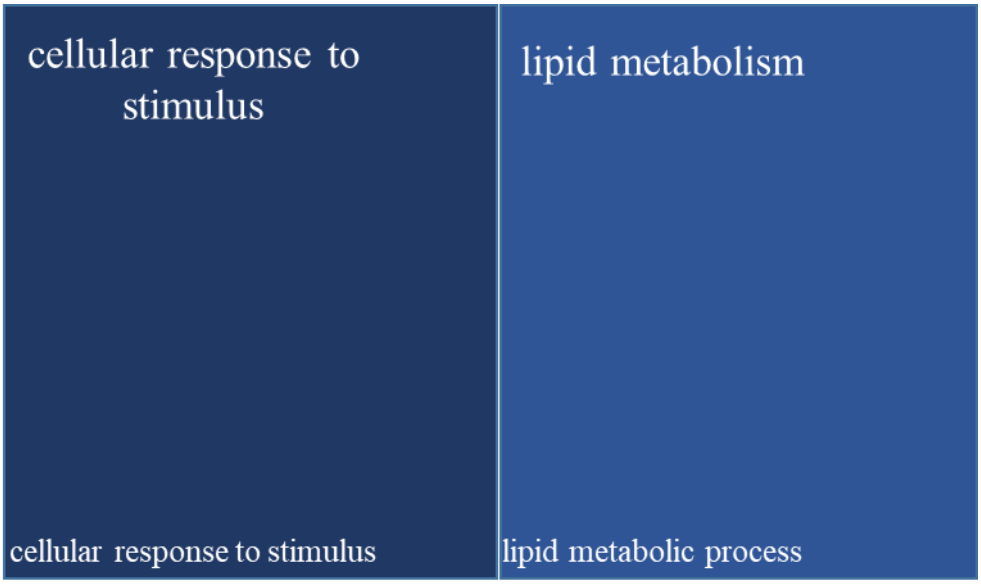

Figure 26. TreeMap view of GO terms generated by REVIGO (29 genes).

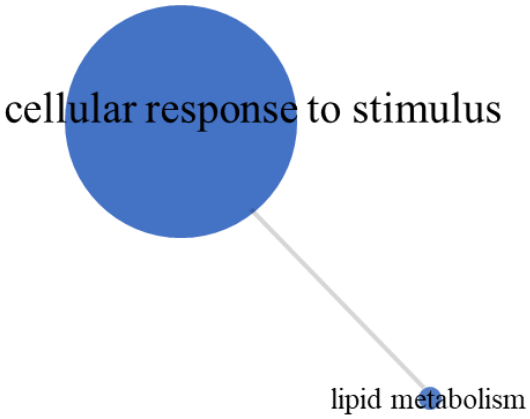

Figure 27. Interactive graph view generated with REVIGO (29 genes).

Dark and pale colors indicate lower and higher *p*-values, respectively. The sizes of circles indicate the frequency of the GO terms in the underlying GOA database.

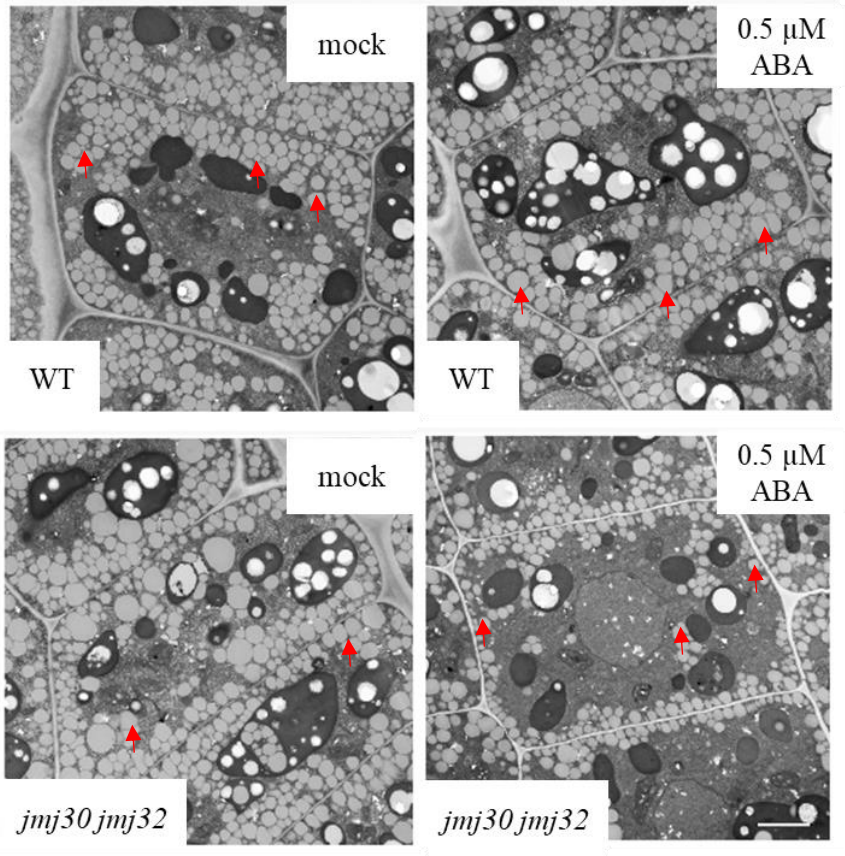

Figure 28. Transmission electron micrographs of wild-type (above) and *jmj30-2 jmj32-1* (below) seedlings grown for 0.5 day on 1/2 MS medium and 2.5 days on 1/2 MS containing 0.5 μM ABA (right). Scale bar = 2 μm.The red arrows represent lipid bodies.

To confirm the RNA-seq results, I next examined the expression of these JMJ30 and JMJ32 downstream genes in the presence and absence of ABA during post-germination growth. I chose several genes from different GO term categories. *SnRK2.8*, *AT2G43530*, and *AT4G23670* are linked to "response to organic substance" (Atias et al. 2009; Sahr et al. 2005; Umezawa et al. 2004). There was no obvious expression difference in those three genes between mock-treated wild-type and *jmj30-2 jmj32-1* plants (Fig. 29). In the presence of ABA, however, the expression of all three genes was significantly higher in the wild type, but this ABA-dependent induction was compromised in the *jmj30-2 jmj32-1* double mutant background ($p < 0.05$ by one-way ANOVA test) (WT + ABA vs. the other samples: $p < 0.05$ by post-hoc Tukey's HSD) (Fig. 29). Similarly, the *MICROTUBULE-ASSOCIATED PROTEIN18* (*MAP18*), the type-A *AUTHENTIC RESPONSE REGULATOR9* (*ARR9*), and the glycosyl hydrolase family 32 protein gene *AT1G62660* were categorized into "response to stimulus", "signal transmission", and "signaling", respectively (Wang et al. 2013; Zhu et al. 2013). Expression levels of all three of these genes were significantly decreased in the ABA-treated *jmj30-2 jmj32-1* double mutant compared to the wild type ($p < 0.05$ by one-way ANOVA test) (WT + ABA vs. the other samples: $p < 0.05$ by post-hoc Tukey's HSD) (Fig. 29). Likewise, I confirmed upregulation of three downstream genes in response to ABA in the *jmj30-2 jmj32-1* double mutant background ($p < 0.05$ by one-way ANOVA test) (*jmj30 jmj32* + ABA vs. the other samples: $p < 0.05$ by post-hoc Tukey's HSD) (Fig. 30).

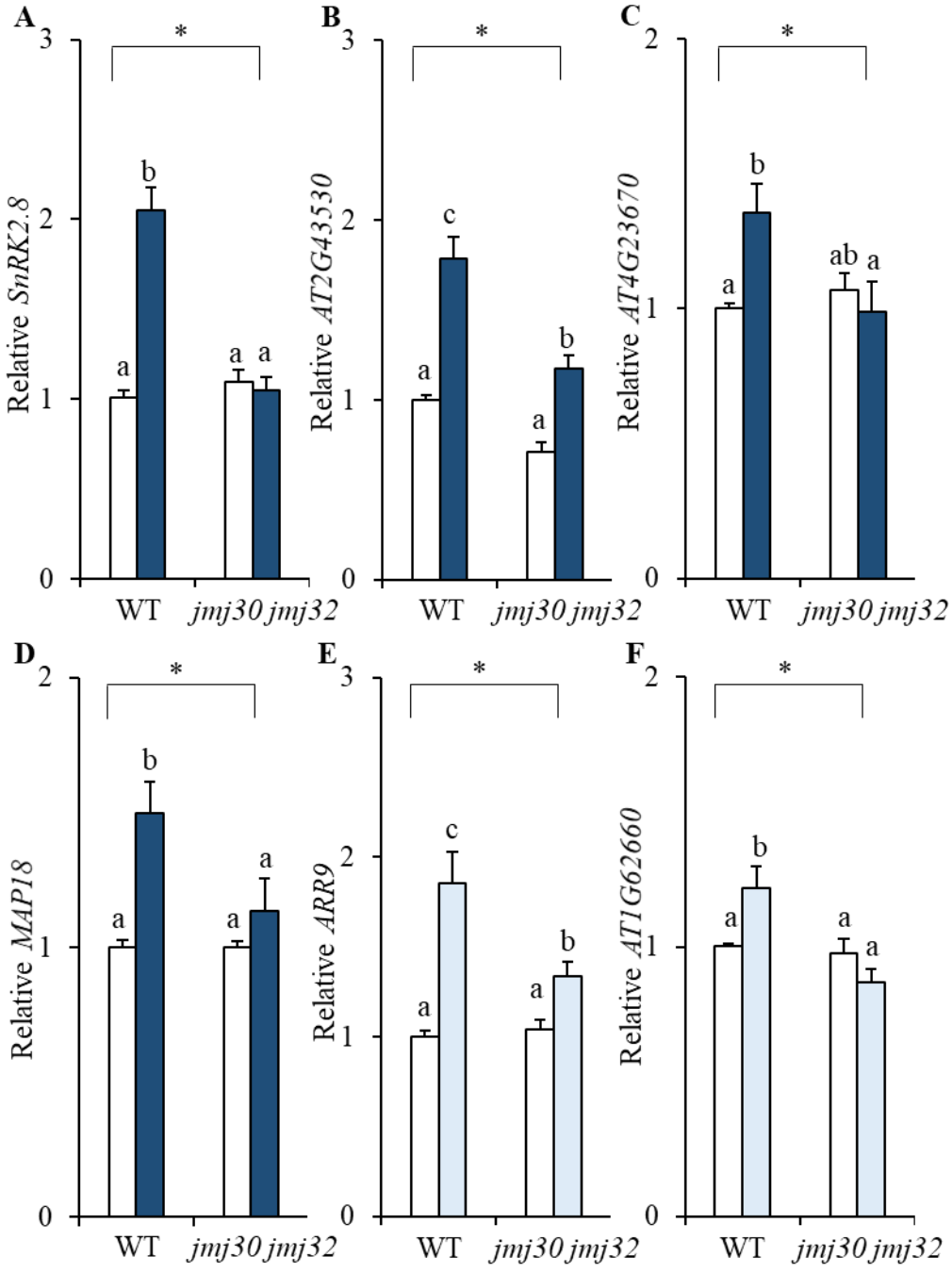

Figure 29. Genes downregulated in ABA-treated *jmj30-2 jmj32-1* mutants compared to ABA-treated wild-type plants by RT-qPCR; (A) *SnRK2.8.* (B) *AT2G43530.* (C) *AT4G23670.* (D) *MAP18*. (E) *ARR9*. (F) *AT1G62660*. White and colored bars represent mock- and ABA-treated samples, respectively. Genes indicated by navy blue, blue, sky blue, and light blue are categorized in 'response to organic substance', 'response to stimulus', 'signal transmission', and

'signaling' in Fig. 24, respectively. The WT with 5 hour mock treatment was set to 1.0 and the relative expressions were calculated.Values are mean ± SEM from three independent experiments. Asterisks indicate significant differences based on one-way ANOVA test. $p < 0.05$. Different letters indicate significant differences, while same letters indicate non-significant differences based on post-hoc Tukey's HSD test. $p < 0.05$.

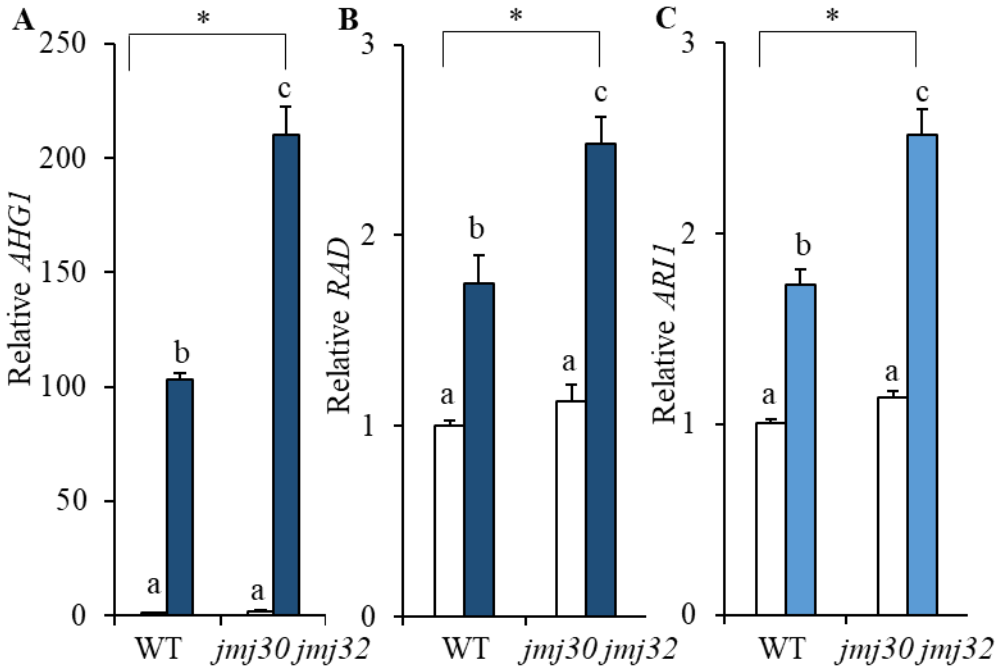

Figure 30. Genes upregulated in ABA-treated *jmj30-2 jmj32-1* compared to ABA-treated wild type by RT-qPCR; (A) *AHG1.* (B) *RAD4.* (C) *ARI1.* White and colored bars represent mock- and ABA-treated samples, respectively. Genes indicated by yellow, blue green, light green, dark blue, and light blue are categorized in 'cellular response to carbohydrate stimulus', 'lipid localization', 'dormancy process', 'positive regulation of cellular process', and 'phenylpropanoid metabolism' in Fig. 24, respectively. The WT with 5 hour mock treatment was set to 1.0 and the relative expressions were calculated. Values are mean ± SEM from three independent experiments. Asterisks indicate significant differences based on one-way ANOVA test. $p < 0.05$. Different letters indicate significant differences, while same letters indicate non-significant differences based on post-hoc Tukey's HSD test. $p < 0.05$.

4.5 Several JMJ30- and JMJ32-regulated genes are enriched by H3K27me3 or JMJ30 in response to ABA during post-germination

To identify direct targets of JMJ30 and JMJ32 in response to ABA during the post-germination stage, I first searched the differentially expressed genes for H3K27me3-bound and ABA-regulated genes. I then enriched the data set for the H3K27me3 mark by searching the genes that were differentially expressed in the *jmj30-2 jmj32-1* double mutant following ABA treatment against a published genome-wide chromatin immunoprecipitation (ChIP)-seq dataset obtained in the absence of ABA (Charron et al. 2009). I found that of the 60 differentially expressed genes, 25 gene had the repressive H3K27me3 mark (Fig. 31, Table 7). I next asked how many of the JMJ30- and JMJ32-dependent genes were also significantly differentially expressed during post-germination (after germination to seedling development) using a publicly available dataset that measures changes in gene expression for 1 to 60 hours after ABA treatment (Song et al. 2016). Twelve of the 60 genes fulfilled this criterion (Fig. 32). Six of the 12 genes had the repressive H3K27me3 mark at least in the absence of ABA (Fig. 31). Fig. 32 shows a clustered heatmap of the expression changes observed in all datasets. Eight genes were upregulated and four genes were downregulated following ABA treatment. Most of the 8 genes co-regulated by JMJs and ABA had almost reached their highest expression levels by 4 hours after ABA treatment (Fig. 32-33). Similarly, four genes were at their lowest expression levels 8 hours after ABA treatment (Fig. 32-33).

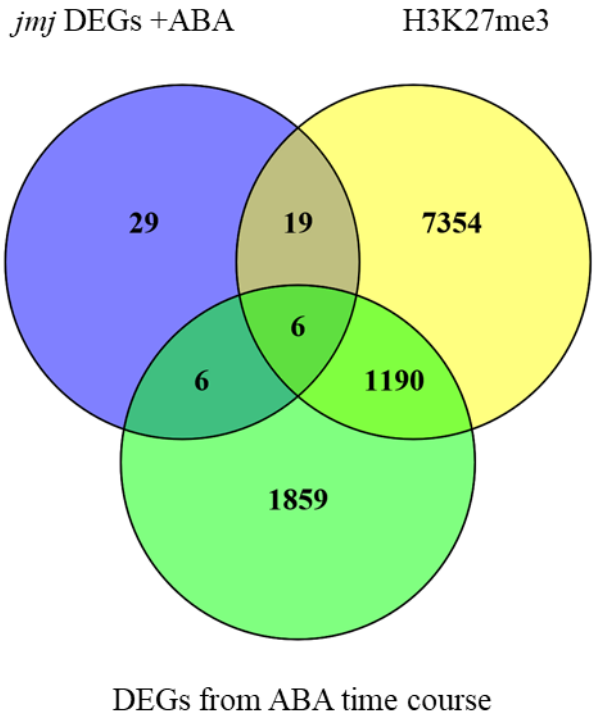

Figure 31. Venn diagram showing the number of genes differentially expressed in ABA-treated wild-type (WT) and *jmj30-2 jmj32-1* seedlings, and their overlap with H3K27me3 and differentially expressed genes following ABA treatment.

Table 7 Overlapped genes between different omics data.

33 overlap genes in "WT vs jmj +ABA" and "H3K27me3"	17 overlap genes in "DE genes from ABA time course" and "H3K27me3"	9 overlap genes in "WT vs jmj +ABA", "H3K27me3", and "DE genes from ABA time course"
AT1G13430	AT1G78290	AT1G13420
AT1G14940	AT2G44970	AT1G48130
AT1G17410	AT4G21490	AT1G62660
AT1G27565	AT4G31830	AT3G06770
AT1G52905	AT4G37420	AT4G23670
AT1G53490	AT5G01250	AT4G27140
AT1G72970	AT5G01300	AT4G27160
AT1G73860	AT5G48430	AT4G28520
AT3G11220	AT1G13420	AT5G51760
AT3G47990	AT1G48130	
AT3G55646	AT1G62660	
AT4G11190	AT3G06770	
AT4G12510	AT4G23670	
AT4G12520	AT4G27140	
AT4G20260	AT4G27160	
AT4G32850	AT4G28520	
AT5G10140	AT5G51760	
AT5G15360		
AT5G41810		
AT5G44610		
AT5G46900		
AT5G56370		
AT5G57380		
AT5G62800		
AT1G13420		
AT1G48130		
AT1G62660		
AT3G06770		
AT4G23670		
AT4G27140		
AT4G27160		
AT4G28520		
AT5G51760		

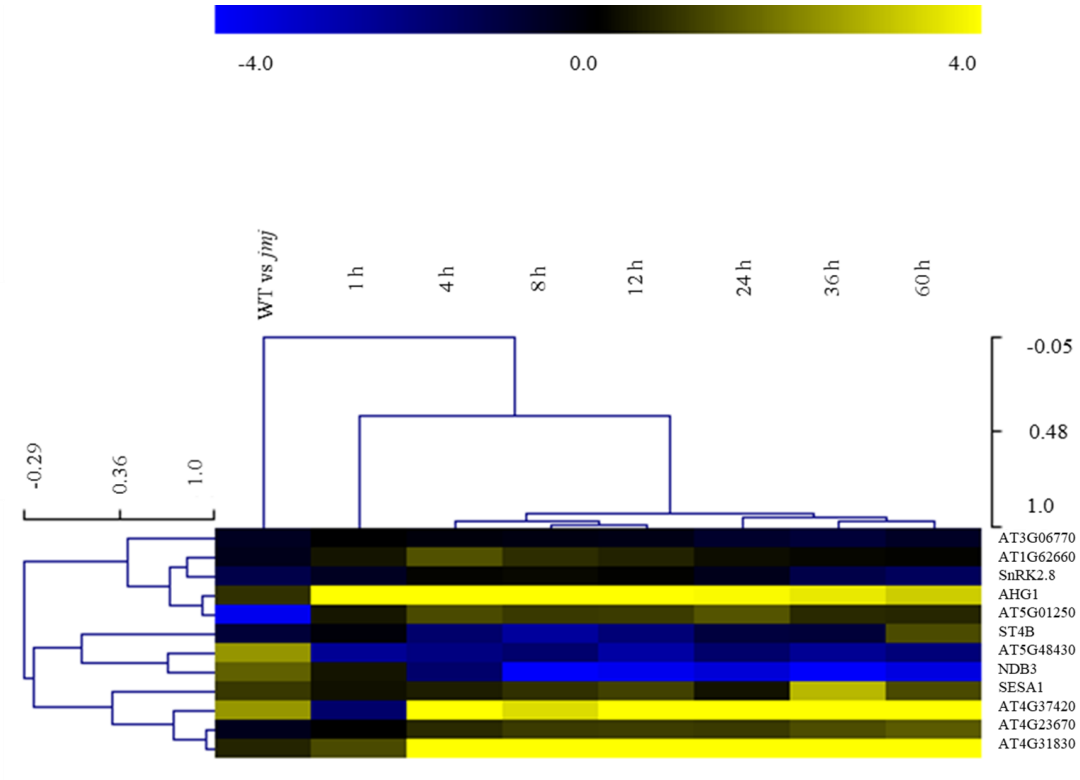

Figure 32. Heatmap displaying the $\log_2$ expression changes of the 12 H3K27me3 targets based on two transcriptome datasets. WT vs *jmj* represents $\log_2$ expression changes between ABA-treated WT and ABA-treated *jmj30-2 jmj32-1* which from the raw data from RNA-Seq. The time course data from a public transcriptome dataset (Song et al. 2016).

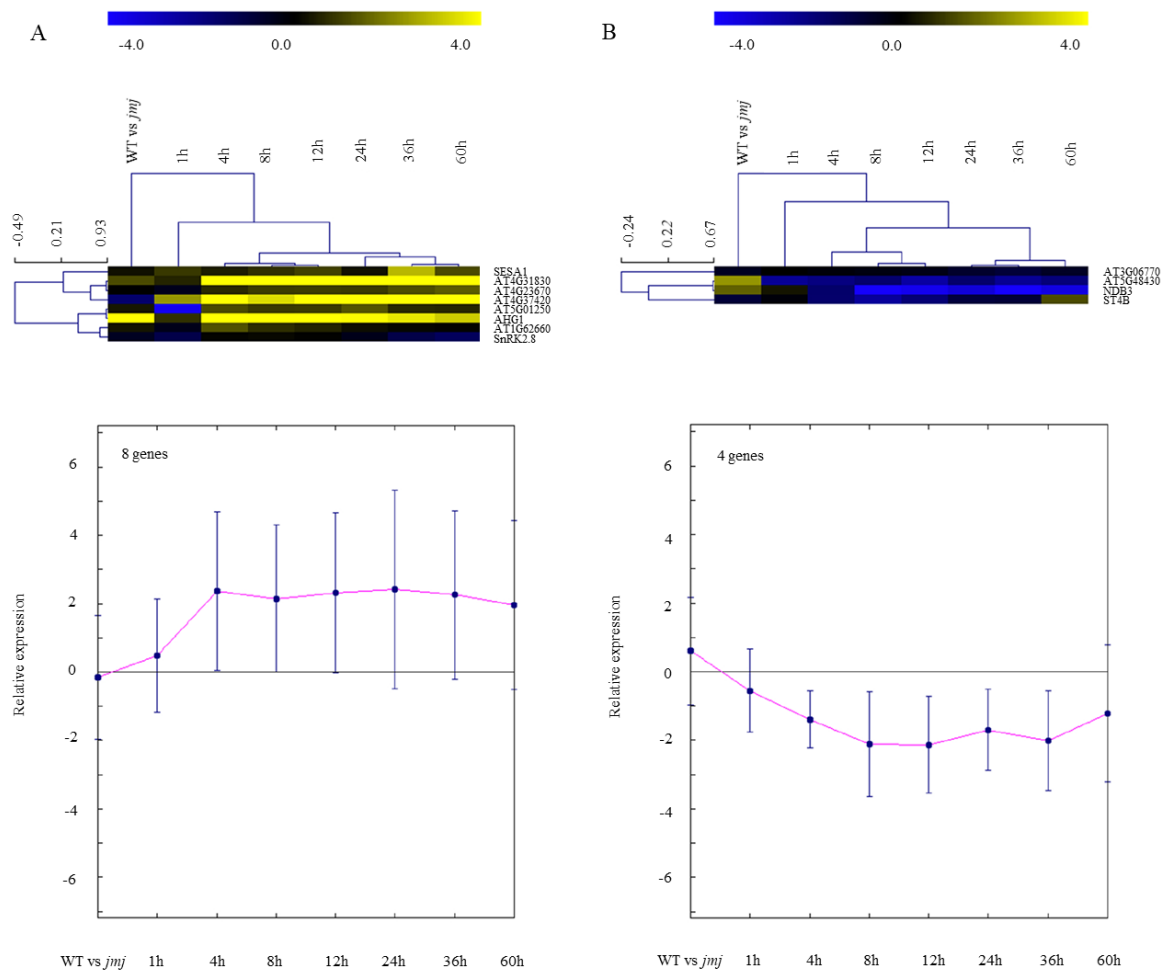

Figure 33. Clustering of differentially expressed genes in the *jmj30 jmj32* mutant in response to ABA during post-germination. (A, B) A k-means clustering of differentially expressed genes in the *jmj30 jmj32* mutant in response to ABA during post-germination. WT vs *jmj* represents $\log_2$ expression changes between ABA-treated WT and ABA-treated *jmj30-2 jmj32-1* which from the raw data from RNA-Seq.. Heatmap (above) and graph (below) display the log2 expression changes of the 8 upregulated (A) and 4 downregulated (B) genes upon ABA treatment based on a public transcriptome dataset (Song et al. 2016).

To assess H3K27me3 levels with and without ABA treatment, I performed a ChIP assay with a H3K27me3 antibody followed by quantitative PCR (qPCR) (Fig. 34). H3K27me3 was associated with a region approximately 2 kb upstream of the transcription start site at *SnRK2.8* (fragment P2) in mock-treated wild type and *jmj30-2 jmj32-1* mutants (Fig. 34A). Upon ABA treatment, H3K27me3 levels were decreased in the wild type. However, this reduction was not observed in ABA-treated *jmj30-2 jmj32-1* mutants (P2: $p < 0.05$ by one-way ANOVA test) (ABA-treated wild type vs. the other samples: $p < 0.05$ by post-hoc Tukey's HSD) (Fig. 34A). I also detected a reduction in H3K27me3 levels in the exon regions (P2 and P5) of *AT1G62660* in mock-treated wild type compared to that in ABA-treated wild type and mock- or ABA-treated *jmj30-2 jmj32-1* mutants (Fig. 34B) ($p < 0.05$ by one-way ANOVA test) (ABA-treated wild type vs. the other samples: $p < 0.05$ by post-hoc Tukey's HSD). Likewise, greater enrichment of H3K27me3 in the first and second exons of *AT4G23670* was observed in mock-treated wild type and mock- and ABA-treated *jmj30-2 jmj32-1* mutants (P2 and P4: $p < 0.05$ by one-way ANOVA test) (ABA-treated wild type vs. the other samples: $p < 0.05$ by post-hoc Tukey's HSD) (Fig. 34C). These results suggest that JMJ30 and/or JMJ32 activities are necessary to remove H3K27me3 in response to ABA.

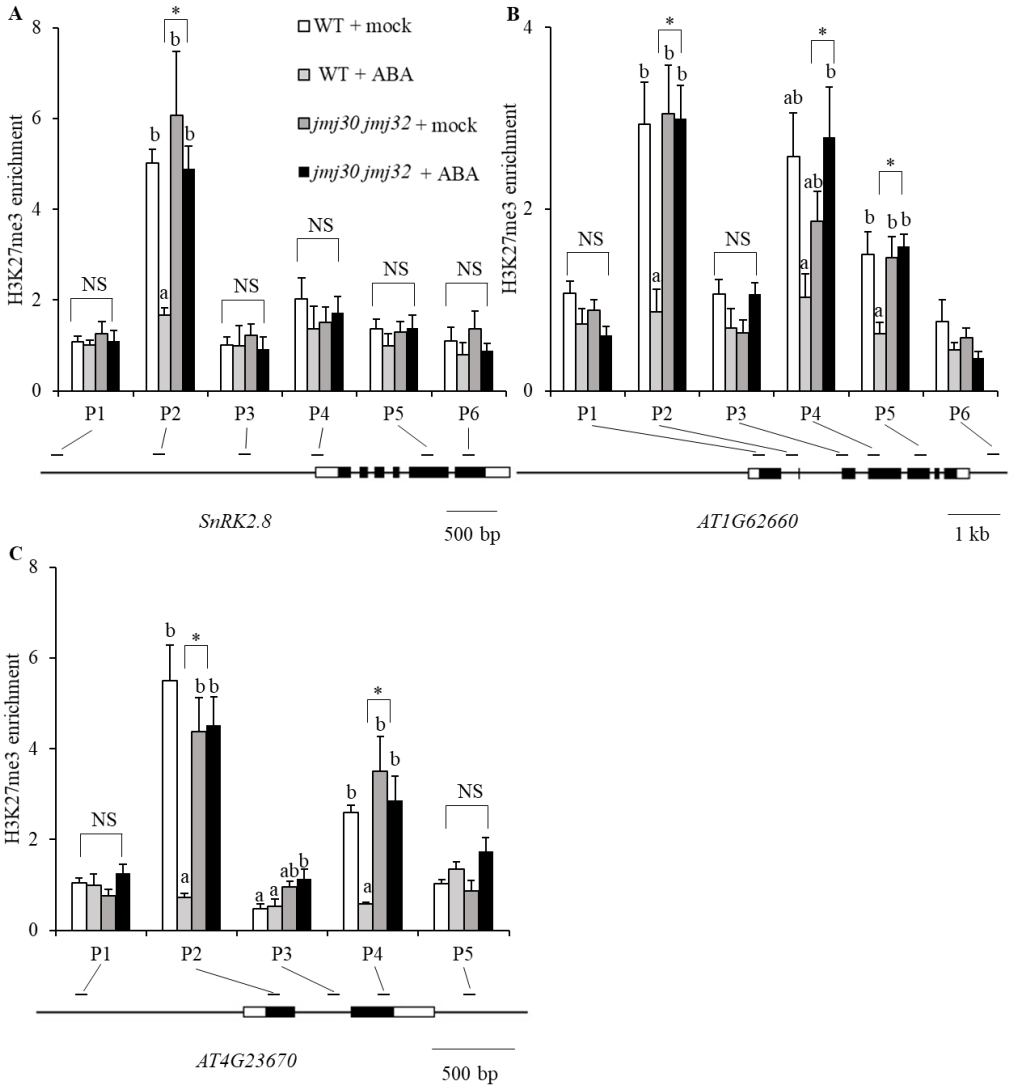

Figure 34. H3K27me3 ChIP at the *SnRK2.8* (A), *AT1G62660* (B), and *AT4G23670* (C) loci in ABA-treated WT and *jmj30-2 jmj32-1* seedlings. PCR fragments (P) and schematic diagram of genes are shown above the ChIP data. White bars, untranslated regions; black bars, protein coding regions. The WT with 5 hour mock treatment (P1 locus) was set to 1.0 and the relative enrichment were calculated after normalization of the input DNA. Values are mean ± SEM from three independent experiments. Asterisks indicate significant differences based on one-way ANOVA test. $p < 0.05$. Different letters indicate significant differences, while same letters indicate non-significant differences based on post-hoc Tukey's HSD test. $p < 0.05$.

To address whether those three genes are regulated by JMJ30 directly, I carried out ChIP-qPCR with a published human influenza hemagglutinin (HA) epitope-tagged and biologically active JMJ30 protein (the *pJMJ30::JMJ30-HA* line) (Fig. 35). Consistent with the H3K27me3 ChIP result, I detected JMJ30-HA association with a region approximately 1–2 kb upstream of the *SnRK2.8* start codon in the 5' promoter region only when ABA treatment was conducted (P2 and P3: $p < 0.05$ by one-way ANOVA test) (ABA-treated JMJ30-HA vs. the other samples: $p < 0.05$ by post-hoc Tukey's HSD) (Fig. 35A). In addition, I tested JMJ30 binding to the *AT1G62660* and *AT4G23670* regulatory regions (Fig. 35B, C). I detected JMJ30-HA association with the P2, P4, and P5 regions of the *AT1G62660* exons, but I did not detect any enrichment signals at *AT4G23670* using five different amplicons (Fig. 35B, C). Since I observed H3K27me3 deposition at *AT4G23670*, this deposition could be due to JMJ32 or other histone demethylases. These findings reveal a direct link between histone demethylases and ABA-dependent responses in some genes detected by transcriptome.

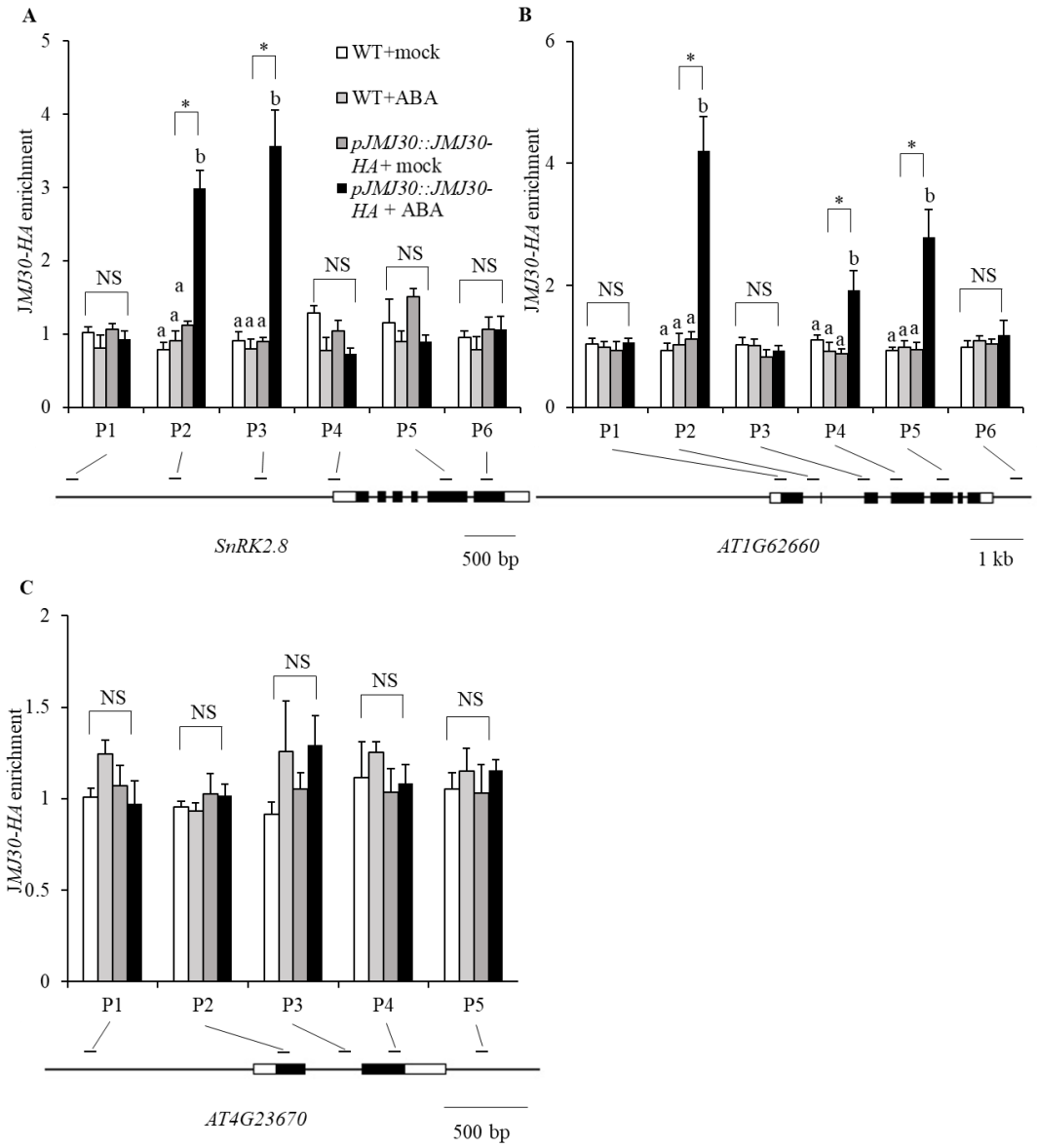

Figure 35. JMJ30-HA ChIP at the *SnRK2.8* (A), *AT1G62660* (B), and *AT4G23670* (C) loci in ABA-treated WT and *pJMJ30::JMJ30-HA* seedlings. Values are mean ± SEM from three independent experiments. The WT with 5 hour mock treatment (P1 locus) was set to 1.0 and the relative enrichment were calculated after normalization of the input DNA. Values are mean ± SEM from three independent experiments. Asterisks indicate significant differences based on one-way ANOVA test. $p < 0.05$. Different letters indicate significant differences, while same letters indicate non-significant differences based on post-hoc Tukey's HSD test. $p < 0.05$.

4.6 SnRK2.8 plays a key role in JMJ-mediated growth arrest in response to ABA during post-germination

Previous researches reported that SnRK2.8 positively regulates ABA response and drought tolerance (Kim et al. 2012a; Umezawa et al. 2004). Since my data suggest that *SnRK2.8* is a downstream target of JMJ30, it is worthwhile to check the function of JMJ-SnRK2.8 modules in ABA responses. To understand the role of SnRK2.8 in JMJ-mediated growth arrest, I conducted a rescue experiment of the ABA insensitivity in *jmj30 jmj32* double mutants. I overexpressed *SnRK2.8* under the control of the ubiquitous 35S promoter (*SnRK2.8ox*) in the double mutants. Among the resulting independent lines, *jmj30-2 jmj32-1 SnRK2.8ox* line 1 (L1) had a similar expression level of *SnRK2.8* to ABA-treated wild type (Fig. 36). I also identified two *jmj30-2 jmj32-1 SnRK2.8ox* lines that the expression levels of *SnRK2.8* are more than 10-fold as compared with ABA-treated wild-type seedlings (Fig. 36). Consistent with the previous publication (Kim et al. 2012a), *SnRK2.8ox* L11 show delay of germination phenotype (Fig. 37). However, I did not see a similar effect when I used the weak L1 line (Fig. 37- 38). I therefore used the L1 line for my further phenotypic analyses. In the absence of ABA, wild type, *jmj30-2 jmj32-1*, and *jmj30-2 jmj32-1 SnRK2.8ox* L1 all grew normally (Fig. 38A-D, Fig 39-40). Although the percentage of arrested plants in *jmj30-2 jmj32-1* double mutants was significantly decreased by 0.25 μM ABA treatment (WT + 0.25 μM ABA vs. *jmj30-2 jmj32-1* + 0.25 μM ABA: $p = 3.2 \times 10^{-26}$), no such reduction was observed when *SnRK2.8* was overexpressed (WT

+ 0.25 μM ABA vs. *jmj30-2 jmj32-1 SnRK2.8ox* L1 + 0.25 μM ABA: $p > 0.05$) (Fig. 38E-H, Fig. 39-40). Likewise, the ABA-less sensitive phenotype seen in *jmj30-2 jmj32-1* double mutants was not observed in the *jmj30-2 jmj32-1 SnRK2.8ox* L1 in the presence of 0.5 μM ABA (WT + 0.5 μM ABA vs. *jmj30-2 jmj32-1 SnRK2.8ox* L1 + 0.5 μM ABA: $p > 0.05$) (Fig. 38I-L, Fig. 39-40). Thus, I concluded that the direct target of JMJ, *SnRK2.8*, regulates growth arrest in response to ABA.

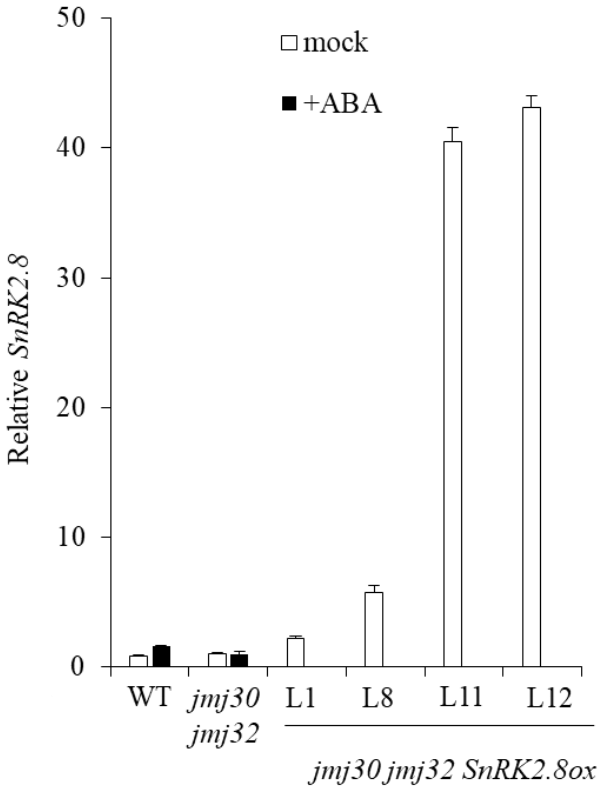

Figure 36. *SnRK2.8* expression in *jmj30 jmj32* double mutants.

Expression of *SnRK2.8* in four independent *jmj30-2 jmj32-1 SnRK2.8ox* lines. The WT with 5 hour mock treatment was set to 1.0 and the relative expressions were calculated. Results are from three independent experiments. Values represent mean ± SEM.

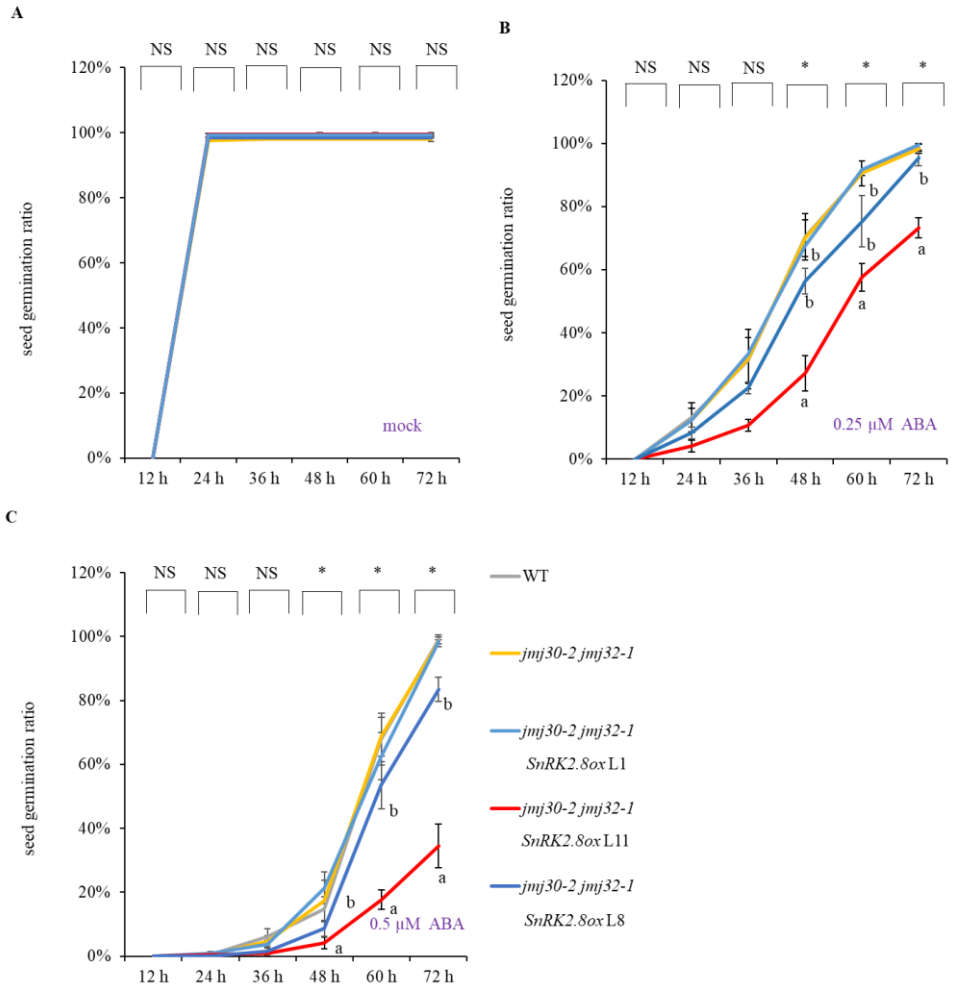

Figure 37. Germination rates between wild type, *jmj30 jmj32* and *jmj30 jmj32 SnRK2.8ox* lines with and without ABA.

Rates of seed germination on 1/2 MS agar plates in the absence (A) and in the presence of 0.25 µM (B) and 0.5 µM (C) ABA. Values represent mean ± SD. Asterisks indicate statistical significance based on Chi-Squared test.

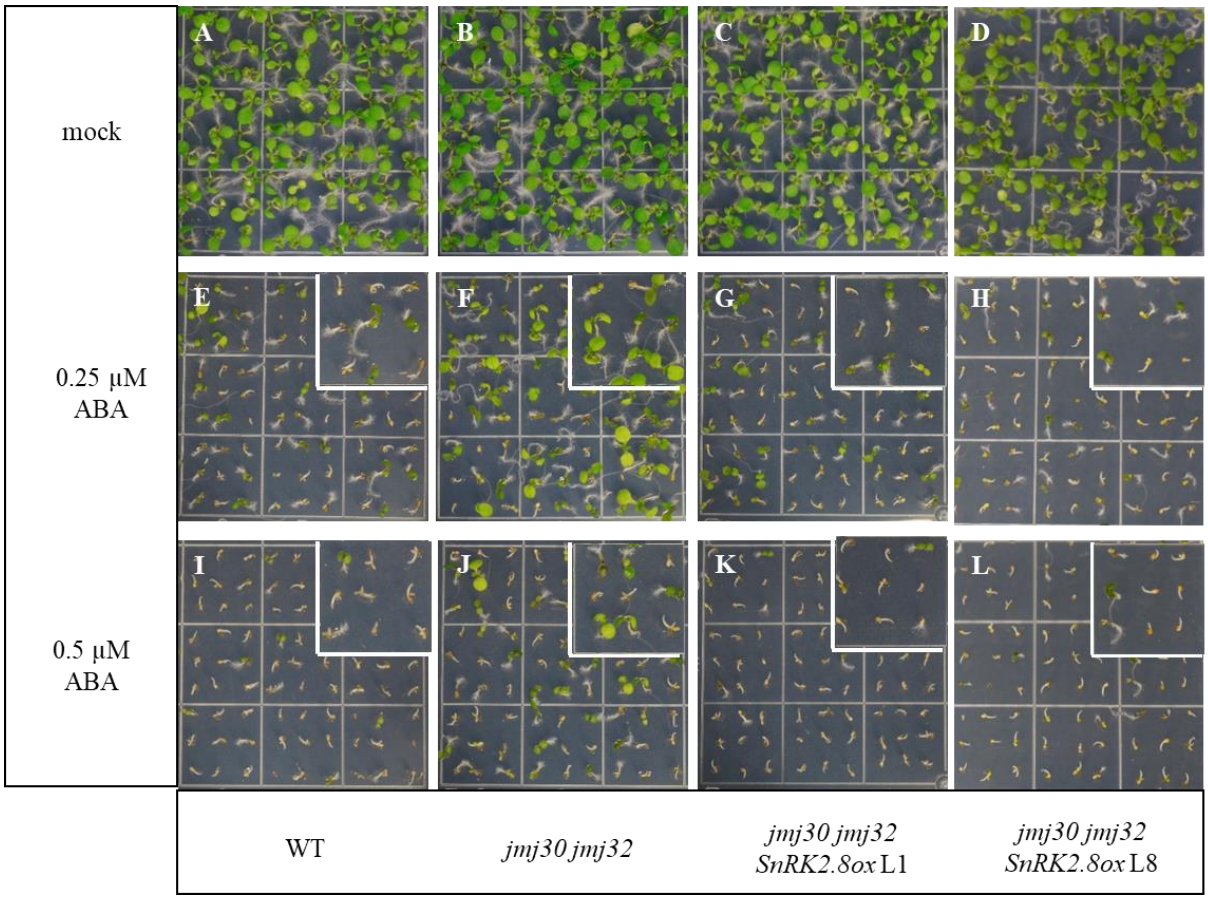

Figure 38. Ectopic expression of *SnRK2.8* rescued the ABA less sensitive phenotype seen in the ABA-treated *jmj30 jmj32* double mutant.

(A-I) Representative images of wild-type (A, E, I), *jmj30-2 jmj32-1* (B, F, J), *jmj30-2 jmj32-1 SnRK2.8ox* L1 (C, G, K)), and *jmj30-2 jmj32-1 SnRK2.8ox* L1 (D, H, L) seedlings grown for 5.5 days on 1/2 MS medium containing 0 μM (A-D), 0.25 μM (E-H), and 0.5 μM ABA (I-L). Insets in E-L show close-ups of representative seedlings.

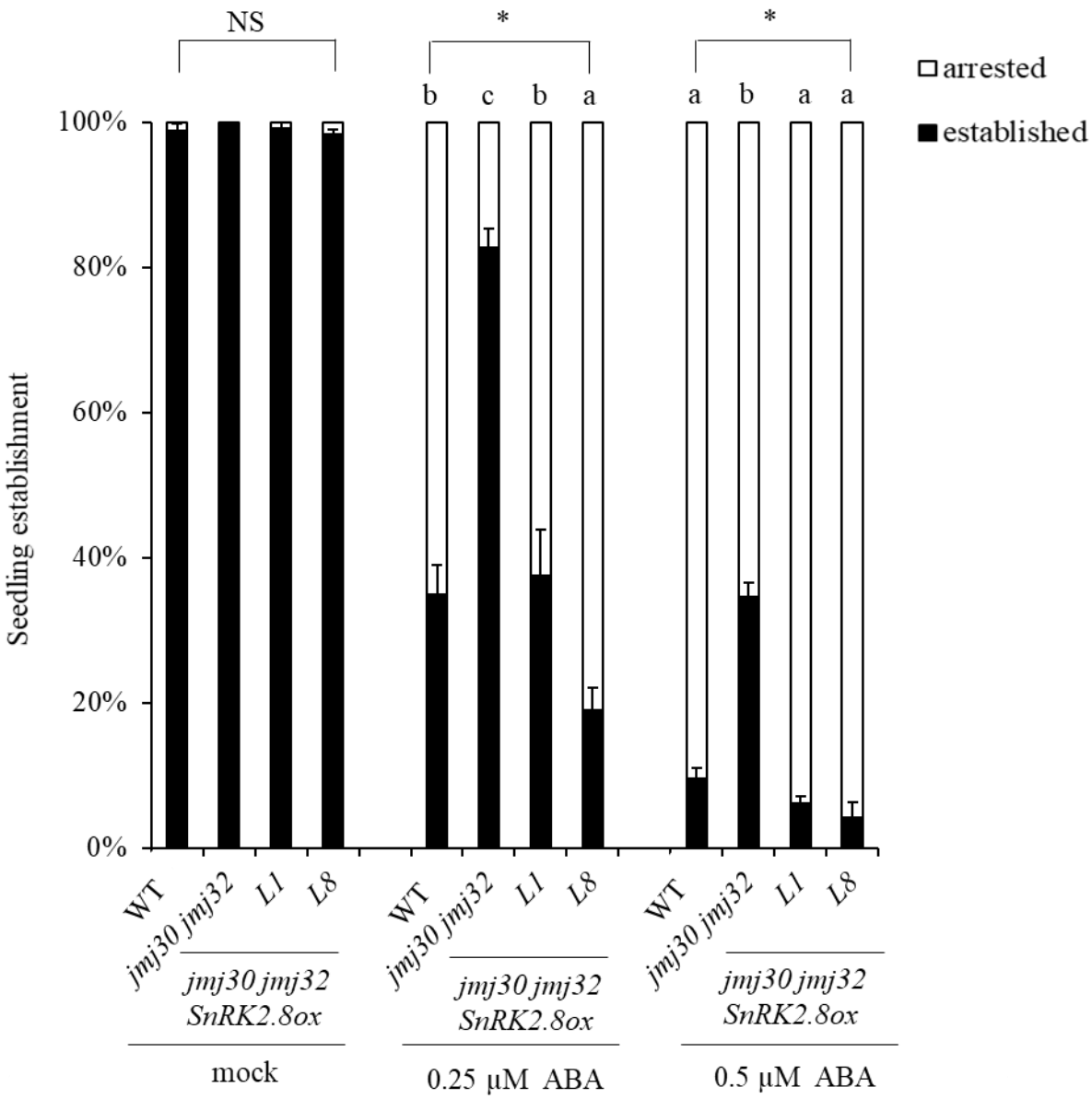

Figure 39. Percentages of established and arrested seedlings in *jmj30-2 jmj32-1*, *jmj30-2 jmj32-1 SnRK2.8 ox* L1, and *jmj30-2 jmj32-1 SnRK2.8 ox* L8 plants in the absence and presence of ABA. Asterisks indicate significant differences based on one-way ANOVA test. $p < 0.05$. Different letters indicate significant differences based on post-hoc Tukey's HSD test. $p < 0.01$. n = 243. NS, non significant. Values representS mean ± SEM of 243 and 81 plants, respectively.

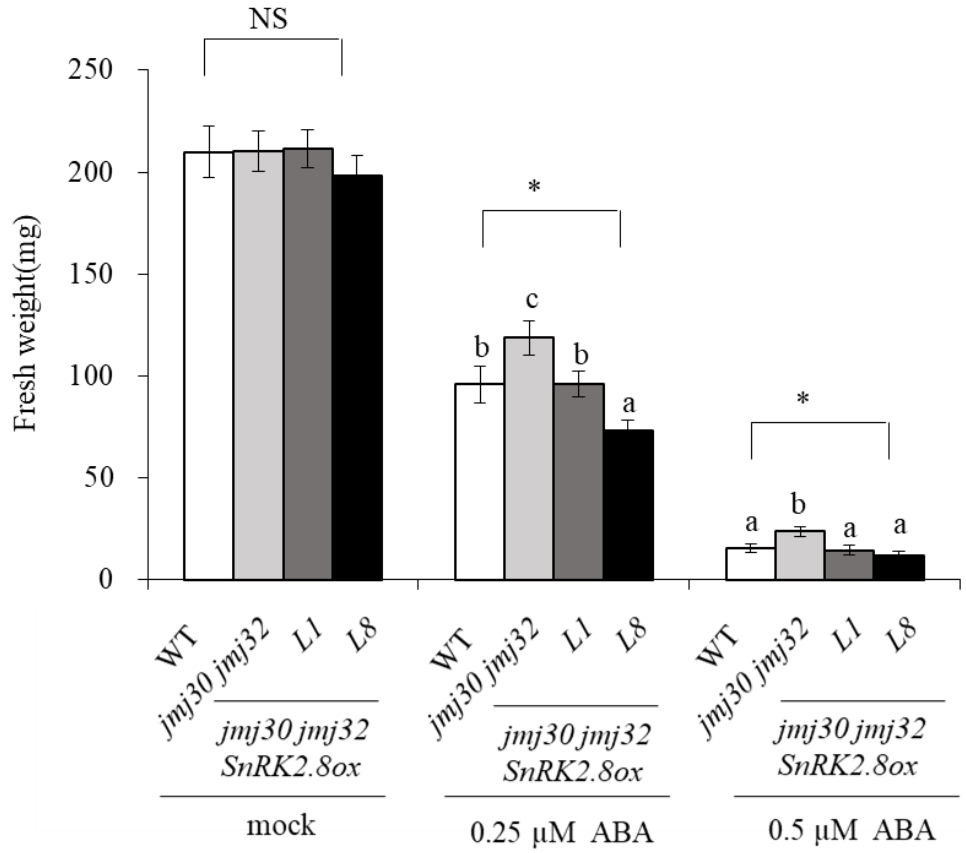

Figure 40. Measurement of the fresh weight of *jmj30-2 jmj32-1, jmj30-2 jmj32-1 SnRK2.8 ox* L1, and *jmj30-2 jmj32-1 SnRK2.8 ox* L8 seedlings in the absence and presence of ABA. Asterisks indicate significant differences based on one-way ANOVA test. $p < 0.05$. Different letters indicate significant differences based on post-hoc Tukey's HSD test. $p < 0.01$. NS, non significant. Values representS mean ± SEM of 243 and 81 plants, respectively.

5. Discussion

5.1 JMJ30 and JMJ32 act redundantly in ABA response

Here, I demonstrated that JMJ30 and JMJ32 are necessary for ABA-dependent growth arrest during post-germination. Two lines of evidences support this conclusion. Firstly, phenotypical analysis indicated that only *jmj30-2 jmj32-1* double mutant showed reduced sensitivity to ABA; however, *jmj30-2* nor *jmj32-1* single mutant displayed no difference in ABA sensitivity as compared to WT (Fig. 14-20). On the other hand, I found out that *JMJ30* expression between WT and *jmj32* mutant showed no significant difference under either mock or ABA treatment condition based on expression analysis (Fig. 21). Up-regulation of *JMJ30* induced by ABA treatment indicates that it might have an important role in compensating the loss or reduction of histone demethylase activity in response to environmental stress. Certain levels of JMJ32 activity may contribute to the maintenance of H3K27me3, possibly through the counteraction of histone methyltransferases activities. Thus, this might be the reason of *jmj30* mutation sensitized in *jmj32* background. These results implied that JMJ32 is important to maintain the ABA response. Secondly, the RT-qPCR results showed that only *JMJ30* but not *JMJ32* induced by ABA treatment and this was correlated with my GUS assay result (Fig. 4 and Fig. 6). JMJ30-GUS expression was highly localized in the root meristem region and root differentiation area with GUS signals increased after ABA treatment (Fig. 4). However, JMJ32-GUS accumulation in root meristem was not affected by ABA treatment (Fig. 7). Although

JMJ32 was not ABA inducible, it cannot be ruled out that JMJ32 is important for ABA-mediated growth arrest. As consistent well with the phenotype of high-temperature-mediated early flowering only performed in *jmj30 jmj32* double mutants (Gan et al. 2014), these results also suggest that JMJ30 and JMJ32 both contribute to execute ABA-dependent growth arrest.

5.2 ABA-inducible JMJ30 depends on the function of ABI3

ABI3 was reported as a master regulator of ABA-dependent growth arrest (Giraudat et al. 1992; Lopez-Molina et al. 2002). Previous studies have revealed that ABA-dependent *ABI3* expression is under the control of histone modification (Perruc et al. 2007; Pfluger and Wagner 2007; Aichinger et al. 2009; Uddenberg et al. 2011; Kim et al. 2012b; Han et al. 2012). Although the upstream regulation of *ABI3* is well characterized, information about the downstream cascade pathways ABI3 leading to ABA-dependent growth arrest is very limited. Only *ABI5* has been identified as a downstream target of ABI3 involved in growth arrest. *ABI5* up-regulation upon ABA treatment depends on the function of ABI3 (Lopez-Molina et al. 2002). Furthermore, overexpression of *ABI5* rescues growth arrest phenotype of *abi3* (Lopez-Molina et al. 2002). I showed here that *JMJ30* is induced in part via ABI3 (Fig. 8 and Fig. 10). ABA-induced ABI3 promotes the expression of *JMJ30* (Fig. 8, Fig. 10-13). Since the mutation of the RY motif in the *JMJ30* promoter caused a reduction in *JMJ30* expression upon ABA treatment, transcriptional regulation of *JMJ30* by ABI3 could be a direct effect (Fig. 8, Fig. 10-13). My

findings provide an insight to complete the molecular mechanism of epigenetic program changes for growth arrest by ABI3 in response to ABA.

5.3 *SnRK2.8* is a key target of JMJ30 and JMJ32 in response to ABA

Here, I identified several genes regulated by JMJ proteins during ABA-dependent growth arrest. I found links between JMJ30 and JMJ32 under the GO terms "response to organic substance", "response to stimulus", "signaling", and "lipid metabolism" (Fig. 23-24). For germination, plants must utilize organic substances, lipids, and phosphates as energy sources. Thus, it is reasonable that JMJ30 and JMJ32 could direct a process to "respond to" those materials and induce a return to the quiescent state under ABA-mediated stress response during the post-germination stage. Indeed, *jmj30 jmj32* double mutants were not only rescued from arrest growth by ABA treatment, but it also did not retain proper amounts of lipids (Fig. 28).

Of clearer relevance, I found that a direct target of JMJ30 was *SnRK2.8*, which regulated ABA-mediated growth arrest. Overexpression of *SnRK2.8* rescued the ABA less sensitive phenotype of *jmj30 jmj32* double mutants. Identification of this target sheds light on the question of how ABI3-activated JMJ30 directs growth arrest. SnRK2.8 belongs to the serine/threonine kinase superfamily, and the phosphorylated SnRK2s mediated the phosphorylation key transcription factors that mediate ABA responses (Lee et al. 2015; Mustilli et al. 2002; Nakashima et al. 2009; Umezawa et al. 2009; Umezawa et al. 2004). Moreover,

ABI3 is phosphorylated by SnRK2s (Kobayashi et al. 2005; Yang et al. 2017). Thus, a positive feedback loop from JMJ30-SnRK2.8 to ABI3 may lock ABA signaling in the ON state to keep reactivating the stress-tolerance program.

Based on GO term analysis, *MAP18* has been categorized as "related to extracellular stimuli" in cellular responses (Fig. 24). In general, MAP kinase signaling is initiated by stimulus and triggers the activation of a MAP kinase kinase kinase (MAP3K). MAP3K activation leads to phosphorylation to activate MAP kinase kinases (MAP2K). Subsequently, the MAP2K phosphorylates the MAPK for further phosphorylation of substrates, such as transcription factors (Plotnikov et al. 2011). Recently, this MAPK cascade was shown to act downstream of SnRKs in plant stress signaling (Zhu 2016). Detailed characterization of *MAP18* during the post-germination stage needs to be examined in the future.

I identified *AT1G62660* as a direct target of JMJ30. Previous quantitative trait locus （QTL） analysis identified that *AT1G62660* is as regulators for Arabidopsis root elongations (Sergeeva et al. 2006). *AT1G62660* belongs to the glycosyl hydrolase family and it catalyzes the hydrolysis of glycosidic bonds in sugar complexes (Cabello et al. 2014). Therefore, *AT1G62660* might have a role in modulating cell wall remodeling though degradation of cellulose, hemicellulose, and starch. Although I could not identify the direct target(s) of JMJ30 responsible for carbohydrate or lipid metabolism in the *jmj30 jmj32* mutant phenotype thus far, my results support the idea that precise metabolic regulation of energy sources by JMJ30 and

JMJ32 may have important roles during ABA-dependent growth arrest (Fig. 28). *AT4G23670* belongs to the polyketide cyclase/dehydrase and lipid transport super family (Carter et al. 2004). This gene was transcriptionally regulated by JMJ30 and JMJ32 and had higher levels of H3K27me3 deposited in the *jmj30-2 jmj32-1* background than in the wild type (Fig. 34), but I did not observe any direct binding of JMJ30 to this genomic locus (Fig. 35). This indicated the regulation could be due to direct regulation by JMJ32 or a secondary effect. The functions of *AT1G62660* during the post-germination stage need to be checked in the future.

6. Conclusion

Here, I provide new insights into how histone demethylases contribute to stress hormone ABA-dependent growth arrest. ABI3-activated upregulation of *JMJ30* is required for the growth arrest. JMJ30 and JMJ32 redundantly execute this role through removal of H3K27me3 from their downstream target genes. My study reveals that the feedback activation loop of the ABI3 transcription factor, JMJ histone demethylases, and SnRK2.8 kinase makes a key regulatory pathway in ABA-dependent growth arrest.

This study started from the confirmation that *JMJ30* is induced by ABA during seedling establishment. The upregulation of *JMJ30* by ABA depends on the function of *ABI3*. Further genetic and biochemical analysis showed that ABI3 binds to the RY motif of the *JMJ30* promoter and activated *JMJ30* expression. I also identified that *SnRK2.8* was served as one of the downstream targets of *JMJ30* in an ABA-dependent pathway. Consistently, the *jmj30 jmj32* mutant display weakened ABA-mediated growth arrest during post-germination. These findings demonstrate an ABA-dependent feedback pathway that ABI3 activated *SnRK2.8* via JMJ30/JMJ32-mediated H3K27me3 demethylation (Fig. 41).

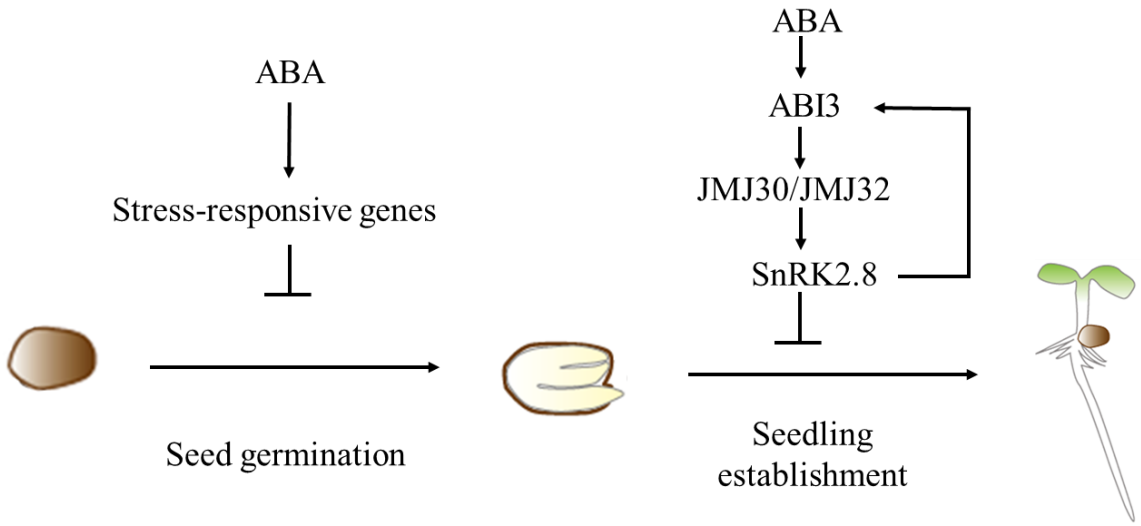

Figure 41. Model for the role of JMJ30 and JMJ32 in response to ABA during the post-germination stage. Roles of ABA at two different stages. In unfavorable conditions, ABA inhibits seed germination after imbibition. This inhibition is independent of JMJ30 and JMJ32. ABA also inhibits later growth of seedling development such as emergence of root hair and cotyledon greening. This pathway is JMJ30 and JMJ32 dependent. Stage-specific function of JMJ30 and JMJ32 are critical for proper growth arrest upon ABA treatment.

Part II JMJ30 and JMJ32 control root elongation in response to abscisic acid in *Arabidopsis*

Abstract

In response to various stresses, abscisic acid (ABA) plays critical roles during plant growth and development. In part I, I reported that *Arabidopsis* histone demethylases JUMONJI-C DOMAIN-CONTAINING PROTEIN30 (JMJ30) and JMJ32 control ABA-mediated growth arrest during the post-germination stage (2–3 days after germination). However, the role of JMJ30 and JMJ32 on ABA response at later stage of plant development remains largely unknown. Here, I show that JMJ30 and JMJ32 mediate ABA response during root development. In the presence of ABA, *jmj30 jmj32* double mutants displayed longer primary root phenotype than wild type. Loss-of-function mutation in the *SNF1-RELATED PROTEIN KINASE 2.8* (*SnRK2.8*) gene also led to longer primary root phenotype in response to ABA. My expression analysis suggests that *JMJ30/JMJ32* and *SnRK2.8* act in the same pathway to mediate ABA response during root elongation at seedling stage. My findings highlight the importance of JMJ30/JMJ32-SnRK2.8 module at two different developmental stages.

1. Introduction

Abscisic acid (ABA) is a key stress hormone (Verma et al. 2016; Finkelstein 2013). In response to stress such as water deficit and salt stress, not only the amount of ABA, but also ABA perception and response are properly mediated. Stress triggers the biosynthesis of ABA. The resulting ABA accumulates in the cytosol and binds to the ABA receptors PYRABACTIN RESISTANCE1 (PYR1)/PYR1-LIKE(PYL)/REGULATORY COMPONENTS OF ABA RECEPTORS (RCAR) (Cutler et al. 2010; Park et al. 2009). The activated ABA receptors bind to phosphatases 2C (PP2C) like ABSCISIC ACID-INSENSITIVE1 (ABI1) or ABI2 and inhibit catalytic activity of PP2C (Merlot et al. 2001). Then, SNF1-RELATED PROTEIN KINASE 2 (SnRK2) kinases are released from PP2C-mediated inactivation and trigger gene expression through phosphorylation (Kulik et al. 2011; Nakashima et al. 2009; Umezawa et al. 2009). After reaching certain threshold of ABA concentration or signaling, stomata is closed and gene expression is changed. Although mechanism of opening and closing the stomata by ABA is well-characterized, how ABA-dependent gene expression is controlled in a flexible and reversible manner remains unknown.

Histone modifications have functions both positively and negatively in the regulation of gene expression (Sun et al. 2014; You et al. 2017). H3 histones are modified with acetylation, phosphorylation, methylation and ubiquitination post-translationally (Bannister and Kouzarides 2011). Histone modification enzymes specify when and where histones need to be modified.

Especially, catalyzation of reversible lysine methylation by those enzymes are central to the epigenetic regulation. Despite their importance, the role of histone modification enzymes on ABA response are not characterized.

In part I, I reported that histone demethylases JUMONJI-C DOMAIN-CONTAINING PROTEIN30 (JMJ30) and JMJ32 control ABA-mediated growth arrest during the post-germination stage. To pass through unfavorable stress condition, the B3 domain transcription factor ABSCISIC ACID INSENSITIVE3 (ABI3) is activated by ABA (Kagaya et al. 2005) . ABA-activated ABI3 promotes the expression levels of JMJ30, presumably by direct binding via the evolutionally conserved RY motif. Then, JMJ30 and JMJ32 remove repressive H3K27me3 marks at the *SnRK2.8* locus to activate its expression. Upregulated *SnRK2.8* promotes ABA-dependent gene expression and feedbacks to ABI3 activation.

2. Objective of this study

1. To examine the JMJs induction by ABA during vegetative stages

2. To investigate the ABA sensitivity between wild type and *jmj* mutant during vegetative stages

3. To validate the role of JMJ-SnRK2.8 during vegetative stages

3. Materials and Methods

3.1 Plant Materials and Growth Conditions

The *snrk2.8-1* (SALK_073395) mutant was obtained from the Arabidopsis Biological Resource Center (ABRC) with the Columbia (Col-0) background. Prior to grow mutants, genotype was confirmed by PCR using Emerald Amp polymerase (Takara). The primers for genotyping are as follows: jmj30-2 genotyping-FW; CAAACTCTGCTGCAATCGATTTC, jmj30-2 genotyping-RV; GAAAATGTCACAAGCTCTTGCTTC, jmj32-1 genotyping-FW; GACTGAGAAAACCTGAACTCAGC, jmj32-1 genotyping-RV; GTCGTGTAAAGGACTGAAGGTTG, snrk2.8-1 genotyping-FW; CAAACCATGACACATCAGCAC, snrk2.8-1 genotyping-RV; AGGCTCCTGTTAATCACCAGG . All of the plants were grown at 22°C growth chamber under continuous light condition after stratification at 4°C for 3 days.

3.2 Phenotypic and Statistical Analyses

The 1/2 MS plate preparation and seed surface sterilization were describe previously (Part I 3.3). For root elongation assay, the sterilized wild-type, *jmj30-2 jmj32-1* and *snrk2.8-1* seeds were placed on the 1/2 MS plates, stratified at 4°C for 3 days, and then placed in a growth chamber at 22°C under continuous light for 3 days. 3-day-old plants were transplanted onto 1/2 MS plates with 1% sucrose supplemented with 0 μM, 5 μM ABA or 10 μM ABA and grown

vertically under 24-hour light condition for additional 7 days. The primary root length was measured then statistical analyses were conducted by Excel. Statistical significance was computed using two-tailed Student's *t*-test.

3.3 Expression analysis

For ABA treatment, 4-day-old plants after stratification grown on 1/2 MS plates with 1% sucrose were treated with 10 μM ABA to induce rapid changes in gene expression. After 3 hour treatment, the harvested seedlings were used for RNA extraction. The RNA isolation and RT-qPCR methods were followed the previous protocol (Yamaguchi et al. 2017). Three independent biological replicates were performed for the qPCR analyses and four technical replicates were conducted for each experiment. Statistical significance was computed using either one-way ANOVA test followed by post-hoc Tukey's HSD test and two-tailed Student's *t*-test for multiple and single pair comparisons, respectively. The primers for expression analyses are as follows: EIF4A1-FW; TCTTGGTGAAGCGTGATGAG, EIF4A1-RV; AATCAACCTTACGCCTGGTG, JMJ30-FW; GAATCACTTGGACTACCTCAATGC, JMJ30-RV; CATTGGAGACGATTTATTGGTCC, JMJ32-FW; GTTTCATTGTACTGTCAAGGCTGG, JMJ32-RV; CATACTTGATGTCAAACTGCATGTC, ABI3-FW; ATGTATCTCCTCGAGAACAC, ABI3-RV; CCCTCGTATCAAATATTTGCC, ABI5-FW; ACCTAATCCAAACCCGAACC, ABI5-RV; TACCCTCCTCCTCCTGTCCT,

SnRK2.8-FW; GTTGCCAACCCTGAAAAGAG, SnRK2.8-RV; CCGAGCTTCTTCAATGATCC.

4. Results

4.1 JMJ30 and JMJ32 positively regulate ABA responses in root elongation

Previous comprehensive expression study for the *JUMONJI-C DOMAIN-CONTAINING PROTEIN* genes in response to stress revealed that JMJ30 is upregulated by ABA during vegetative stage (Qian et al. 2015). However, nothing is known about the function of JMJ30 and JMJ32 in ABA response during vegetative stages. To understand their roles, I performed phenotypic analysis using *jmj30 jmj32* double mutants in the absence or presence of ABA at vegetative stages (Fig. 42). The 3-day-old wild-type and *jmj30-2 jmj32-1* double mutant seedlings were transferred to 1/2 MS plates with or without ABA to observe the role of JMJ30/JMJ32 at vegetative stages. When grown and transferred on 1/2 MS plates without ABA, wild-type and *jmj30-2 jmj32-1* plants showed no obvious difference in their phenotypes (Fig. 42A). Both plants displayed normal size and color of leaves and well-grown primary root with a lot of lateral roots (Fig. 42A). No significant difference in primary root length was observed between wild type and *jmj30-2 jmj32-1* without ABA ($p > 0.05$ by two-tailed Student's *t*-test) (Fig. 42D). Both ABA-treated plants had smaller and paler leaves and shorter roots compared to control plants (Fig. 42A-C). In the presence of 5 μM ABA, length of primary root in wild type was 3.7 ± 0.1. On the other hand, root length of 5 μM ABA-treated *jmj30-2 jmj32-1* plants was 4.2 ± 0.1 and significant difference was observed between them ($p < 0.01$ by two-tailed Student's *t*-test). In the presence of 10 μM ABA, root elongation was inhibited more than those

in 5 μM ABA-treated plants (Fig. 42B, C). There were still significant differences in root length between 10 μM ABA-treated wild type and *jmj30-2 jmj32-1* ($p < 0.01$ by two-tailed Student's *t*-test) (Fig. 42D). These results suggest that JMJ30 and JMJ32 are required for ABA-dependent root growth inhibition during vegetative stage.

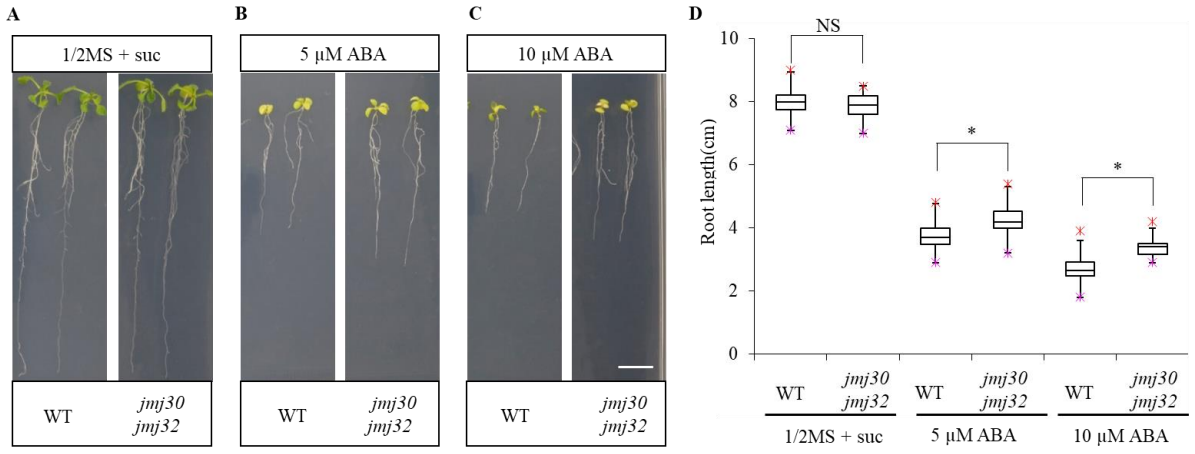

Figure 42. *jmj30 jmj32* double mutants are less sensitive to ABA. (A-C) Representative images of wild-type and *jmj30-2 jmj32-1* plants in the absence and presence of ABA. The wild-type and *jmj30-2 jmj32-1* seeds were sown on 1/2 MS with 1% sucrose and stratified at 4 °C for 3 days. The plants were grown under 24-hour light condition for 3 days. 3-day-old wild-type and *jmj30-2 jmj32-1* plants were then transplanted onto 1/2 MS plates with 1% sucrose supplemented with 0 μM ABA (A), 5 μM ABA (B) or 10 μM ABA (C) and grown vertically under 24-hour light condition for additional 7 days. Scale bar = 1 cm. (D) Quantification of root length in wild-type and *jmj30-2 jmj32-1* plants in Figure 42A-C. Asterisks indicate significant differences based on two-tailed Student's *t*-test. $p < 0.01$. NS, non significant. Values represent mean ± SD of 24 plants.

4.2 SnRK2.8 positively regulates ABA response in root elongation

To understand the role of SnRK2.8 in ABA-mediated root elongation at vegetative stages, phenotypic analyses were conducted in wild-type and *snrk2.8-1* plants. When grown and transferred on 1/2 MS plates without ABA, wild-type and *snrk2.8-1* plants showed no significant difference in their phenotypes ($p > 0.05$ by two-tailed Student's *t*-test) (Fig. 43A, C). When transferred onto 10 μM ABA plates, root growth was inhibited in both wild type and *snrk2.8-1* (Fig. 43B). However, ABA sensitivity was different between wild type and *snrk2.8-1* mutant. *snrk2.8-1* mutant was less sensitive to ABA, as seen in *jmj30-2 jmj32-1* double mutants ($p < 0.01$ by two-tailed Student's *t*-test) (Fig. 43C). These results suggest that SnRK2.8 is required for ABA-dependent root growth inhibition during vegetative stages.

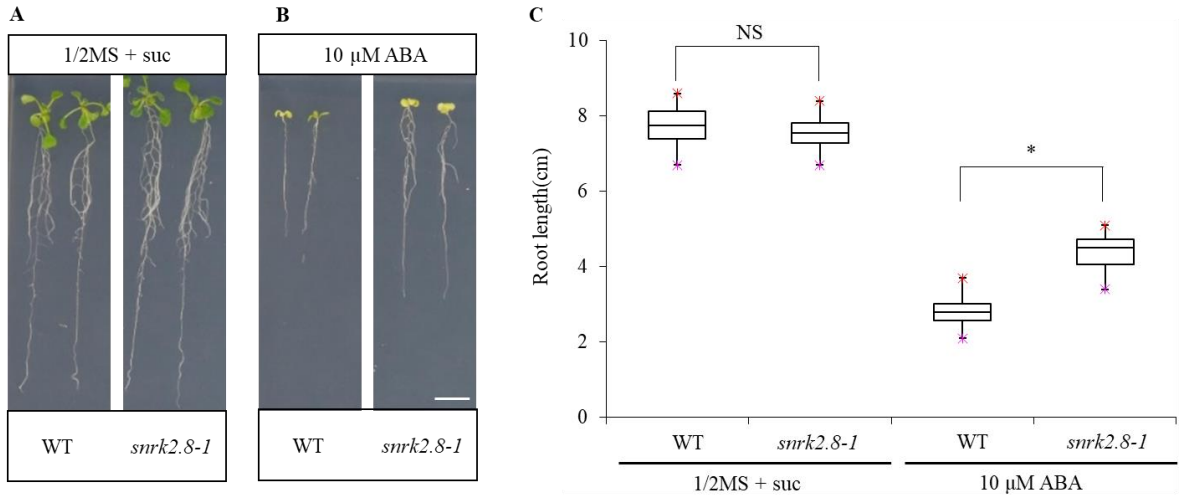

Figure 43. *snrk2.8* mutants are less sensitive to ABA. (A, B) Representative images of wild-type and *snrk2.8-1* plants in the absence and presence of ABA. The wild-type and *snrk2.8-1* seeds were sown on 1/2 MS with 1% sucrose and stratified at 4 °C for 3 days. The plants were

grown under 24-hour light condition for 3 days. 3-day-old wild-type and *snrk2.8-1* plants were then transplanted onto 1/2 MS plates with 1% sucrose supplemented with 0 μM ABA (A), or 10 μM ABA (B) and grown vertically under 24-hour light condition for additional 7 days. Scale bar = 1 cm. (C) Quantification of root length in wild-type and *snrk2.8-1* plants in Figure 43A-B. Asterisk indicates significant difference based on two-tailed Student's *t*-test. $p < 0.01$. NS, non significant. Values represent mean ± SD of 24 plants.

4.3 *SnRK2.8* expression is controlled by JMJ30 in response to ABA during vegetative phase

To examine the relationship between JMJ30/JMJ32 and SnRK2.8 in response to ABA during vegetative stage, quantitative real-time polymerase chain reaction (qRT-PCR) analysis was conducted (Fig. 44A-D). In response to ABA, *JMJ30* is upregulated in ABI3 during post-germination stage. To understand *JMJ30* and *JMJ32* expression in response to ABA during vegetative stage, I first examined *JMJ30* and *JMJ32* expression levels (Fig. 44A-B). Consistent well with the previous publication, *JMJ30* was upregulated in response to ABA ($p < 0.01$ by two-tailed Student's *t*-test) (Fig. 44A). Similar to post-germination stage, upregulation was not observed in *JMJ32* expression (Fig. 44B). To further confirm whether JMJ30 upregulation in response to ABA is dependent on the ABI3 function, I tested *ABI3* expression at vegetative stage. Although I observed significant difference in ABI5 expression in response to ABA, it was not observed in the *ABI3* gene (Fig. 44C-D). Taken together, my data suggest that JMJ30 is

upregulated by a factor other than ABI3. I next addressed the expression levels of *SnRK2.8* (Fig. 44E). ABA-treated WT had more *SnRK2.8* transcripts than mock-treated wild type ($p < 0.01$ by one-way ANOVA test) (WT with ABA vs. WT without ABA: $p < 0.01$ by post-hoc Tukey's HSD) (Fig. 44E). In addition, there is no upregulation of *SnRK2.8* in the *jmj30-2 jmj32-1* background with and without ABA treatment (WT with ABA vs. WT without ABA: $p > 0.05$ by post-hoc Tukey's HSD) (Fig. 44E). This result implies that *SnRK2.8* expression is controlled by JMJ30 in response to ABA during vegetative phase.

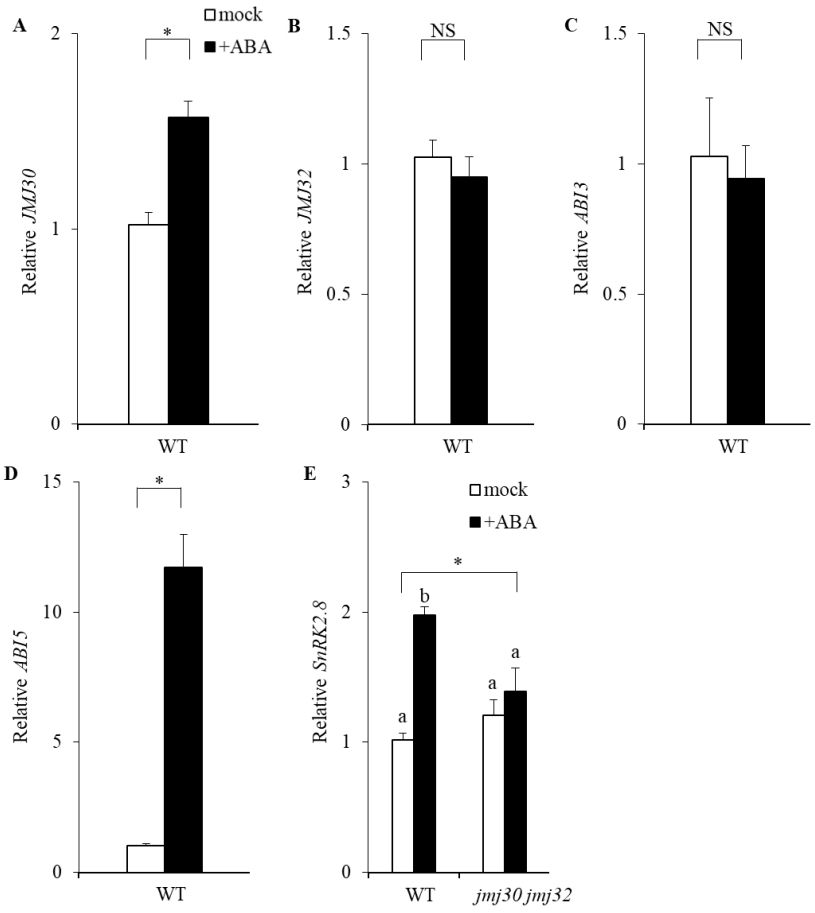

Figure 44. *JMJ30* and *SnRK2.8* expression are induced by ABA. (A-D) Expression of *JMJ30* (A), *JMJ32* (B), *ABI3* (C), and *ABI5* (D) in wild-type plants in response to 10 μM ABA after 5

hours treatment. Results are from three independent experiments. Values represent mean ± SEM. Asterisks indicate significant differences based on two-tailed Student's *t*-test. $p < 0.01$. (E) Expression of *SnRK2.8* in wild-type and *jmj30-2 jmj32-1* plants in response to 10 μM ABA. Results are from three independent experiments. Values represent mean ± SEM. The WT with 5 hour mock treatment was set to 1.0 and the relative expressions were calculated. Asterisk indicates significant differences based on one-way ANOVA test. $p < 0.01$. Different letters indicate significant differences based on post-hoc Tukey's HSD test. $p < 0.01$.

5. Summary

In part I, I showed that the function of JMJ30/JMJ32-SnRK2.8 module is dependent of the ABA-dependent transcription factor, ABI3 during post-germination stage. Here, I demonstrated the role of JMJ30/JMJ32-SnRK2.8 module in response to ABA during root elongation at vegetative stage. Although function of JMJ30/JMJ32-SnRK2.8 module in response to ABA was conserved between two different stages, upstream regulators were different. Thus, I conclude that factor X(s) activates JMJ30 in response to ABA during root elongation at vegetative stage (Fig. 45). It will be interesting to identify such factor in the future. SnRK2.8 plays a role in JMJ-mediated growth arrest in response to ABA during vegetative stage.

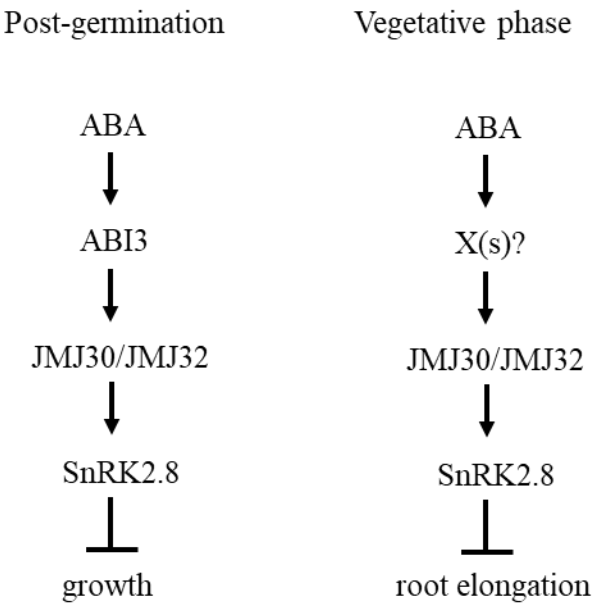

Figure 45. Current model of ABA-mediated hitsone modification.

Acknowledgements

Firstly, I would like to express my gratitude and respect to my supervisor, Dr. Toshiro Ito for his supervision, support and guidance during my Ph.D course. It is my honor to learn under him, not only scientific thinking, time management, and enthusiasm. Truly, I appreciate a lot for his kindness and patience throughout my study.

I am grateful to my mentor, Dr. Nobutoshi Yamaguchi. I don't think I would be able to finish my research without his kind assistance. He is always being helpful to give me technical advices and ideas to produce good research. Besides that, his effective way of conducting experiments and writing has inspired me to pursue my future career.

I would also like to thank the members of my PhD Thesis Committees and Entrance Examination Committees, who are Dr. Taku Demura and Dr. Yusuke Saijo for spending their time to examine my work and provide me valuable comments.

Moreover, the support and assistance from the members in Plant Stem Cell Regulation and Floral Patterning laboratory. Assistant professors, Dr. Makoto Shirakawa and Dr. Yuko Wada, Post-doctoral fellow, Dr. Looi Liang-Sheng, students Ze Hong Lee and Yukun Wang are also the keys for me to accomplish my work.

The financial support from Ministry of Education, Culture, Sports, Science and Technology (MEXT) provided Japanese government allows me to concentrate on my study without worrying about my daily expenses. Specially, I would like to thank Dr. Satoko Maki

for her effort in improving my English language and oral presenting skills.

Last but not least, I want to say a great big heartfelt thanks to my grandmother, parents and sister, for their encouragements and supports, and my beloved partner, Xiaoming Cheng.

References

Aichinger E, Villar CB, Farrona S, Reyes JC, Hennig L, Kohler C (2009) CHD3 proteins and polycomb group proteins antagonistically determine cell identity in Arabidopsis. PLoS Genet 5 (8):e1000605. doi:10.1371/journal.pgen.1000605

Arroyo A, Bossi F, Finkelstein RR, Leon P (2003) Three genes that affect sugar sensing (abscisic acid insensitive 4, abscisic acid insensitive 5, and constitutive triple response 1) are differentially regulated by glucose in Arabidopsis. Plant Physiol 133 (1):231-242

Asami T, Nakagawa Y (2018) Preface to the Special Issue: Brief review of plant hormones and their utilization in agriculture. J Pestic Sci 43 (3):154-158. doi:10.1584/jpestics.M18-02

Atias O, Chor B, Chamovitz DA (2009) Large-scale analysis of Arabidopsis transcription reveals a basal co-regulation network. BMC Syst Biol 3:86. doi:10.1186/1752-0509-3-86

Bannister AJ, Kouzarides T (2011) Regulation of chromatin by histone modifications. Cell Res 21 (3):381-395. doi:10.1038/cr.2011.22

Bentsink L, Koornneef M (2008) Seed dormancy and germination. Arabidopsis Book 6:e0119. doi:10.1199/tab.0119

Bewley JD (1997) Seed Germination and Dormancy. The Plant Cell 9 (7):1055-1066.

doi:10.1105/tpc.9.7.1055

Boros J, Arnoult N, Stroobant V, Collet JF, Decottignies A (2014) Polycomb repressive complex 2 and H3K27me3 cooperate with H3K9 methylation to maintain heterochromatin protein 1alpha at chromatin. Mol Cell Biol 34 (19):3662-3674. doi:10.1128/MCB.00205-14

Boyes DC, Zayed AM, Ascenzi R, McCaskill AJ, Hoffman NE, Davis KR, Gorlach J (2001) Growth stage-based phenotypic analysis of Arabidopsis: a model for high throughput functional genomics in plants. The Plant Cell 13 (7):1499-1510

Cabello S, Lorenz C, Crespo S, Cabrera J, Ludwig R, Escobar C, Hofmann J (2014) Altered sucrose synthase and invertase expression affects the local and systemic sugar metabolism of nematode-infected Arabidopsis thaliana plants. J Exp Bot 65 (1):201-212. doi:10.1093/jxb/ert359

Carter C, Pan S, Zouhar J, Avila EL, Girke T, Raikhel NV (2004) The vegetative vacuole proteome of Arabidopsis thaliana reveals predicted and unexpected proteins. The Plant Cell 16 (12):3285-3303. doi:10.1105/tpc.104.027078

Charron JB, He H, Elling AA, Deng XW (2009) Dynamic landscapes of four histone modifications during deetiolation in Arabidopsis. The Plant Cell 21 (12):3732-3748. doi:10.1105/tpc.109.066845

Chatterjee C, Muir TW (2010) Chemical approaches for studying histone modifications. J

Biol Chem 285 (15):11045-11050. doi:10.1074/jbc.R109.080291

Clough SJ, Bent AF (1998) Floral dip: a simplified method for Agrobacterium-mediated transformation of Arabidopsis thaliana. Plant J 16 (6):735-743

Crevillen P, Yang H, Cui X, Greeff C, Trick M, Qiu Q, Cao X, Dean C (2014) Epigenetic reprogramming that prevents transgenerational inheritance of the vernalized state. Nature 515 (7528):587-590. doi:10.1038/nature13722

Cui X, Lu F, Qiu Q, Zhou B, Gu L, Zhang S, Kang Y, Cui X, Ma X, Yao Q, Ma J, Zhang X, Cao X (2016) REF6 recognizes a specific DNA sequence to demethylate H3K27me3 and regulate organ boundary formation in Arabidopsis. Nat Genet 48 (6):694-699. doi:10.1038/ng.3556

Cutler SR, Rodriguez PL, Finkelstein RR, Abrams SR (2010) Abscisic acid: emergence of a core signaling network. Annu Rev Plant Biol 61:651-679. doi:10.1146/annurev-arplant-042809-112122

Cutter AR, Hayes JJ (2015) A brief review of nucleosome structure. FEBS Lett 589 (20 Pt A):2914-2922. doi:10.1016/j.febslet.2015.05.016

Dekkers BJ, He H, Hanson J, Willems LA, Jamar DC, Cueff G, Rajjou L, Hilhorst HW, Bentsink L (2016) The Arabidopsis DELAY OF GERMINATION 1 gene affects ABSCISIC ACID INSENSITIVE 5 (ABI5) expression and genetically interacts with ABI3 during Arabidopsis seed development. Plant J 85 (4):451-465.

doi:10.1111/tpj.13118

Delmas F, Sankaranarayanan S, Deb S, Widdup E, Bournonville C, Bollier N, Northey JG, McCourt P, Samuel MA (2013) ABI3 controls embryo degreening through Mendel's I locus. Proc Natl Acad Sci USA 110 (40):E3888-3894. doi:10.1073/pnas.1308114110

Ficz G, Heintzmann R, Arndt-Jovin DJ (2005) Polycomb group protein complexes exchange rapidly in living Drosophila. Development 132 (17):3963-3976. doi:10.1242/dev.01950

Finkelstein R (2013) Abscisic Acid synthesis and response. Arabidopsis Book 11:e0166. doi:10.1199/tab.0166

Finkelstein RR, Gampala SS, Rock CD (2002) Abscisic acid signaling in seeds and seedlings. The Plant Cell 14 Suppl:S15-45

Finkelstein RR, Lynch TJ (2000) The Arabidopsis abscisic acid response gene ABI5 encodes a basic leucine zipper transcription factor. The Plant Cell 12 (4):599-609

Gan ES, Xu Y, Ito T (2015) Dynamics of H3K27me3 methylation and demethylation in plant development. Plant Signal Behav 10 (9):e1027851. doi:10.1080/15592324.2015.1027851

Gan ES, Xu Y, Wong JY, Goh JG, Sun B, Wee WY, Huang J, Ito T (2014) Jumonji demethylases moderate precocious flowering at elevated temperature via regulation of FLC in Arabidopsis. Nat Commun 5:5098. doi:10.1038/ncomms6098

Giraudat J, Hauge BM, Valon C, Smalle J, Parcy F, Goodman HM (1992) Isolation of the Arabidopsis ABI3 gene by positional cloning. The Plant Cell 4 (10):1251-1261. doi:10.1105/tpc.4.10.1251

Grossniklaus U, Paro R (2014) Transcriptional silencing by polycomb-group proteins. Cold Spring Harb Perspect Biol 6 (11):a019331. doi:10.1101/cshperspect.a019331

Han SK, Sang Y, Rodrigues A, Biol F, Wu MF, Rodriguez PL, Wagner D (2012) The SWI2/SNF2 chromatin remodeling ATPase BRAHMA represses abscisic acid responses in the absence of the stress stimulus in Arabidopsis. The Plant Cell 24 (12):4892-4906. doi:10.1105/tpc.112.105114

Harshman SW, Young NL, Parthun MR, Freitas MA (2013) H1 histones: current perspectives and challenges. Nucleic Acids Res 41 (21):9593-9609. doi:10.1093/nar/gkt700

Hong Q, Shao ZM (2011) Ubiquitination/deubiquitination and acetylation/deacetylation: making DNMT1 stability more coordinated. Acta Pharmacol Sin 32 (2):139-140. doi:10.1038/aps.2011.3

Javaid N, Choi S (2017) Acetylation- and Methylation-Related Epigenetic Proteins in the Context of Their Targets. Genes (Basel) 8 (8). doi:10.3390/genes8080196

Jones MA, Covington MF, DiTacchio L, Vollmers C, Panda S, Harmer SL (2010) Jumonji domain protein JMJD5 functions in both the plant and human circadian systems. Proc Natl Acad Sci USA 107 (50):21623-21628. doi:10.1073/pnas.1014204108

Kagaya Y, Okuda R, Ban A, Toyoshima R, Tsutsumida K, Usui H, Yamamoto A, Hattori T (2005) Indirect ABA-dependent regulation of seed storage protein genes by FUSCA3 transcription factor in Arabidopsis. Plant Cell Physiol 46 (2):300-311. doi:10.1093/pcp/pci031

Kahn TG, Dorafshan E, Schultheis D, Zare A, Stenberg P, Reim I, Pirrotta V, Schwartz YB (2016) Interdependence of PRC1 and PRC2 for recruitment to Polycomb Response Elements. Nucleic Acids Res 44 (21):10132-10149. doi:10.1093/nar/gkw701

Kim MJ, Park MJ, Seo PJ, Song JS, Kim HJ, Park CM (2012a) Controlled nuclear import of the transcription factor NTL6 reveals a cytoplasmic role of SnRK2.8 in the drought-stress response. Biochem J 448 (3):353-363. doi:10.1042/BJ20120244

Kim SY, Lee J, Eshed-Williams L, Zilberman D, Sung ZR (2012b) EMF1 and PRC2 cooperate to repress key regulators of Arabidopsis development. PLoS Genet 8 (3):e1002512. doi:10.1371/journal.pgen.1002512

Kobayashi Y, Murata M, Minami H, Yamamoto S, Kagaya Y, Hobo T, Yamamoto A, Hattori T (2005) Abscisic acid-activated SNRK2 protein kinases function in the gene-regulation pathway of ABA signal transduction by phosphorylating ABA response element-binding factors. Plant J 44 (6):939-949. doi:10.1111/j.1365-313X.2005.02583.x

Kulik A, Wawer I, Krzywinska E, Bucholc M, Dobrowolska G (2011) SnRK2 protein kinases--key regulators of plant response to abiotic stresses. OMICS 15 (12):859-872.

doi:10.1089/omi.2011.0091

Lafos M, Kroll P, Hohenstatt ML, Thorpe FL, Clarenz O, Schubert D (2011) Dynamic regulation of H3K27 trimethylation during Arabidopsis differentiation. PLoS Genet 7 (4):e1002040. doi:10.1371/journal.pgen.1002040

Lee HJ, Park YJ, Seo PJ, Kim JH, Sim HJ, Kim SG, Park CM (2015) Systemic Immunity Requires SnRK2.8-Mediated Nuclear Import of NPR1 in Arabidopsis. The Plant Cell 27 (12):3425-3438. doi:10.1105/tpc.15.00371

Lehmann L, Ferrari R, Vashisht AA, Wohlschlegel JA, Kurdistani SK, Carey M (2012) Polycomb repressive complex 1 (PRC1) disassembles RNA polymerase II preinitiation complexes. J Biol Chem 287 (43):35784-35794. doi:10.1074/jbc.M112.397430

Li D, Zhang L, Li X, Kong X, Wang X, Li Y, Liu Z, Wang J, Li X, Yang Y (2018) AtRAE1 is involved in degradation of ABA receptor RCAR1 and negatively regulates ABA signalling in Arabidopsis. Plant, cell & environment 41 (1):231-244. doi:10.1111/pce.13086

Li G, Reinberg D (2011) Chromatin higher-order structures and gene regulation. Curr Opin Genet Dev 21 (2):175-186. doi:10.1016/j.gde.2011.01.022

Lim S, Park J, Lee N, Jeong J, Toh S, Watanabe A, Kim J, Kang H, Kim DH, Kawakami N, Choi G (2013) ABA-insensitive3, ABA-insensitive5, and DELLAs Interact to activate

the expression of SOMNUS and other high-temperature-inducible genes in imbibed seeds in Arabidopsis. The Plant cell 25 (12):4863-4878. doi:10.1105/tpc.113.118604

Liu X, Yang S, Yu CW, Chen CY, Wu K (2016) Histone Acetylation and Plant Development. Enzymes 40:173-199. doi:10.1016/bs.enz.2016.08.001

Liu X, Zhang H, Zhao Y, Feng Z, Li Q, Yang HQ, Luan S, Li J, He ZH (2013) Auxin controls seed dormancy through stimulation of abscisic acid signaling by inducing ARF-mediated ABI3 activation in Arabidopsis. Proc Natl Acad Sci USA 110 (38):15485-15490. doi:10.1073/pnas.1304651110

Lopez-Molina L, Mongrand S, Chua NH (2001) A postgermination developmental arrest checkpoint is mediated by abscisic acid and requires the ABI5 transcription factor in Arabidopsis. Proc Natl Acad Sci USA 98 (8):4782-4787. doi:10.1073/pnas.081594298

Lopez-Molina L, Mongrand S, McLachlin DT, Chait BT, Chua NH (2002) ABI5 acts downstream of ABI3 to execute an ABA-dependent growth arrest during germination. Plant J 32 (3):317-328

Lu F, Cui X, Zhang S, Jenuwein T, Cao X (2011) Arabidopsis REF6 is a histone H3 lysine 27 demethylase. Nat Genet 43 (7):715-719. doi:10.1038/ng.854

Lu F, Li G, Cui X, Liu C, Wang XJ, Cao X (2008) Comparative analysis of JmjC domain-containing proteins reveals the potential histone demethylases in Arabidopsis and rice. J Integr Plant Biol 50 (7):886-896. doi:10.1111/j.1744-7909.2008.00692.x

Marino-Ramirez L, Kann MG, Shoemaker BA, Landsman D (2005) Histone structure and nucleosome stability. Expert Rev Proteomics 2 (5):719-729. doi:10.1586/14789450.2.5.719

Mathiyalagan P, Keating ST, Du XJ, El-Osta A (2014) Chromatin modifications remodel cardiac gene expression. Cardiovasc Res 103 (1):7-16. doi:10.1093/cvr/cvu122

Merlot S, Gosti F, Guerrier D, Vavasseur A, Giraudat J (2001) The ABI1 and ABI2 protein phosphatases 2C act in a negative feedback regulatory loop of the abscisic acid signalling pathway. Plant J 25 (3):295-303

Mustilli AC, Merlot S, Vavasseur A, Fenzi F, Giraudat J (2002) Arabidopsis OST1 protein kinase mediates the regulation of stomatal aperture by abscisic acid and acts upstream of reactive oxygen species production. The Plant Cell 14 (12):3089-3099

Nakashima K, Fujita Y, Kanamori N, Katagiri T, Umezawa T, Kidokoro S, Maruyama K, Yoshida T, Ishiyama K, Kobayashi M, Shinozaki K, Yamaguchi-Shinozaki K (2009) Three Arabidopsis SnRK2 protein kinases, SRK2D/SnRK2.2, SRK2E/SnRK2.6/OST1 and SRK2I/SnRK2.3, involved in ABA signaling are essential for the control of seed development and dormancy. Plant Cell Physiol 50 (7):1345-1363. doi:10.1093/pcp/pcp083

Nambara E, Suzuki M, Abrams S, McCarty DR, Kamiya Y, McCourt P (2002) A screen for genes that function in abscisic acid signaling in Arabidopsis thaliana. Genetics 161

(3):1247-1255

Narusaka Y, Nakashima K, Shinwari ZK, Sakuma Y, Furihata T, Abe H, Narusaka M, Shinozaki K, Yamaguchi-Shinozaki K (2003) Interaction between two cis-acting elements, ABRE and DRE, in ABA-dependent expression of Arabidopsis rd29A gene in response to dehydration and high-salinity stresses. Plant J 34 (2):137-148

Nee G, Xiang Y, Soppe WJ (2017) The release of dormancy, a wake-up call for seeds to germinate. Curr Opin Plant Biol 35:8-14. doi:10.1016/j.pbi.2016.09.002

Park SY, Fung P, Nishimura N, Jensen DR, Fujii H, Zhao Y, Lumba S, Santiago J, Rodrigues A, Chow TF, Alfred SE, Bonetta D, Finkelstein R, Provart NJ, Desveaux D, Rodriguez PL, McCourt P, Zhu JK, Schroeder JI, Volkman BF, Cutler SR (2009) Abscisic acid inhibits type 2C protein phosphatases via the PYR/PYL family of START proteins. Science 324 (5930):1068-1071. doi:10.1126/science.1173041

Penfield S (2017) Seed dormancy and germination. Curr Biol 27 (17):R874-R878. doi:10.1016/j.cub.2017.05.050

Perruc E, Kinoshita N, Lopez-Molina L (2007) The role of chromatin-remodeling factor PKL in balancing osmotic stress responses during Arabidopsis seed germination. Plant J 52 (5):927-936. doi:10.1111/j.1365-313X.2007.03288.x

Pfluger J, Wagner D (2007) Histone modifications and dynamic regulation of genome accessibility in plants. Curr Opin Plant Biol 10 (6):645-652.

doi:10.1016/j.pbi.2007.07.013

Piskurewicz U, Tureckova V, Lacombe E, Lopez-Molina L (2009) Far-red light inhibits germination through DELLA-dependent stimulation of ABA synthesis and ABI3 activity. EMBO J 28 (15):2259-2271. doi:10.1038/emboj.2009.170

Plotnikov A, Zehorai E, Procaccia S, Seger R (2011) The MAPK cascades: signaling components, nuclear roles and mechanisms of nuclear translocation. Biochim Biophys Acta 1813 (9):1619-1633. doi:10.1016/j.bbamcr.2010.12.012

Qian S, Wang Y, Ma H, Zhang L (2015) Expansion and Functional Divergence of Jumonji C-Containing Histone Demethylases: Significance of Duplications in Ancestral Angiosperms and Vertebrates. Plant Physiol 168 (4):1321-1337. doi:10.1104/pp.15.00520

Rodrigues A, Adamo M, Crozet P, Margalha L, Confraria A, Martinho C, Elias A, Rabissi A, Lumbreras V, Gonzalez-Guzman M, Antoni R, Rodriguez PL, Baena-Gonzalez E (2013) ABI1 and PP2CA phosphatases are negative regulators of Snf1-related protein kinase1 signaling in Arabidopsis. The Plant Cell 25 (10):3871-3884. doi:10.1105/tpc.113.114066

Rossetto D, Avvakumov N, Cote J (2012) Histone phosphorylation: a chromatin modification involved in diverse nuclear events. Epigenetics 7 (10):1098-1108. doi:10.4161/epi.21975

Ryu H, Cho H, Bae W, Hwang I (2014) Control of early seedling development by BES1/TPL/HDA19-mediated epigenetic regulation of ABI3. Nat Commun 5:4138. doi:10.1038/ncomms5138

Sahr T, Voigt G, Schimmack W, Paretzke HG, Ernst D (2005) Low-level radiocaesium exposure alters gene expression in roots of Arabidopsis. New Phytol 168 (1):141-148. doi:10.1111/j.1469-8137.2005.01485.x

Sakata Y, Nakamura I, Taji T, Tanaka S, Quatrano RS (2010) Regulation of the ABA-responsive Em promoter by ABI3 in the moss Physcomitrella patens: role of the ABA response element and the RY element. Plant Signal Behav 5 (9):1061-1066

Sergeeva LI, Keurentjes JJ, Bentsink L, Vonk J, van der Plas LH, Koornneef M, Vreugdenhil D (2006) Vacuolar invertase regulates elongation of Arabidopsis thaliana roots as revealed by QTL and mutant analysis. Proc Natl Acad Sci USA 103 (8):2994-2999. doi:10.1073/pnas.0511015103

Silva AT, Ribone PA, Chan RL, Ligterink W, Hilhorst HW (2016) A Predictive Coexpression Network Identifies Novel Genes Controlling the Seed-to-Seedling Phase Transition in Arabidopsis thaliana. Plant Physiol 170 (4):2218-2231. doi:10.1104/pp.15.01704

Song L, Huang SC, Wise A, Castanon R, Nery JR, Chen H, Watanabe M, Thomas J, Bar-Joseph Z, Ecker JR (2016) A transcription factor hierarchy defines an environmental stress response network. Science 354 (6312). doi:10.1126/science.aag1550

Sun B, Looi LS, Guo S, He Z, Gan ES, Huang J, Xu Y, Wee WY, Ito T (2014) Timing mechanism dependent on cell division is invoked by Polycomb eviction in plant stem cells. Science 343 (6170):1248559. doi:10.1126/science.1248559

Supek F, Bosnjak M, Skunca N, Smuc T (2011) REVIGO summarizes and visualizes long lists of gene ontology terms. PLoS One 6 (7):e21800. doi:10.1371/journal.pone.0021800

Suzuki M, Kao CY, McCarty DR (1997) The conserved B3 domain of VIVIPAROUS1 has a cooperative DNA binding activity. The Plant Cell 9 (5):799-807. doi:10.1105/tpc.9.5.799

Takeuchi T, Watanabe Y, Takano-Shimizu T, Kondo S (2006) Roles of jumonji and jumonji family genes in chromatin regulation and development. Dev Dyn 235 (9):2449-2459. doi:10.1002/dvdy.20851

Teaster ND, Motes CM, Tang Y, Wiant WC, Cotter MQ, Wang YS, Kilaru A, Venables BJ, Hasenstein KH, Gonzalez G, Blancaflor EB, Chapman KD (2007) N-Acylethanolamine metabolism interacts with abscisic acid signaling in Arabidopsis thaliana seedlings. The Plant Cell 19 (8):2454-2469. doi:10.1105/tpc.106.048702

Tian T, Liu Y, Yan H, You Q, Yi X, Du Z, Xu W, Su Z (2017) agriGO v2.0: a GO analysis toolkit for the agricultural community, 2017 update. Nucleic Acids Res 45 (W1):W122-W129. doi:10.1093/nar/gkx382

Uddenberg D, Valladares S, Abrahamsson M, Sundstrom JF, Sundas-Larsson A, von Arnold S (2011) Embryogenic potential and expression of embryogenesis-related genes in conifers are affected by treatment with a histone deacetylase inhibitor. Planta 234 (3):527-539. doi:10.1007/s00425-011-1418-8

Uemura A, Yamaguchi N, Xu Y, Wee W, Ichihashi Y, Suzuki T, Shibata A, Shirasu K, Ito T (2018) Regulation of floral meristem activity through the interaction of AGAMOUS, SUPERMAN, and CLAVATA3 in Arabidopsis. Plant Reprod 31 (1):89-105. doi:10.1007/s00497-017-0315-0

Umezawa T, Sugiyama N, Mizoguchi M, Hayashi S, Myouga F, Yamaguchi-Shinozaki K, Ishihama Y, Hirayama T, Shinozaki K (2009) Type 2C protein phosphatases directly regulate abscisic acid-activated protein kinases in Arabidopsis. Proc Natl Acad Sci USA 106 (41):17588-17593. doi:10.1073/pnas.0907095106

Umezawa T, Yoshida R, Maruyama K, Yamaguchi-Shinozaki K, Shinozaki K (2004) SRK2C, a SNF1-related protein kinase 2, improves drought tolerance by controlling stress-responsive gene expression in Arabidopsis thaliana. Proc Natl Acad Sci USA 101 (49):17306-17311. doi:10.1073/pnas.0407758101

Verma V, Ravindran P, Kumar PP (2016) Plant hormone-mediated regulation of stress responses. BMC Plant Biol 16:86. doi:10.1186/s12870-016-0771-y

Vogler C, Huber C, Waldmann T, Ettig R, Braun L, Izzo A, Daujat S, Chassignet I, Lopez-

Contreras AJ, Fernandez-Capetillo O, Dundr M, Rippe K, Langst G, Schneider R (2010) Histone H2A C-terminus regulates chromatin dynamics, remodeling, and histone H1 binding. PLoS Genet 6 (12):e1001234. doi:10.1371/journal.pgen.1001234

Waese J, Pasha A, Wang TT, van Weringh A, Guttman DS, Provart NJ (2016) Gene Slider: sequence logo interactive data-visualization for education and research. Bioinformatics 32 (23):3670-3672. doi:10.1093/bioinformatics/btw525

Wang W, Qin JJ, Voruganti S, Nag S, Zhou J, Zhang R (2015) Polycomb Group (PcG) Proteins and Human Cancers: Multifaceted Functions and Therapeutic Implications. Med Res Rev 35 (6):1220-1267. doi:10.1002/med.21358

Wang Y, Li L, Ye T, Lu Y, Chen X, Wu Y (2013) The inhibitory effect of ABA on floral transition is mediated by ABI5 in Arabidopsis. J Exp Bot 64 (2):675-684. doi:10.1093/jxb/ers361

Weitbrecht K, Muller K, Leubner-Metzger G (2011) First off the mark: early seed germination. J Exp Bot 62 (10):3289-3309. doi:10.1093/jxb/err030

Wu X, Johansen JV, Helin K (2013) Fbxl10/Kdm2b recruits polycomb repressive complex 1 to CpG islands and regulates H2A ubiquitylation. Mol Cell 49 (6):1134-1146. doi:10.1016/j.molcel.2013.01.016

Yamagishi K, Tatematsu K, Yano R, Preston J, Kitamura S, Takahashi H, McCourt P, Kamiya Y, Nambara E (2009) CHOTTO1, a double AP2 domain protein of Arabidopsis

thaliana, regulates germination and seedling growth under excess supply of glucose and nitrate. Plant Cell Physiol 50 (2):330-340. doi:10.1093/pcp/pcn201

Yamaguchi N, Huang J, Tatsumi Y, Abe M, Sugano SS, Kojima M, Takebayashi Y, Kiba T, Yokoyama R, Nishitani K, Sakakibara H, Ito T (2018) Chromatin-mediated feed-forward auxin biosynthesis in floral meristem determinacy. Nat Commun 9 (1):5290. doi:10.1038/s41467-018-07763-0

Yamaguchi N, Huang J, Xu Y, Tanoi K, Ito T (2017) Fine-tuning of auxin homeostasis governs the transition from floral stem cell maintenance to gynoecium formation. Nat Commun 8 (1):1125. doi:10.1038/s41467-017-01252-6

Yamaguchi N, Winter CM, Wu MF, Kwon CS, William DA, Wagner D (2014) PROTOCOLS: Chromatin Immunoprecipitation from Arabidopsis Tissues. Arabidopsis Book 12:e0170. doi:10.1199/tab.0170

Yang W, Zhang W, Wang X (2017) Post-translational control of ABA signalling: the roles of protein phosphorylation and ubiquitination. Plant Biotechnol J 15 (1):4-14. doi:10.1111/pbi.12652

You Y, Sawikowska A, Neumann M, Pose D, Capovilla G, Langenecker T, Neher RA, Krajewski P, Schmid M (2017) Temporal dynamics of gene expression and histone marks at the Arabidopsis shoot meristem during flowering. Nat Commun 8:15120. doi:10.1038/ncomms15120

Zhang S, Wei Y, Lu Y, Wang X (2009) Mechanisms of brassinosteroids interacting with multiple hormones. Plant Signal Behav 4 (12):1117-1120

Zhu JK (2016) Abiotic Stress Signaling and Responses in Plants. Cell 167 (2):313-324. doi:10.1016/j.cell.2016.08.029

Zhu L, Zhang Y, Kang E, Xu Q, Wang M, Rui Y, Liu B, Yuan M, Fu Y (2013) MAP18 regulates the direction of pollen tube growth in Arabidopsis by modulating F-actin organization. The Plant Cell 25 (3):851-867. doi:10.1105/tpc.113.110528

Publications

Jinfeng Wu, Yasunori Ichihashi, Takamasa Suzuki, Arisa Shibata, Ken Shirasu, Nobutoshi Yamaguchi & Toshiro Ito (2019) Abscisic acid-dependent histone demethylation during postgermination growth arrest in *Arabidopsis*. Plant, Cell & Environment, 42: 2198-2214. https://doi.org/10.1111/pce.13547

Jinfeng Wu, Nobutoshi Yamaguchi & Toshiro Ito (2019) Histone demethylases control root elongation in response to stress-signaling hormone abscisic acid. Plant Signaling & Behavior, 14:7. DOI: 10.1080/15592324.2019.1604019